Improvement of Energy and Control Performance in Water Hydraulic Transmissions

by PHAM, Ngoc Pha

Dissertation submitted to the Functional Control Systems,
Graduate School of Engineering at
Shibaura Institute of Technology
in partial fulfilment of the requirements for the degree of

Doctor of Engineering

September 2014

I would like to dedicate this thesis to my loving family $\cdots$

Acknowledgements

This research has been performed at the Environmental Systems Control Laboratory, Department of Machinery and Control Systems, College of Systems Engineering and Science, Shibaura Institute of Technology, Japan, under the supervision of Prof. Kazuhisa Ito.

First and foremost, I would like to express my deeply gratitude to Prof. Kazuhisa Ito for his whole-hearted guidance and support.

I also extend my sincere thanks to Prof. Shigeru Ikeo, Department of Engineering and Applied Sciences, Sophia University for proving kind help and support when I did experiment at his university.

My deepest gratitude is due to the staffs of all associated departments who made my study possible from the initial to final stages.

I am grateful to all my dear Japanese friends from Environmental Systems Control Laboratory, Shibaura Institute of Technology, for their unlimited supports.

Especially, I would like to give my special thanks to my family who gave me tremendous spiritual encouragements.

Pham Ngoc Pha

Abstract

The low energy efficiency and high installation cost of water hydraulics are the main obstacles to its widespread application. This thesis introduces two novel systems that overcome these challenges: fluid switching transmission (FST) and pump motor transmission (PMT). These systems only use an inexpensive ON/OFF valve to lower the initial cost and greatly reduce the energy consumption compared to a conventional water hydraulic servo motor system (SMS). Both systems can also recover the kinetic energy of a flywheel for use in the next working cycle. The experimental results showed that the energy consumption of the FST and PMT systems was drastically reduced in comparison with the SMS. The FST system only required 33.2%–47.3% of the total energy consumption of the SMS to complete a full cycle while the PMT system required 14.0%–24.0%. A method was developed to estimate the saved energy stored in the accumulator and was found to recover 8.2%–11.6% and 8.7%–13.7% of the total energy consumptions by the FST and PMT systems, respectively. The SMS had better transient response with the shortest rise time and smallest overshoot, while the steady-state error was only slightly smaller than that of the PMT system. The steady-state error of the FST system was relatively large but stayed almost the same for all reference velocities; thus, this transmission is appropriate for high-velocity systems. With an acceptable velocity response and greatly improved energy efficiency, the PMT system is a promising candidate to replace conventional water hydraulic systems.

Contents

List of Figures

List of Tables

Nomenclature

Roman Symbols

A The area of the piston bore

A_0 The cross section area of an orifice

A_h The heat transfer area of the accumulator

$A_{\max}$ The maximum opening area of an ON/OFF valve

$A_{\mathrm{ON/OFF}}$ The cross section area of an ON/OFF valve

C_v The specific heat at constant volume of the internal gas

D The diameter of the cycle of bore center of the hydraulic pump

d The diameter of the bore the hydraulic pump

d_0 The diameter of an orifice

$E_{\mathrm{con.PMT}}$ The total energy consumption of the PMT

$E_{\mathrm{con.}i}$ The total energy consumption in *Case i*

$e_{\max}$ The percentage for error of maximum rotational velocity

$e_{\min}$ The percentage for error of minimum rotational velocity

$E_{\mathrm{net.PMT}}$ The net energy consumption of PMT

$E_{\mathrm{net.}i}$ The net energy consumption in *Case i*

$E_{\mathrm{re}.i}$ The recovered energy to the accumulator ACC_2 in *Case i*

$E_{\mathrm{save.PMT}}$ The saved energy of the PMT

$E_{\mathrm{save}.i}$ The saved energy in *Case i*

E_{waste} The relative wasted energy of FST to PMT

f The frequency of electrical power supply to the electric motor

G_m The reference model

G_{Pc} The transfer function of PID controller for PMT

G_{Sc} The transfer function of PID controller for servo motor system

h The heat transfer coefficient into the accumulator

h The stroke length of the piston of the hydraulic pump

I_{PM} The moment of inertia of the hydraulic pump/motor

K_{PD} The derivative gain of the PID controller for PMT

K_{PI} The integral gain of the PID controller for PMT

K_{PP} The proportional gain of the PID controller for PMT

K_{SD} The derivative gain of the PID controller for servo motor system

K_{SI} The integral gain of the PID controller for servo motor system

K_{SP} The proportional gain of the PID controller for servo motor system

m The mass of the gas inside the accumulator

n The rotational velocity of the driven shaft of the hydraulic pump

P The number of poles of the electric motor

p_0 The precharge pressure of the accumulator

p_g The internal gas pressure of the accumulator

$p_{\mathrm{ACC}_2.i}$ The pressure of the fluid inside the accumulator ACC_2

P_{M} The number of poles of the electric motor

PO_F The percentage overshoot of the FST system

PO_P The percentage overshoot of the PMT system

PO_S The percentage overshoot of servo motor system

Q_{P} The flow rate of the hydraulic pump

Q_h The heat energy transferred into the accumulator

$Q_{\mathrm{ACC}_2.i}$ The flow rate charged into the accumulator ACC_2 in the deceleration processes corresponding to *Case i*

$Q_{\mathrm{ON/OFF}}$ The flow rate through an ON/OFF valve

Q_{orifice} The flow rate through an orifice

R The ideal gas constant

T The time constant of an ON/OFF valve

T_g The temperature of the gas inside the accumulator

T_w The temperature of the accumulator wall

t_w The operation time in Phase 1 and Phase 2

t_{end} The time at the end of a cycle

$T_{\mathrm{PM,L}}$ The load torque of the motor

t_{start} The time at the beginning of a cycle

u The internal energy per unit of mass

u_{M} The control signal sent to the frequency converter

V_g The internal gas volume of the accumulator

W The external work of the accumulator

z The number of cylinders

Greek Symbols

α The title angle

α_d The discharge coefficient of an orifice

ΔP_{HL} The pressure difference between the high/low pressure ports of the hydraulic pump/motor

$\Delta P_{\mathrm{ON/OFF}}$ The pressure difference of input/output ports of an ON/OFF valve

$\Delta P_{\mathrm{Orifice}}$ The pressure difference between input/output ports of an orifice

η_{PMT} The saved energy index of the PMT

η_{PM} The volumetric efficiency of the motor

η_{P} The volumetric efficiency of the hydraulic pump

η_w The ratio between the relative wasted energy and net energy consumption of FST

$\omega_{\max}$ The maximum velocity in the constant Phase

$\omega_{\min}$ The minimum velocity in the constant Phase

ω_{ref} The reference velocity

ρ The fluid density

τ The thermal time constant of the accumulator

τ_a The thermal time constant when all the gas was released

τ_n The time constant of the electric motor

ε The frequency coefficient

φ The angular of the hydraulic pump/motor shaft

Chapter 1

Introduction

1.1 Water Hydraulics

1.1.1 Historical View

Water hydraulics has a long history [6]; however, water hydraulic system did not have an important position in industry until recent years when the world faces environmental pollution, industrial wastes, unsafe situation in some specification fields such as coal extraction, food processing, etc. Because of these benefits, water hydraulics is considered as the future drive system. The brief development of water hydraulic systems will be introduced in the following section.

Water hydraulics has a very early starting point, almost all investigators agreed that the ideas and the tangible “hydraulic” devices produced by the Greeks of 5^{th} century BC onwards. However, until Aristotle (384 BC – 322 BC) who regarded as the first person laid the foundation for researching academically on water with his postulate “water is a continuum”, water hydraulic started studying naturally. Aristotle was also respected with the title “Father of Hydraulics”.

The application of water considered as the first mechanical system was made by Egyptian named Ktesibios in about 250BC. It is a very simple musical instrument - water powered organ that remained the standard for such instrument until late Middle Ages.

In the early Modern Era, Blaise Pascal (1623 – 1662) is the person who had the most important contribution to the development of hydraulics. He proved mathematically that the pressure at a point in a fluid at rest is equal from all sides. For his work in the field of fluid power the S.I. unit of pressure bears his Pascal's name. The first industrial application of the hydraulic press (using water as the working fluid) based on Pascal's theory was performed later on by Josef Bramah (1748 – 1814), in 1795, in London.

Following the invention of the steam engine by James Watt (1736 – 1819), hydrostatic machines were widely used in England for energy exchange in the form of pressurized water network. Pumps driven by steam engines were employed to generated pressurized water, which was in turn used to actuate pistons driving the processing machines.

In the second half of the 19^{th} century, William George Armstrong (1810 – 1900) developed many hydrostatic machines and devices, primarily for use in shipbuilding. Some of these control devices still resemble those used today.

Fluid power technology has then developed mainly from the beginning of the 20^{th} century. Early 20^{th} century, Professor Harvey D William, professor of Engineering at Cornell University began work on a new design of pump/motor combination. He and an American engineer named Reynolds Jenney cooperated to develop the first variable hydrostatic transmission, something the hydraulic industry really needed. Williams and Jenney's development was the first hydraulic components requiring the medium to be an efficient lubricant. This was the one requirement to make oil had important position in hydraulic field. Another requirement to make oil hydraulic gained its major role is avoiding leakage because of poor quality of seals.

In 1940's, it marked the huge increase in use of oil hydraulic because of demand of heavy presses, particularly of forging presses, demand of aircraft and marine application. However, after an accident concerning with use of oil hydraulic system in a coal mine in Belgium called Bitter Heart Mine in the summer of 1956, the use of oil hydraulic system in some specific and dangerous areas was limited, and water hydraulic presented many outstanding advantages in such areas.

Today, the world faces with very serious situation of environmental pollution and industrial wastes. Moreover, safety standards in work and products are getting more and more stringent. Therefore, development safe and clean technologies are required urgently. From late 1990's, water hydraulic drive systems were developed and considered as the 4th driving source.

1.1.2 Modern Water Hydraulics

1.1.2.1 The Development of Water Hydraulics

Nowadays, the most important requirement for technical application is that the systems and devices need to be safe, clean, and environmental friendly; from this point of view, water hydraulics that uses pure tap water as pressure medium emerges as an important solution and it is considered as the fourth driving source beside electricity, pneumatics, and conventional oil hydraulics, especially in the field of food and medicine processing, steel and glass production, ocean exploration, under water robotics [7], nuclear power generation [8], under water gait-training orthosis [9], wave and wind power generation systems, and mining machinery [10].

Water hydraulic has a very long story as mentioned in [6]; however, it has been paid much attention by researchers only since late 1990s because of the limitations including oxidation and rust, poor lubricity, low viscosity of water, bacterial growth, and particles contaminants present as shown and indicated the remedies in [1, 2]. Recencly, advances in material and machining technology bring longer lifetime, higher flow rate and pressure for water hydraulic components [11] and especially, current researches on the improvement of water hydraulic devices such as pumps [7, 12, 13], valves [10, 14, 15], and actuators [16, 17, 18] or other studies on tribology of materials under water lubrication [19] even in high temperature and pressure [20] bring a bright future and wider applications for water hydraulics.

The application trends of water hydraulics versus oil hydraulics were presented clearly in [1, 21]. Figure 1.1 shows the hydraulics (oil vs. water) application trends and key milestones. The first water-hydraulic press, inverted by Bramah, was granted a British patent in 1795. In 1906, Williams and Janney coined in the idea of replacing water-based fluid by oil, thus avoiding corrosion, lubrication and freezing as well as leakage problems, at high temperature, involving water. The following years saw a tremendous increase in the application of oil hydraulics.

The turning point came in 1994, when Danfoss introduced the first generation of modern tap water components known as the Nessie® family of products for high-pressure tap water hydraulic systems that operate typically up to 140 bar. Since 1997 Danfoss has introduced such a second generation of low-pressure and low-power tap water hydraulic components that operate up to 50 bar.

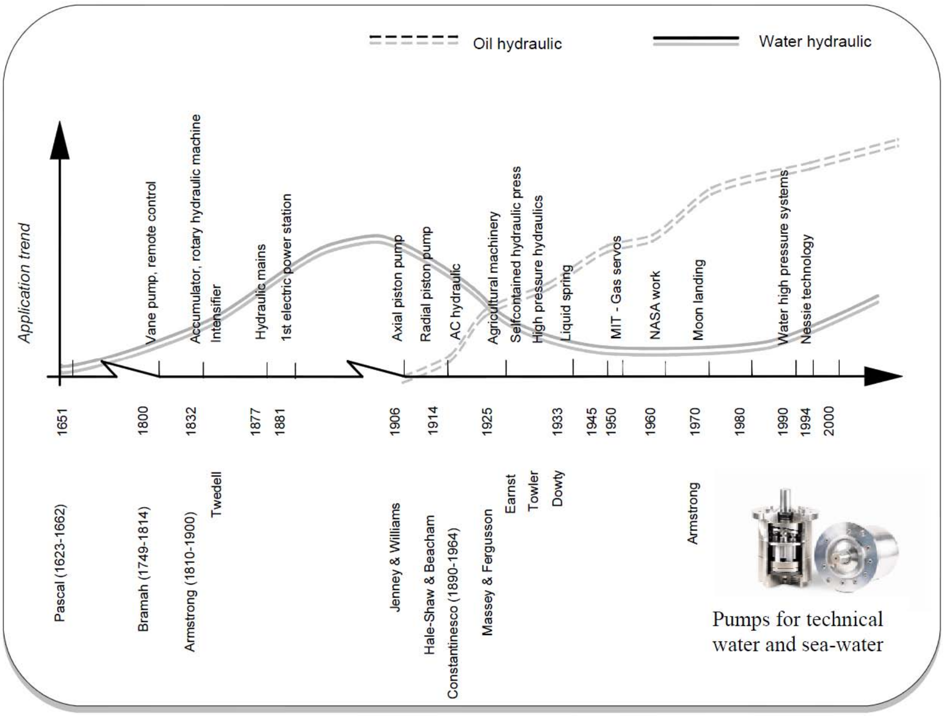

Figure 1.1: *Hydraulics application trends and key milestones [1].*

The business sales history confirms that the use of modern water hydraulics shows a growing turnover as for Danfoss High-Pressure Water Solutions in Fig. 1.2 [1]. Nowadays, many companies are involved in water hydraulics [21]. These include Danfoss [22], Hytar Oy [23], SPX Fluid Power (former Fenner Fluid Power) [24], Hauhinco Trading [25], Elwood Corporation [26], Hunt Valve Company [27], Schrupp Inc. [28], the Oilgear Company [29], Hainzl Industriesysteme GmbH & CoKG [30], Ebara Research Co. Ltd. [31], Kawasaki Heavy Industry Ltd., Kayaba Industry Co. Ltd., Koganei Co., Komatsu Ltd., Mitsubishi Heavy Industries Ltd., Moog Japan Ltd., Nabco Ltd., Nachi Co., SMC Co., Tokyo Precision Instrument Ltd., Yuken Kogyo Co. Ltd., and so on.

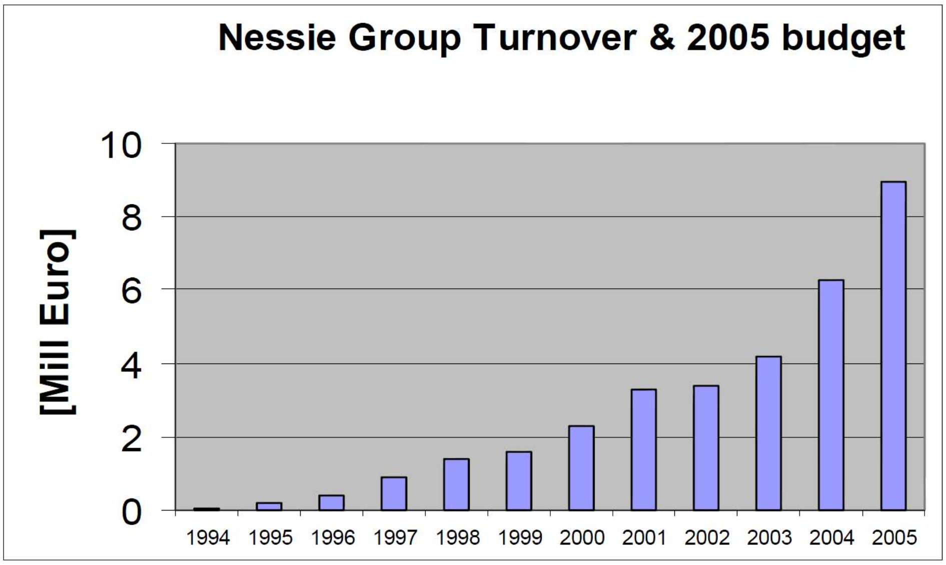

Figure 1.2: *Trend in turnover of Danfoss Nessie Group for water hydraulics [1].*

Institutions interested in modern water-hydraulics are listed as: Institute of Hydraulics and Automation, Tampere University of Technology, Finland, Linkoping University, Sweden, Department of Control and Engineering Design, Technical University of Denmark, University of Wales, Cardiff, Fluid Power Center, University of Bath, Tohoku University, Sophia University, Shibaura Institute of Technology, the State Key Laboratory of Fluid Power Transmission and Control, Zhejiang University, China, Huazhong University of Science and Technology, China, and School of Mechanical and Production Engineering, Nanyang Technological University, Singapore.

Organizations such as FPNI [32], NFPA [33], BFPA [34], VDMA [35], and JFPS [36] are involved in water hydraulics. Some international conferences have occurred in water hydraulics. These include SICFP (Scandinavian International Conference on Fluid Power), Bath International Fluid Power Workshop, Aachen Conferences on Fluid Power Technology, ICFP (International Conference on Fluid Power Transmission and Control), JFPS International Symposium on Fluid Power, and FLUCOME (International Symposium on Fluid Control, Measurement and Visualization).

1.1.2.2 Application of Water Hydraulics

This subsection introduces various applications of water hydraulics, the applications were mentioned in some published conference paper such as [1, 2, 3].

Water hydraulic mobile machines

All hydraulic functions for lifting and filling on the designed Waste Packer Lorries for Gothenburg Municipal, Sweden are shown one of them in Fig. 1.3. The functions are controlled and operated by water hydraulics to protect the environment in the city. The benefits are no risk of oil spill drops or product contamination, and easy to clean. The vehicles have el-hybrid motors.

Figure 1.4 shows a self-propelled water hydraulic vehicle developed at Purdue University. In this project the original oil hydraulic system was replaced with one using water hydraulic components. This vehicle was primarily developed in order to provide an alternative different than oil for the equipment used for maintaining the expensive and delicate grass of golf courses.

Water-based hydraulic systems for longwall mining roof supports

Water hydraulics is very useful for protecting from fire hazard. Thus, it has been used successfully for many years in self-advancing hydraulic roof supports for the longwall mining of minerals such as coal and potash. Some examples of the largest and latest roof supports, or shields are shown in Figs. 1.5 and 1.6. The coal face consists of a line of around 150 of these supports, which support the roof of the mine whilst the shearer cuts the coal along a face length of around 300 m. The operation of such a modern longwall face is now highly automated.

Tap water hydraulic machinery designed for hygiene

Some typical examples of design for hygiene are presented in the following to illustrates application areas where tap water hydraulics can offer a design for hygiene solution in the food processing industry, which cannot been solved by use of a bio-oil based hydraulic system. Compared with pneumatic solutions, water hydraulic solutions have the significant advantages of easy to flush and clean according to the requirements and regulations in the food processing industry,

Figure 1.3: *Water hydraulic waste packer lorry [1].*

Figure 1.4: *Self-propelled water hydraulic vehicle [2].*

Figure 1.5: *1750 ton roof support with 480 mm bore leg cylinder – note the bronze plated rods [3].*

Figure 1.6: *Roof support for 7 m face with 500 mm bore leg cylinders [3].*

lighter weight of cutting tools (saws etc.) due to higher power density, much higher efficiency and saving energy costs. A tap water hydraulic driven meat burger-machine is shown in Fig. 1.7. A motor is driving the spindle for the meat cutting of beef meat, and two water cylinders for motion control are used to form the five meat burgers in one row, and one cylinder for moving the forming tool horizontally. The machine is very environmentally friendly and very easy to clean daily.

Figure 1.7: *Tap water hydraulic driven burger-machine [1].*

An automatic controlled ice fill machine for Tetra Pak Hoyer in Denmark with a capacity of 400 ices per minutes driven by electro water hydraulics with one motor, 3 linear servo cylinders and 3 end cylinders is shown in Fig. 1.8.

An automatic control tobacco cutter machine for Universelle Germany is shown in Fig. 1.9 with two water hydraulic cylinders to avoid no risk of pollution, easy cleaning and save energy.

A water hydraulic drive unit for wing press equipment for the aero plane factory of Palamine in UK wants to avoid no pollution on ground, no fire risk and no oil is shown in Fig. 1.10. Other applications of water hydraulics are shown in Appendix B.

Figure 1.8: *Ice fill machines for 400 ices per minutes [1].*

Figure 1.9: *Automatic control tobacco cutter machine driven by water hydraulics with two cylinders [1].*

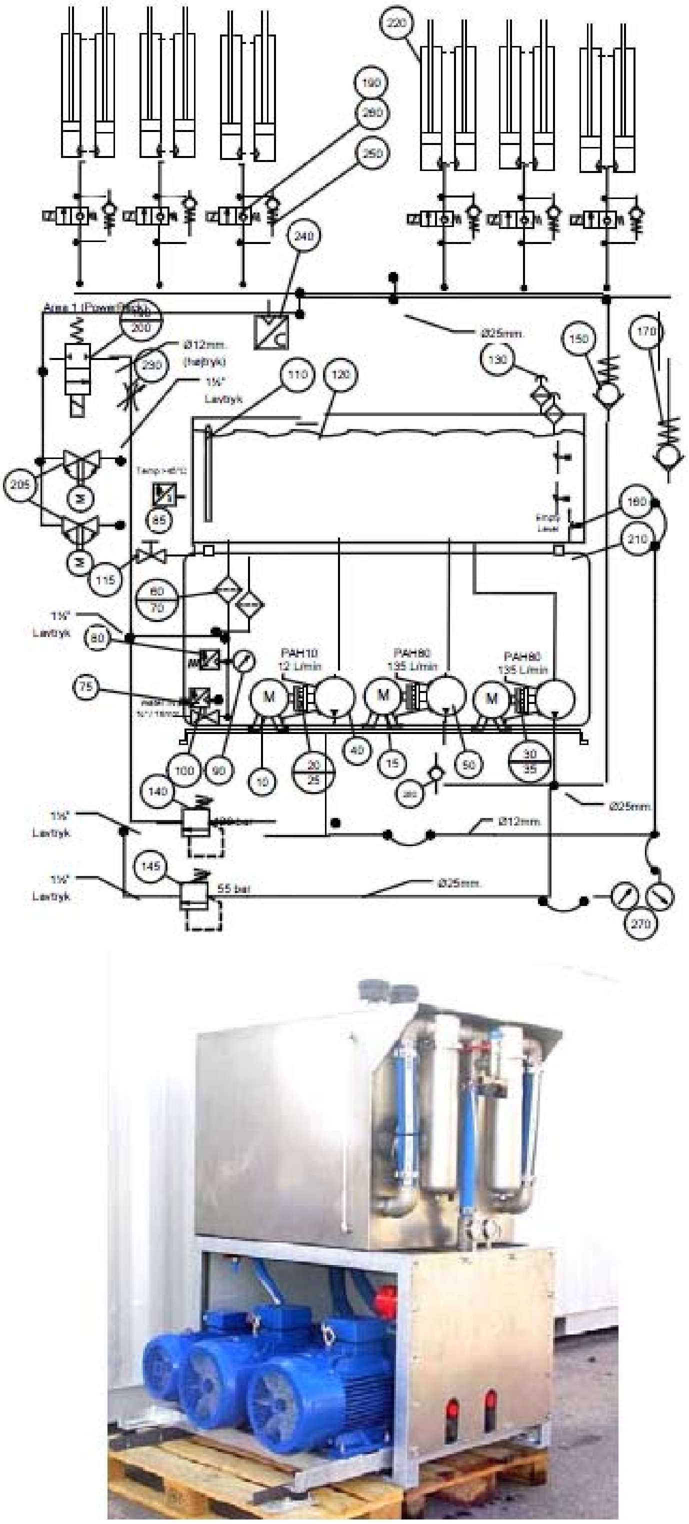

Figure 1.10: *Water hydraulics drives for wing press equipment for an aero plane factory [1].*

1.1.3 Advantages and Disadvantages of Water Hydraulics

According to [1, 2, 21], the benefits of water relative to mineral oil, bio oil and water-oil emulsion are illustrated in Fig. 1.11. The significant advantages and benefits can be listed as follows:

- No pollution of the environment (since most processes create leakage and fluid spills).
- Low operational and power media costs, i.e. purchase, storage, disposal
- Non-flammable explosion-proof fluid, safe and suitable for use in hazardous applications (lower insurance costs, require less cooling capacity etc.)
- High fluid power density, high power efficiency and high torque to inertia ratio compared to electric drives and pneumatic drives.
- Workers do not breathe harmful oil vapors or risk exposure to skin and eyes.
- Readily available and cost effective.

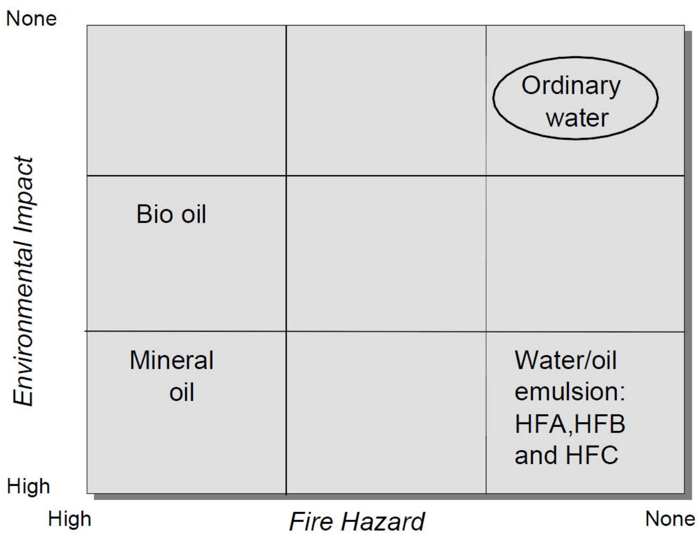

Figure 1.11: *Water versus bio oil, mineral oil and emulsions [1].*

The compressibility gives the liquid its ability to store and transfer energy with a remarkable power density, i.e. a very high torque to inertia ratio. Water contains much less air in solution that may affect the rigidity of hydraulic systems. However the bulk modulus of pure ordinary water is 2.4×10^3 MPa, approximately 50% larger than that for mineral oil (1.6×10^3 MPa), and the velocity of sound in water (1,480 m/s at 20°C) is around 10% faster than the velocity of sound in mineral oil (1,300 m/s at 20°C). Thus water has an advantage for faster operation and control of hydraulic systems.

According to Garcia [2], the major disadvantages of using water in hydraulic systems are listed in Table 1.1

Table 1.1: *Disadvantages of water hydraulics [2].*

Disadvantages	Remedy
Oxidation and Rust	Use of rust resistant materials
Poor lubricity	Improve surface finish and design
Lower viscosity	Tighter tolerances
Bacterial growth	Used treated or deionized water
Particles contaminants present	Use 5μm or better filtration

These challenges have been undertaken by Danfoss and other companies and by researchers. Today, companies have water hydraulic components, systems and solutions on the market, and the number of products and the areas of application are increasing as illustrated in Fig. 1.1 and turnover in Fig. 1.2.

1.2 Research Objective

For conventional water hydraulics, a major research trend has been to find the way to improve control performance by using advanced control theory such as robust control [37], simple adaptive control [11, 38], or sliding mode control combined with a disturbance observer [39] to deal with nonlinearities in water hydraulics components, such as strong friction, considerable leakage, and dead zone characteristics. Another trend has been to improve the accuracy in the valves to raise the control performance [10, 40]. Dispite their obvious merit with regard to the control performance, servo motor systems (SMSs) retain inherent defects such as a low energy efficiency(even lower than oil hydraulics, which has an energy efficiency of 6%–40% depending on applications; and the average efficiency is only 21% [41, 42]) and prohibitive costs because of the complex structure and high technology to overcome the disadvantages of water hydraulics given above. Thus, conventional water hydraulic systems that use servo or proportional valves are only appropriate when very precise control is required; for the other applications, the main problem is finding methods to raise the energy efficiency and lessen the initial expenditure.

Figure 1.12 [4] shows the energy losses in servo systems in conventional case (a), using load sensing unloading valve (variable pressure system) (b), using pressure compensator (variable flow system) (c), and load sensing system (d). In the conventional system, the pressure after the fixed displacement pump is controlled by a relief valve. Its outputs of flow and pressure are in excess of the load requirements. Therefore surplus flow and pressure from hydraulic pump produce large losses. A variable pressure control can minimize the surplus pressure by an unloading valve and a fixed displacement pump can be use in this system. Variable flow control is defined as that it can adapt the pump supply flow to the load motion requirements precisely or rather it has no surplus flow into the system. It can save energy by minimizing the losses dependent on flow. This method requires a variable pump. Variable flow system cannot resolve the problem of pressure surplus and variable pressure system cannot resolve the problem of flow surplus. The load sensing system as shown in Fig. 1.12(d) may be the best choice to improve the system efficiency. The losses in load sensing system are only due to the losses across servo valve. Table 1.2 [4] shows the average energy efficiency of a crane in four cases. The load sensing system is very useful for raising the energy efficiency of servo system; however, the price of such system is very high and the structure is very complex. It is only suitable for using in conventional oil hydraulic system.

Lately, digital and switched fluid power has rapidly gained serious potential; the number of publications in this area has increased very quickly [43] because it only uses ON/OFF valves, which reduce the installation cost and energy consumption. This technology has three main issues: improving the operation of ON/OFF valves [44, 45], application to cylinder systems [46] to improve energy

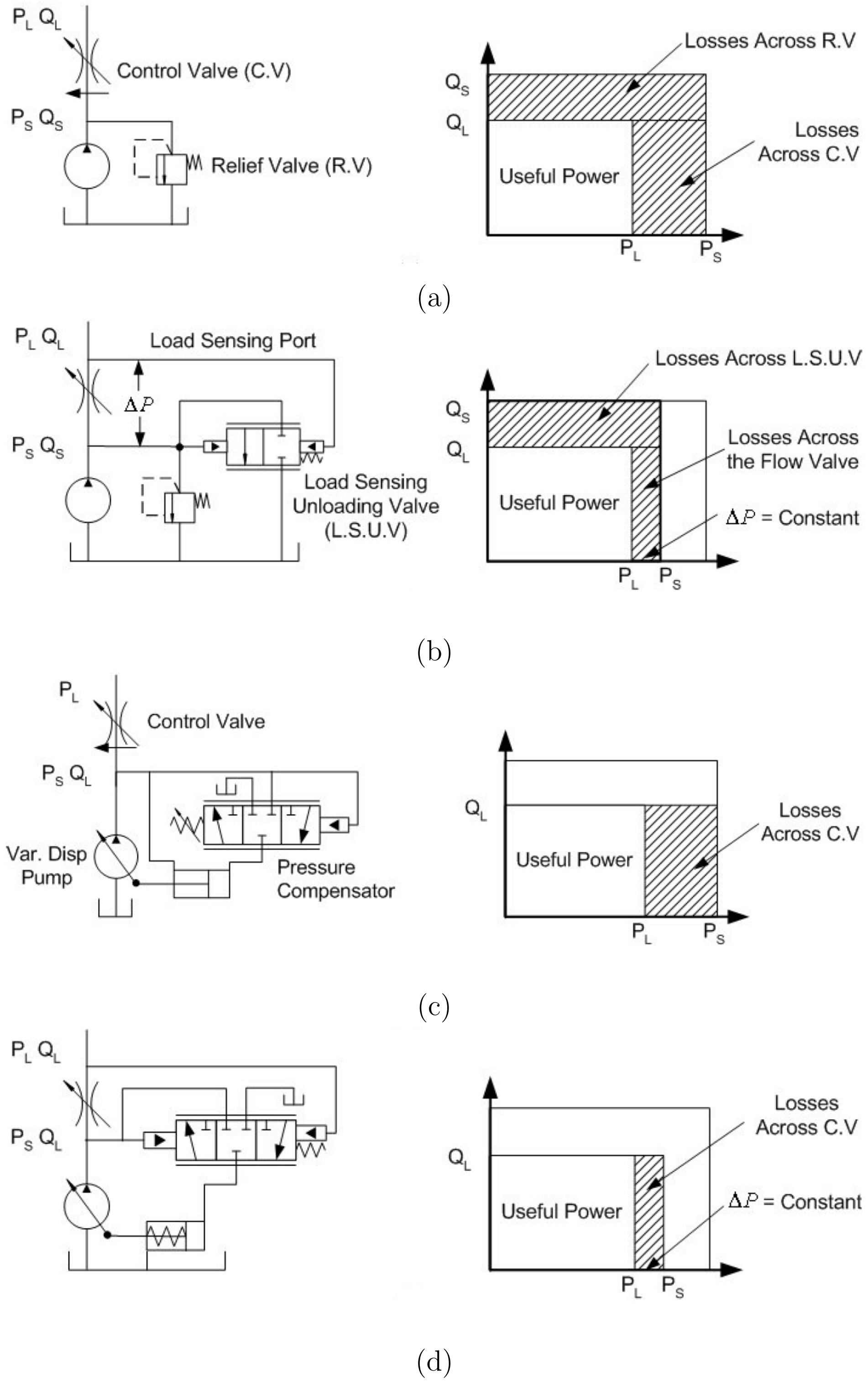

Figure 1.12: *Power losses of servo systems: (a) Conventional system, (b) Variable pressure system, (c) Variable flow system, and (d) Load sensing system [4].*

Table 1.2: *Overall average efficiency of valve-controlled hydraulic crane [4].*

Driving strategies	Conventional system (a)	Variable pressure system (b)	Variable flow system (c)	Load sensing system (d)
Efficiency	10.6%	27.4%	14.4%	35.6%

efficiency [47] or recover potential energy of a load in a vertical cylinder system [48], and analysis of hydraulic motor systems using digital hydraulic transmission such as oil hydraulic fluid switching transmission (FST) [49], water hydraulic FST [50, 51, 52], and pump motor transmission (PMT) [53, 54].

The FST system only uses ON/OFF valves to control the performance, which not only reduces the initial costs because these valves are much cheaper than servo or proportional valves but also increases the energy efficiency. The FST system can also recover the kinetic energy of the load in the deceleration phase into high-pressure fluid energy stored in an accumulator for reuse in the acceleration process of the next working cycle [50, 52]. These properties of the FST system are very important to its use in applications. However, the FST system possesses inherent limitations that need to be overcome. First, FST requires fast switching logic to control the velocity; thus, the ON/OFF valves switch many times under high-pressure fluid conditions, and the hydraulic motor changes the working and braking states for each switch. This causes an unbearable noise and shortens the service life of the hydraulic motor. Second, the velocity of the load needs to be controlled through the setting of a velocity threshold to make the velocity theoretically work within the prescribed bounds however, the steady-state error goes beyond these bounds because of the time delay of the devices. The main methods to reduce the error are using quick-response devices and restricting the velocity threshold [52]; the effectiveness of the restriction is limited depending on the characteristics of the ON/OFF valves, which means that the steady-state error inherently remains in the control logic. However, the steady-state error in the FST system does not change much when the reference velocity varies. Thus, the ratio between the steady-state error and the reference velocity tends to decrease with increasing reference velocity; therefore, the FST system is only appropriate for use in high-velocity systems.

To maintain the viability and reduce the limitations of the FST system, this paper introduces a novel water hydraulic transmission that directly connects a water hydraulic pump and motor and is called water hydraulic pump motor transmission. In the past, very few studies have considered directly connecting a hydraulic pump and actuator [55, 56]; researchers have only worked on controlling the displacement of a cylinder and the systems cannot recover energy in the deceleration phase. This paper presents a PMT system as an improvement over the FST system. It works more smoothly and reduces noise drastically because the ON/OFF valves only switch once in the entire cycle, which consists of acceleration, working (or constant), and deceleration phases. In addition, the service lives of the hydraulic motor and ON/OFF valves are lengthened because of the stable working pressure and fewer changes in state.

1.3 Outline of the Dissertation

This research is to analysis the velocity response and energy consumption of the two cheap water hydraulic FST and PMT systems and compare with a conventional servo motor system to show the advantages of the FST and PMT systems mainly in energy efficiency. This dissertation consists of following chapters.

Chapter 2 Water Hydraulic Fluid Switching Transmission: this chapter introduces the overview of FST system, the mathematical models of key devices, the control algorithms for the solenoid ON/OFF valves, and four methods to improve the energy efficiency. After that the experimental results for both velocity response and energy performance are shown and analyzed.

Chapter 3 Water Hydraulic Pump Motor Transmission: a novel transmission for water hydraulics is presented. In this chapter, the overview and control logic of the PMT system are discussed. And then, the performances for both velocity and energy are shown.

Chapter 4 Comparison among FST, PMT, and Servo Motor System: a conventional servo motor system was set up similarly to the FST and PMT system for comparing the velocity responses and energy performances of three systems to achieve the conclusions on the two cheap FST and PMT systems.

Chapter 5 Conclusions: summarizes and concludes on the obtained results.

Chapter 2

Water Hydraulic Fluid Switching Transmission

2.1 FST System

2.1.1 Overview of the FST System

In this section, a simple FST circuit used for experiments in this research will be introduced (Fig. 2.1). The system consisted of following main elements: a fixed displacement pump (P) connected to an electric motor (M), a fixed displacement pump/motor (PM), two accumulators (ACC$_i$, i = 1, 2), and three ON/OFF valves (VS$_i$, i=1, 2, 3). The two accumulators ACC$_1$ and ACC$_2$ were used as a pressure surge absorber and energy storage, respectively. The fluid energy with pressure p_s generated by the pump P was considered as the input energy and limited to 12 MPa in all experiments. The flywheel (FW) connected to the PM was was considered as a working load. Table A.1 presents the specifications of the main experimental devices.

The measurement devices of the FST system consisted of four pressure gauges to measure the supply pressure p_s, working pressure p_1, pressures in two ports of the PM p_2 and p_3, two flow meters to measure the supply flow rate Q_1 and recovered flow rate Q_2, and an encoder to measure the velocity of the FW. The signals out of the pressure gauges were voltage and sent to the dSPACE channel after amplifiers. The flow meters generated the outputs in currents and they

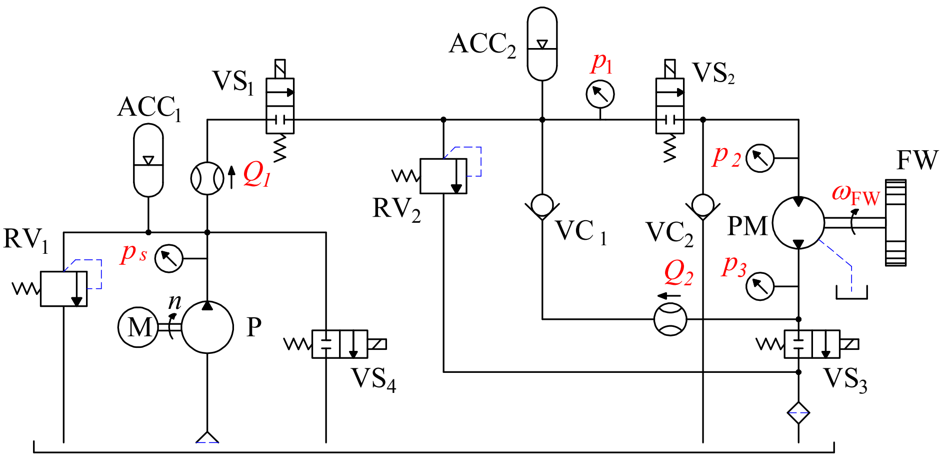

Figure 2.1: *Schematic of water hydraulic FST System.*

were changed to voltages after resistances and the voltage signals were sent to the dSPACE channels. The encoder generated the signal in frequency. On the feedback loop, a frequency voltage (FV) converter was applied and the voltage signal after the FV converter was sent to the dSPasce channel. The specification of the measurement devices are shown in Table A.2

To have visual look on the FST, PMT, and SMS, some imagines of experimental systems are shown in this section as well. Figure 2.2 shows the supply response, which consists of the electric motor M, hydraulic pump P, relief valve RV$_1$, pressure gauge p_s, ON/OFF valve VS$_4$, which acts as an unload valve, Accumulator ACC$_1$, and some other devices such as the reservoir and control box for the electric motor M. Figure 2.3 shows the valve control circuits of the all three systems. For the FST and PMT systems, the valve control circuits consist three ON/OFF valves and SMS uses servo valve to control the velocity response of the flywheel FW. The flywheel, encoder, and hydraulic pump/motor PM are shown in Fig. 2.4.

The goal was to control the flywheel velocity to meet the desired constant velocity during the working period. Drive pattern of the flywheel FW consisted of three phases: an acceleration phase (Phase 1), a working (or constant) phase (Phase 2), and a deceleration phase (Phase 3). In the acceleration phase, the ON/OFF valves are not controlled, they are opened to make water flow directly from the pump P to the pump/motor PM. After the desired constant velocity

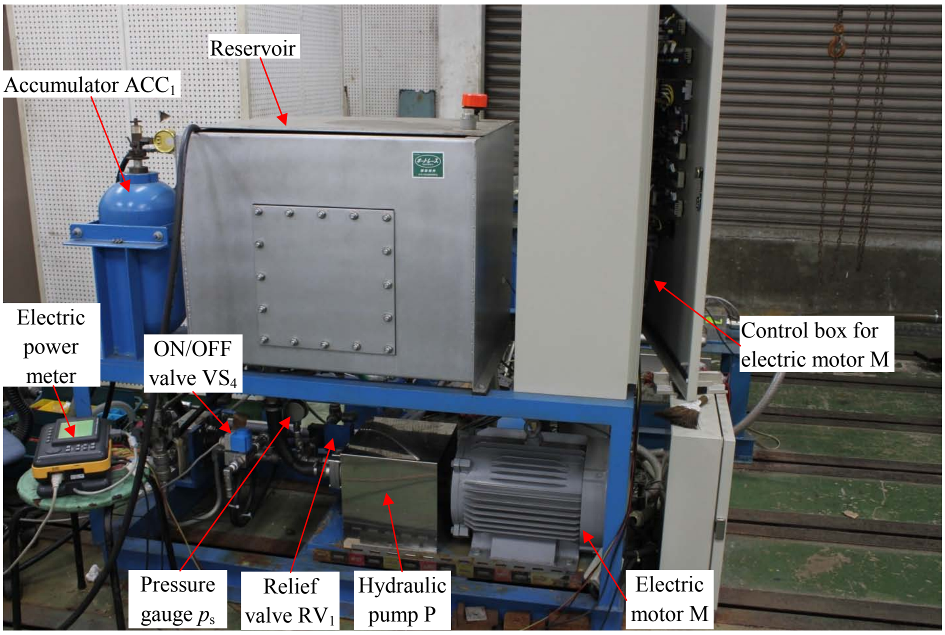

Figure 2.2: *Supply response.*

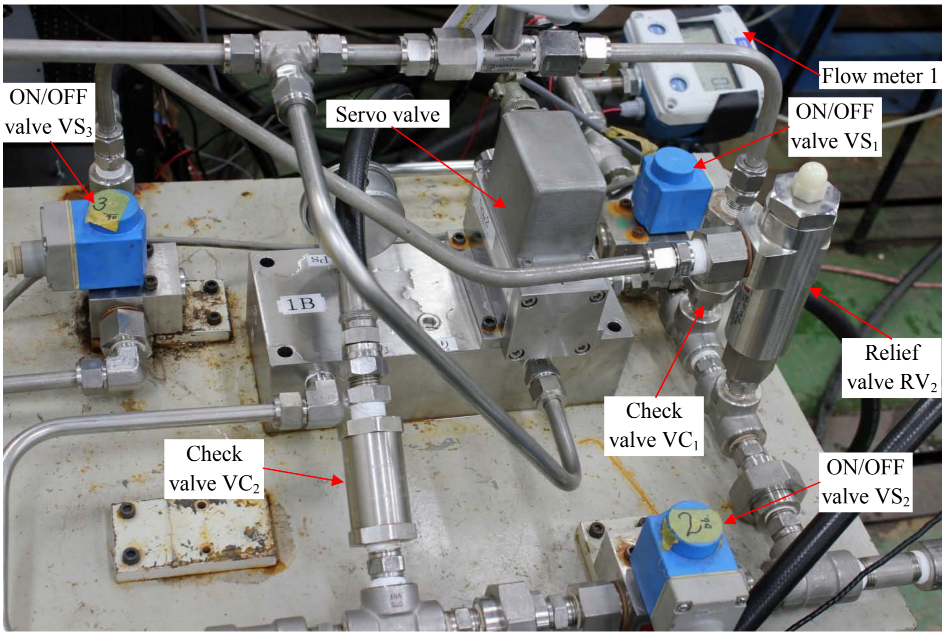

Figure 2.3: *Control valve circuit for all systems.*

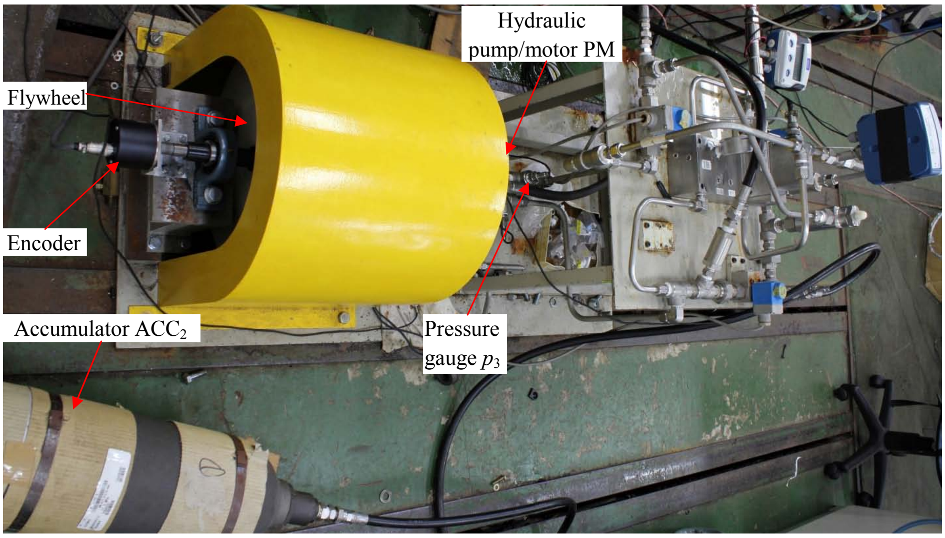

Figure 2.4: *Control valve circuit with load.*

is achieved, the state of the system changes to the working phase. At this time, the control logics for the ON/OFF valves are used to regulate the velocity of the flywheel around the constant value. When the working phase is completed, the system turns to the deceleration phase. All ON/OFF valves are in a closed state; however, the pump/motor PM still works because of the kinetic energy of the flywheel FW and it acts as a hydraulic pump to convert the kinetic energy into high-pressure fluid stored in the accumulator ACC_2. The pump/motor PM is supplied with water via the suction line that contains the check valve VC_2. This energy is one part of the recovered energy; more energy is recovered in the working phase when the velocity of the flywheel FW decreases.

2.1.2 Mathematical Model of Key Devices

The characteristics of all main devices of the FST system, which are pump, relief valves, accumulators, ON/OFF valves, pump/motor and flywheel, and velocity transducer, in order are introduced in this section. The devices are presented in constitution, operation, and characteristic parameters.

2.1.2.1 Hydraulic Pump

The simple model of an axial piston pump is shown in Fig. 2.5. Here, the pistons are arranged axially parallel to each other around the circumferential periphery of the cylinder block. The cam plate was fixed and the angle of the working surface and vertical direction is α. The pistons were connected with the shoe plate via piston shoes. When the cylinder block rotates, the position of the cylinder block and the cam plate interchanged; accordingly, the pistons are driven to and fro inside a number of bores in the cylinder barrel. Controlled by ball valves, the fluid is sucked in or pumped out, the flow rate of the pump at a given rotational speed remaining constant. However, the flow rate can vary if the speed of rotational of the prime mover is altered or the angle between the axis of the cam plate and the barrel is changed.

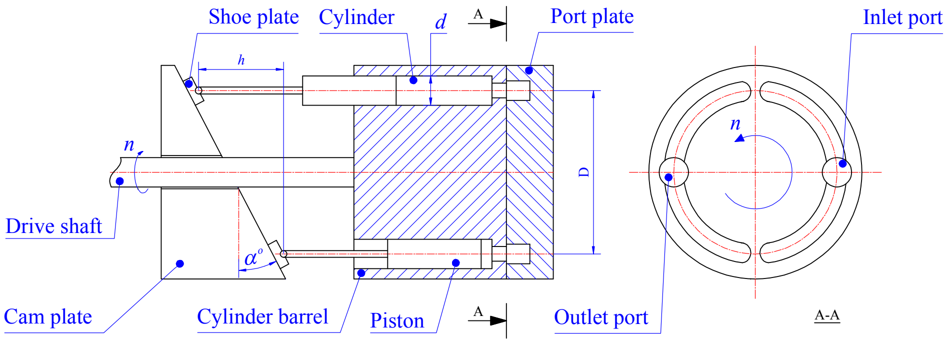

Figure 2.5: *Model of axial piston pump.*

Flow rate of the hydraulic pump can be calculated as following equation [5]:

$$Q_{\mathrm{P}} = \eta_{\mathrm{P}} Ahzn \tag{2.1}$$

where A is the area of piston bore and η_{P} is volumetric efficiency of the pump. Equation (2.1) can also be written as follows:

$$Q_{\mathrm{P}} = \frac{\pi d^2}{4}\eta hzn = \frac{\pi d^2}{4}\eta znD\tan\alpha \tag{2.2}$$

where

d: diameter of bore

h: stroke length of the piston, $h = D\tan\alpha$

z: number of cylinders

n: rotational velocity of driven shaft

D: diameter of the cycle of bore center

α: title angle

The pump was driven by an electric motor that can be changed the rotational velocity by changing frequency of the electrical power supply via a frequency converter. Rotational velocity of electric motor can be calculated by following equation [57].

$$n = 120\frac{f}{P} \tag{2.3}$$

where

n: rotational velocity of electric motor

f: frequency of electrical power supply

P: number of poles for which the stator is wound

In the experimental system, the SF-JR electric motor having 4 poles and Variable Frequency Freqrol-A500 that can be changed the frequency from 0.2 to 400 Hz were used. Base on the Eq. 2.3, the rotational velocity of pump can be changed from 4 to 12000 min^{-1}.

2.1.2.2 Relief Valve

A pressure relief valve is a normally closed valve connected between the pressure line and the reservoir. Its main purpose is to limit the pressure in a system to a prescribed maximum by diverting some or all of the pump output to the tank, when the designed pressure is reached [5]. In the FST system, two pressure relief valves were assembled. The first relief valve (RV_1) is to limit the pressure P_s in the discharge side of the pump (P) at 12MPa that acts as supply pressure and the remaining relief valve (RV_2) is to limit the pressure P_1 in the line after ON/OFF valve VS_1, because pressure P_1 can be reached over design pressure when the pump/motor acts as a pump.

A simple relief valve may consist of nothing but a ball or poppet held seated in the valve body by the compressive force of a heavy spring. When the pressure at the inlet is insufficient to overcome the force of the spring the valve remains closed and hence it is very often referred as a normally closed valve. When the preset pressure is reached, the ball unseats and allows flow through outlet to tank. In most of these valves, an adjusting screw is provided to vary the spring force. Thus the valve can be set to open at any pressure within the specified range. The pressure at which the valve first opens is called the cracking pressure. As the flow through the valve increases, the poppet is forced further, the resulting pressure increasing considerably thereby. The difference between the full flow pressure and the initial pressure may sometime be objectionable to other system elements. In certain cases it can result in a considerable amount of wasted power due to the fluid lost through the valve before its maximum setting is reached [5]. Figure 2.6 shows a simple sketch of a pressure relief valve.

In the FST system, Nessie pressure relief valve type VRH60 which has maximum flow rate of 60 l/min is used as relief valve RV_2. The P/Q characteristics of the valve shows in Fig. 2.7 [Danfoss Catalog] with three pressure setting ranges 10 to 40 bar, 25 to 80 bar, and alt. 80 to 140 bar. The cracking pressure of the valve was set up at 14 MPa; therefore, the P/Q characteristic of the valve corresponds to the pressure setting range 10 to 40 bar. Based on the characteristics of the relief valve type VRH60, the logic chart of the relief valve can be simplified in Fig. 2.8 with cracking pressure P_{cr} of 14 MPa, full flow pressure P_{ff} of 19 MPa, and maximum flow rate Q_{max} of 70 l/min.

2.1.2.3 Accumulator

The main function of a hydraulic accumulator is to store hydraulic energy and on demand make the energy available again to the system. In the FST system, two bladder type accumulators were used. A bladder type accumulator consists of a synthetic polymer rubber bladder inside a metal (steel) shell. The bladder is filled with compressed inert gas. A poppet valve located at the discharge port closes the port when the accumulator is completely discharged. The advantage of a bladder type accumulator is that it responds quickly for receiving or expelling

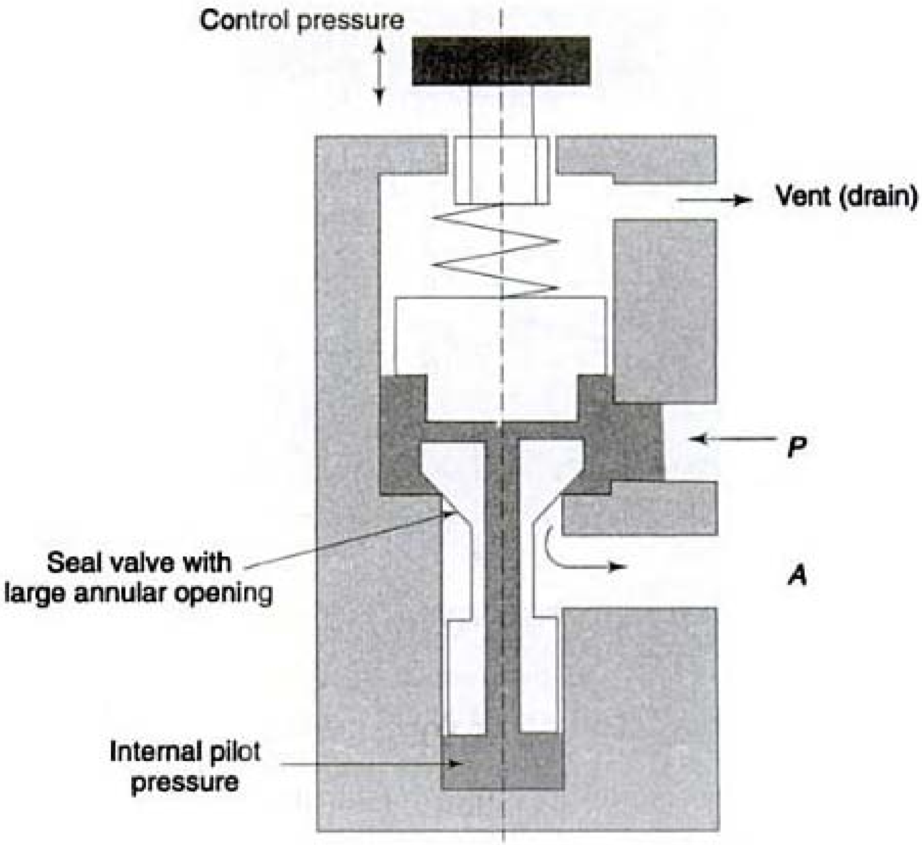

Figure 2.6: *Model of relief valve [5].*

flow of fluid. But major disadvantage is that possibility of bladder failure which is to be taken into consideration [5]. Figure 2.9 shows the component of a bladder type accumulator.

The two accumulators with different functions are used in the system, the fist one ACC_1 contributed as a pressure surge absorber and the other one ACC_2 is to store the recovery energy in the pressure energy that is converted from the kinetic energy of the flywheel mainly in the deceleration phase (Phase 3).

The accumulators in experiments were the bladder type. Thus, the mathematical model of a bladder type accumulator in [58] and [59] was used in this study.

The first law of thermodynamics is applied to obtain the energy balance for the gas in an accumulator

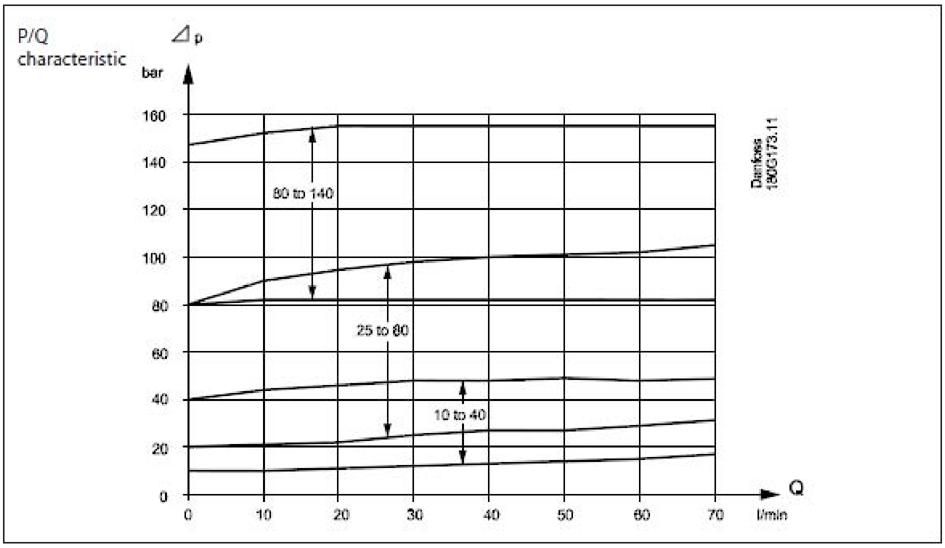

Figure 2.7: *P/Q characteristics of Nessie pressure relief valve type VRH60.*

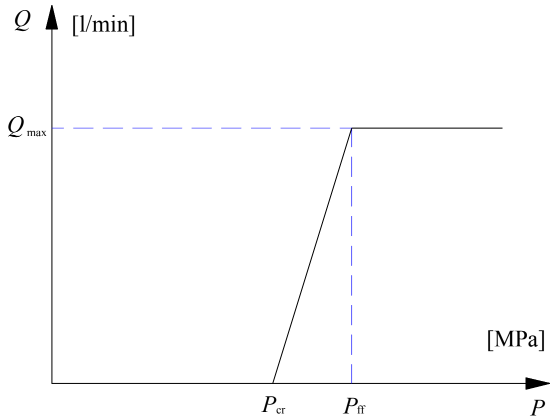

Figure 2.8: *Modeling of P/Q characteristic of relief valve.*

$$m\frac{du}{dt} = \frac{dQ_h}{dt} - \frac{dW}{dt} \tag{2.4}$$

where m is the mass of the gas, u the internal energy per unit mass, Q the heat energy transferring into the accumulator, and W the external work of the accumulator.

Based on Newton's second law of cooling, the heat transfer into the gas can

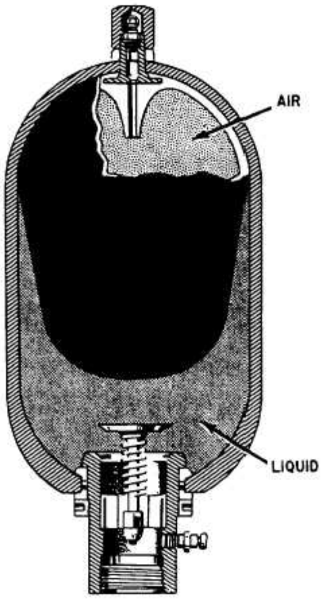

Figure 2.9: *Component of a bladder type accumulator.*

be calculated as follows

$$\frac{dQ}{dt} = hA(T_w - T_g) \tag{2.5}$$

where h is the transfer coefficient, A the heat transfer area, T_g the temperature of the gas, and T_w the temperature of the accumulator wall. Furthermore, in fact, the accumulators were filled with water inside so that it is necessary to consider the temperature of the water. That means the temperature of the water in the accumulators is assumed to be constant and equal to the temperature of the wall.

Moreover, the external work W can be determined by following equation

$$\frac{dW}{dt} = p_g \frac{dV_g}{dt} \tag{2.6}$$

where p_g is the pressure of the internal gas and V_g the volume of the internal gas.

The relationship between the internal energy, the temperature and the volume of the internal gas can be expressed [58]:

$$\frac{du}{dt} = C_v \frac{dT_g}{dt} + \frac{1}{m} \left\{ T_g \left(\frac{\partial p_g}{\partial T_g} \right) - p_g \right\} \frac{dV_g}{dt} \tag{2.7}$$

where C_v is the specific heat at constant volume of the internal gas.

From Eqs. (2.4), (2.5), (2.6), and (2.7), the following expression is derived

$$\frac{dT_g}{dt} = \frac{T_w - T_g}{\tau} - \frac{T_g}{mC_v}\left(\frac{\partial p_g}{\partial T_g}\right)\frac{dV_g}{dt} \tag{2.8}$$

where τ is the thermal time constant of the accumulators and can be defined by following equation

$$\tau = \frac{mC_v}{hA} \tag{2.9}$$

Consider the internal gas of the accumulators as ideal gas; the equation of state of ideal gas will be applied to the internal gas as follows

$$p_g V_g = mRT_g \tag{2.10}$$

where R is the ideal gas constant. Equations (2.8) and (2.10) can be written down by using dimensionless quantities as follows:

$$\frac{dT_g^*}{dt^*} = \frac{1 - T_g^*}{\tau^*} - K_0 \frac{T_g^*}{V_g^*}\frac{dV_g^*}{dt^*} \tag{2.11}$$

$$p_g^* V_g^* = T_g^* \tag{2.12}$$

where $K_0 = R/C_v$, $T_g^* = T_g/T_w$, $V_g^* = V_g/V_0$, $p_g^* = p_g/p_0$, $T_g^* = T_g/T_w$, $t^* = t/\tau_a$, and $\tau^* = \tau/\tau_a$; p_0 is the precharge pressure and τ_a the thermal time constant when all the gas was released.

Moreover, the relationship between τ^* and V_g^* can be expressed by following equation [58]

$$\tau^* = V_g^* + 0.1 \tag{2.13}$$

2.1.2.4 Solenoid ON/OFF Valve

An ON/OFF valve or a solenoid valve is an electromechanical valve controlled by an electric current through a solenoid. Principle of operation of a solenoid valve can be introduced in Fig. 2.10. The main sections of an ON/OFF valve are solenoid, diaphragm or poppet, pressure chamber, pressure relief conduit, input and output port. When solenoid is at rest, it means no electric supplies to the solenoid, valve closes. When solenoid is active, it means electric supplies to the solenoid, fluid from pressure chamber flows through pressure relief conduit to make pressure in output port up; and then the pressure can open the diaphragm or poppet, that is the full open situation of solenoid valve.

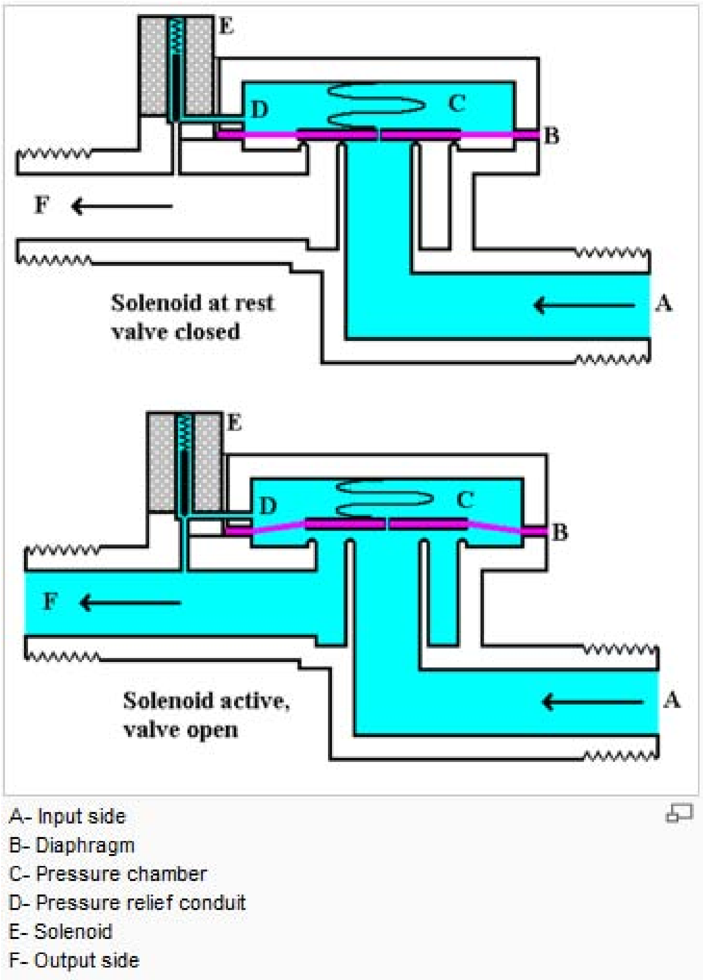

Figure 2.10: *Operation of ON/OFF Valve.*

In the FST system, three ON/OFF valves type VDHT1/2E2/2NC manufactured by Danfoss corporation were assembled. The component of ON/OFF valves is shown in Fig. 2.11 [Danfoss Catalog]. The valves were controlled by 24 voltage electric supply. Maximum flow rate through the solenoid valves are 60 l/min at the pressure of 14 MPa.

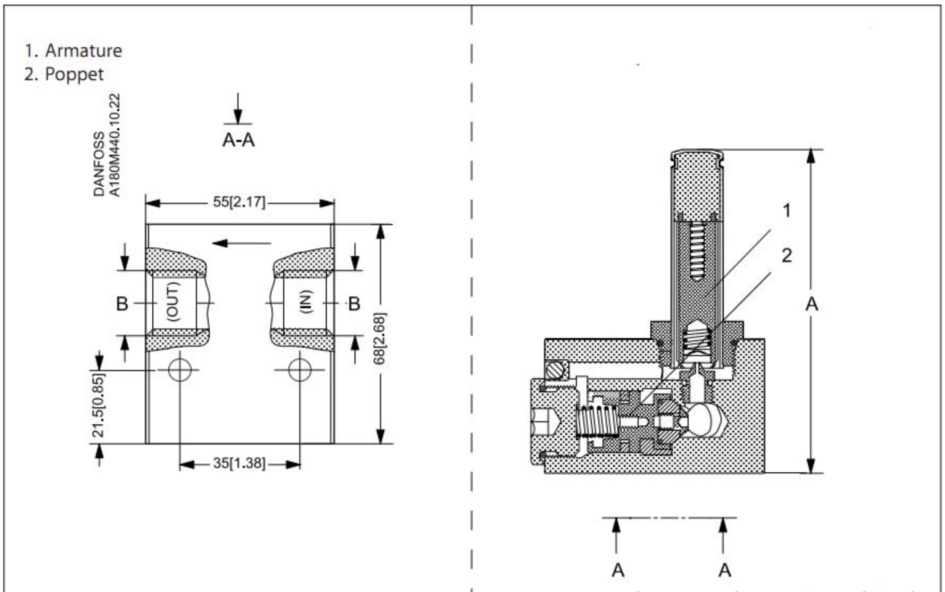

	A	B
VDHT 3/8	NO: 112 [4.41] NC: 102 [4.02]	3/8"
VDHT 1/2	NO: 112 [4.41] NC: 102 [4.02]	1/2"

Figure 2.11: *Component of ON/OFF Valve.*

Flow rate through the ON/OFF valves are calculated based on the orifice equation for turbulent flow. Orifices are sudden restrictions of short length (ideally zero length for a sharp-edged orifice) in the flow passage and may have a fixed or variable area [60]. Figure 2.12 shows turbulent flow through an orifice. Flow rate through an orifice depends on cross sectional area of the orifice and difference of pressures in the two sides of orifice. Borrow from [61], flow rate through an orifice can be calculated as follows:

$$Q_{\text{Orifice}} = \alpha_d A_0 \sqrt{\frac{2}{\rho} \Delta P_{\text{Orifice}}} \tag{2.14}$$

where

α_d: discharge coefficient. Theoretically, $\alpha_d = \frac{\pi}{\pi+2} = 0.611$

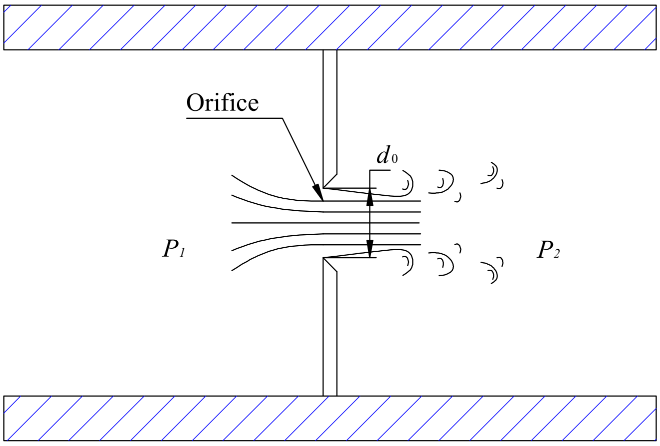

Figure 2.12: *Turbulent flow through an orifice.*

A_0: cross sectional area of orifice, $A_0 = \frac{\pi d_0^2}{4}$

ρ: fluid density

d_0: diameter of orifice

$\Delta P_{\text{Orifice}}$: difference of pressures in the two sides of orifice

Based on equation of flow through orifice, flow rate through ON/OFF valve can be calculated as Eq. (2.15)

$$Q_{\text{ON/OFF}} = \alpha_d A_{\text{ON/OFF}} \sqrt{\frac{2}{\rho} \Delta P_{\text{ON/OFF}}} \tag{2.15}$$

where

$A_{\text{ON/OFF}}$: cross sectional area of poppet inside ON/OFF valve

$\Delta P_{\text{ON/OFF}}$: pressures difference of input/output ports of ON/OFF valve

However, it takes finite time from close state to full open state corresponding with opening area increasing from zero to maximum $A_{\max}$. To simplify, it is assumed that the increasing of opening area obeys the first order equation as follows

$$A_{\text{ON/OFF}} = \frac{A_{\max}}{Ts + 1} \tag{2.16}$$

where

A_{max}: opening area at the full open state

T: time constant that was defined base on the real opening time of the valves

As shown in Fig. 2.13 - the characteristic of the opening area of ON/OFF valve, there are time lags for opening and closing processes, t_{open} and t_{close}, respectively. For simplification, they were approximated as the step response of a first-order system. In this research, coefficient ε will be introduced, and set up at the value of 0.02 in the opening process. That means, when the opening area got 98% of the maximum opening area, the valve was changed to the full open state directly; inversely, in the closing process, when the opening area got 2% of the maximum opening area, the valve was changed to the full close state directly. In the simulation circuit, the time lags for both the opening and closing processes were estimated from test data as shown in section 5 and had values of 40 ms and 100 ms, respectively.

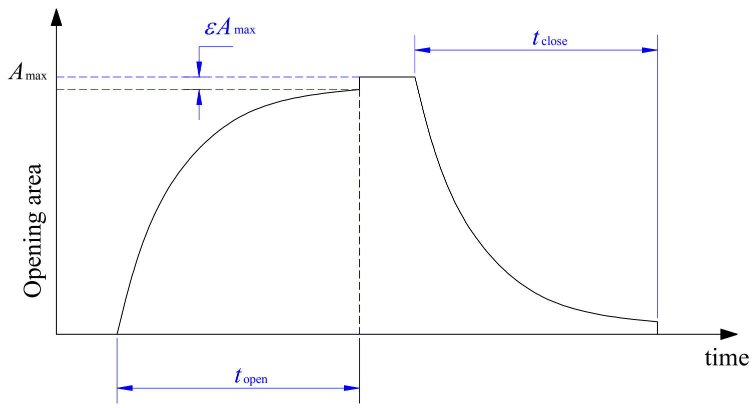

Figure 2.13: *Modeling of opening area of ON/OFF Valve.*

2.1.2.5 Hydraulic Pump/motor

Hydraulic motors closely resemble hydraulic pumps in construction and size. The only difference is that instead of pushing the fluid as the pump does, in a hydraulic motor the rotating elements are pushed by the fluid pressure to enable the motor shaft to rotate and thus develop the necessary turning torque and continuous rotation motion [5].

In this FST system, a pump/motor acted as pump or motor, depends on the situation. When high pressure fluid was supplied according to acceleration process, it acts as a motor and when no supply fluid and flywheel at high speed, it acts as a pump converting the kinetic energy of flywheel to energy as high pressure water stored into the accumulator ACC_2.

Newton's second law is applied to obtain the torque balance equation for the motor [60]

$$I_{\mathrm{PM}}\ddot{\varphi} + T_f = \frac{1}{\eta_{\mathrm{PM}}} T_{\mathrm{PM,th}} - T_{\mathrm{PM,L}} \tag{2.17}$$

where

I_{PM}: moment of inertia of the hydraulic pump/motor
φ: angular of the hydraulic pump/motor shaft
$T_{\mathrm{PM,L}}$: load torque of the hydraulic pump/motor, $T_{\mathrm{PM,L}} = I_{\mathrm{FW}}\ddot{\varphi}$
η_{PM}: volumetric efficiency of the hydraulic pump/motor

The friction torque can be modeled as [60]

$$T_f = T_v\dot{\varphi} + \operatorname{sign}(\dot{\varphi})\left[T_{c0} + T_{s0}\exp\left(-\frac{|\dot{\varphi}|}{c_s}\right)\right] \tag{2.18}$$

where T_v, T_{c0}, T_{s0}, c_s are coefficient of friction.

Displacement volume of hydraulic motor can be defined in the same way as hydraulic pump [60].

$$V_{\mathrm{PM,th}} = \frac{\pi d^2}{4} zD\tan\alpha \tag{2.19}$$

The effective displacement can be calculated using the estimated overall (volumetric and mechanical) efficiency η_{PM} [60]:

$$V_{\mathrm{PM,eff}} = \frac{1}{\eta_{\mathrm{PM}}} V_{\mathrm{PM,th}} \tag{2.20}$$

The theoretical torque is approximated by [60]

$$T_{\mathrm{PM,th}} = \frac{V_{\mathrm{PM,th}}}{2\pi}\Delta P_{\mathrm{HL}} \tag{2.21}$$

where ΔP_{HL} is the pressure difference between the high-pressure line and low-pressure line.

Moreover, the pump/motor flow is determined by

$$Q_{\mathrm{PM}} = \eta_{\mathrm{PM}} \frac{V_{\mathrm{PM,th}}}{2\pi} \ddot{\varphi} \tag{2.22}$$

2.2 Valve Control

As mentioned above, the drive pattern of flywheel shown in Fig. 2.14 (a) consists of three phases: acceleration phase (Phase 1), constant phase (Phase 2), and deceleration phase (Phase 3). The total time for acceleration phase and working phase is t_w depending on experiments. This section introduces the logic depending on the flywheel drive pattern and reference velocity of the flywheel to control the ON/OFF valves (Fig. 2.14 (b) and (c)). The valve VS_1 is opened in both Phase 1 and Phase 2, and only closed in Phase 3. The two valves VS_2 and VS_3 received the same control signal depending on flywheel rotational velocity ω_{FW}. In order to compare the results for the FST system with/without energy recovery, the valve VS_3 was opened during full cycle in without energy recovery case. In following section, the valve switching algorithms corresponding to three phases will be introduced.

2.2.1 Acceleration Phase (Phase 1)

In this phase, the FST accelerates the flywheel FW from the stationary state to a given reference rotational velocity. Once the reference is reached, the control logic switches to Phase 2. The ON/OFF valves are not controlled; they are fully opened to make water flow directly from the pump P to the pump/motor PM. The electric motor M is operated at a velocity of 1200 min^{-1} in Phase 1.

2.2.2 Constant (Working) Phase (Phase 2)

The rotational velocity of the flywheel FW between the prescribed limit ω_{open} and ω_{close} is maintained via control logics, as shown in Fig. 2.14 (b). Table 2.1 presents the control logics of the three ON/OFF valves. In the control logic, when the

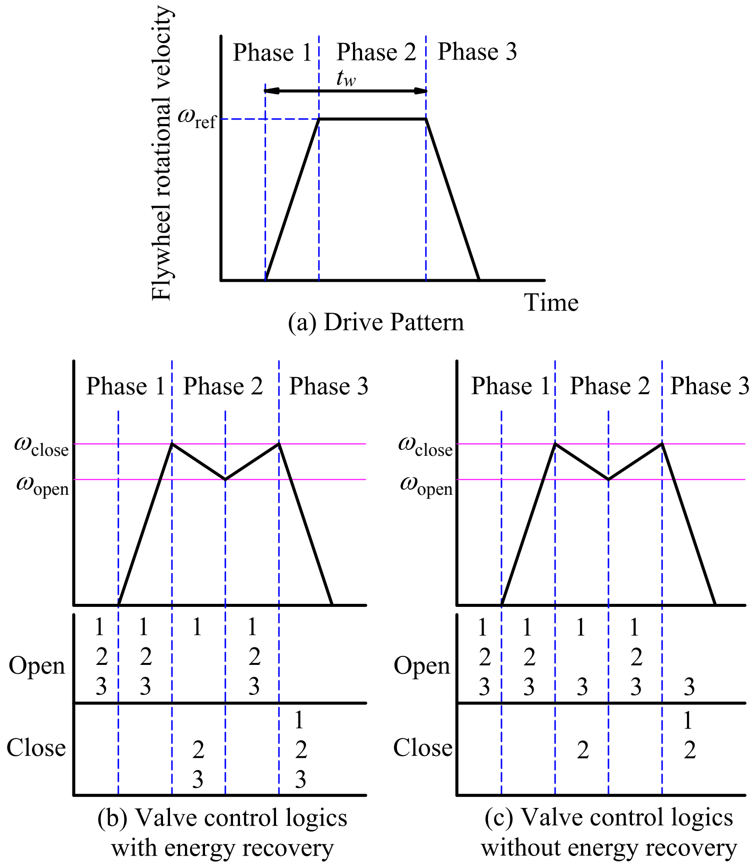

Figure 2.14: *Control logic of ON/OFF valves.*

Table 2.1: *Valve operation logic in Phase 2.*

Valve	Open	Close
VS_1	Open	
VS_2	$\omega_{FW} < 795\ \mathrm{min}^{-1}$	$\omega_{FW} > 805\ \mathrm{min}^{-1}$
VS_3	$\omega_{FW} < 795\ \mathrm{min}^{-1}$	$\omega_{FW} > 805\ \mathrm{min}^{-1}$

velocity of the flywheel exceeds ω_{close}, both of the ON/OFF valves VS_2 and VS_3 are closed to brake the flywheel. Conversely, when the velocity becomes less than ω_{open}, the both ON/OFF valves are opened to supply energy to the hydraulic motor M. By this control logic, the velocity of the flywheel will theoretically oscillates inside the bounds ω_{open} and ω_{close}; however, the steady-state error is larger in practice because of the effect of the time delay of the experimental devices.

2.2.3 Deceleration Phase (Phase 3)

The speed of the flywheel FW decelerates to zero and not that in this phase, no velocity control is performed, all the ON/OFF valves are closed. The ON/OFF valve VS_3 is closed to brake the flywheel and induce the energy recovery process. The ON/OFF valve VS_1 is closed to cut the supplied energy. The ON/OFF valve VS_2 is closed to keep the recovered energy inside the accumulator ACC_2.

2.3 Energy Efficiency Improvement

This section introduces the original FST system,which only uses the constant velocity of the electric motor M, and the methods to reduce the energy consumption of this system.

2.3.1 *Case 1*: Original FST System

In the original FST system, there is no control for the electric motor M and its velocity is maintained at a constant value during all phases. The velocity of electric motor M was chosen to ensure that the system completes a full cycle at a maximum reference velocity of 1000 min^{-1}. Thus, the velocity of the electric motor M was established at 1200 min^{-1} for all phases. This velocity was chosen at a high value to compensate for the energy loss, which is quite difficult to determine precisely.

2.3.2 *Case 2*: Reduced Velocity in the Electric Motor

Based on the working characteristic of a cycle, Phase 1 requires the most energy to accelerate the velocity of the flywheel FW from stationary to reference velocity, Phase 2 requires less energy to maintain the flywheel velocity at the reference value, and Phase 3 requires no energy. The velocity of the electric motor M was set at 1200 min^{-1} for the acceleration phase and 600 min^{-1} for the working phase. These values were determined to ensure that the system would complete the full cycle for all reference velocities, particularly for the highest reference velocity of 1000 min^{-1}, which requires the most supplied energy, and would stop in the deceleration phase.

2.3.3 *Case 3*: Use of Unload Valve

The velocity of the electric motor was selected to maintain the same values for all reference velocities and established at a high value for addressing energy loss and opening the range of reference velocity. Thus, supplied energy to the system is normally higher than the requirement; one fraction is lost via relief valves and another is stored in the accumulator ACC_1 and dissipated after the cycle. Thus, using the unload valve method to limit the pressure $p_{1.3}$ in a prescribed range for all working periods is one method to reduce the energy consumption of the system. Another ON/OFF valve (VS_4) was used to reduce supply pressure, $p_{s.3}$, acting as the load of supply response based on pressure $p_{1.3}$. The control logic of ON/OFF valves VS_1 and VS_4 is listed in Table 2.2. In this research, the bounds of the pressure $p_{1.3}$ are 8.5 and 9 MPa for $p_{1\text{open}}$ and $p_{1\text{close}}$, respectively.

Table 2.2: *Valve operation logic in Phase 2.*

Valve	Open	Close
VS_1	$p_{1.3} < p_{1\text{open}}$	$p_{1.3} \geq p_{1\text{close}}$
VS_4	$p_{1.3} > p_{1\text{close}}$	$p_{1.3} \leq p_{1\text{open}}$

2.3.4 *Case 4*: Use of Idling Stop Method

As in the unload valve method presented above, the idling stop method is based on the pressure $p_{1.4}$ to turn the electric motor M on or off. The control logic for ON/OFF valve VS_1 and electric motor M are listed in Table 2.3. The bounds of the pressure $p_{1.4}$ were also chosen at values of 8.5 and 9 MPa for $p_{1\text{start}}$ and $p_{1\text{stop}}$, respectively. The bounds of the pressure $p_{1.4}$ were chosen as above to ensure that the system was supplied minimal but sufficient energy to complete a full cycle. To ensure the homogeny for easier comparison, the same values as the bounds of the pressure $p_{1.3}$ in *Case 3* were chosen; however, slightly smaller values can also be used.

Table 2.3: *Valve operation logic in Phase 2.*

Valve (Electric motor)	Open (Start)	Close (Stop)
VS_1	$p_{1.4} \leq p_{1\text{start}}$	$p_{1.4} > p_{1\text{stop}}$
M	$p_{1.4} < p_{1\text{start}}$	$p_{1.4} \geq p_{1\text{stop}}$

2.4 Velocity Response

2.4.1 Experimental Results

Table 2.4 shows the results on control performances of the rotational velocity of the flywheel for the reference velocity of 600-1000 min^{-1}. The rotational velocity percentage errors e_{max} and e_{min} in Phase 2 defined in Eqs. (2.23) and (2.24) decreased when the reference velocity ω_{ref} was up and did not exceeding 2.4% at the velocity of 1000 min^{-1}. In case that the reference velocity of the flywheel is 800 min^{-1}, the experimental results of the rotational velocity ω_{FW} and the flow rate q_2 to the accumulator ACC_2 as energy recovery are shown in Figs.2.15 and 2.16, respectively.

$$e_{\text{min}} = \frac{\omega_{\text{ref}} - \omega_{\text{min}}}{\omega_{\text{ref}}} \tag{2.23}$$

$$e_{\max} = \frac{\omega_{\max} - \omega_{\mathrm{ref}}}{\omega_{\mathrm{ref}}} \tag{2.24}$$

Table 2.4: *Control performance of rotational velocity.*

Reference rotational velocity [min^{-1}]	$\omega_{\min}$ [min^{-1}]	$\omega_{\max}$ [%]	$e_{\min}$ [%]	$e_{\max}$
1000	983	1024	1.70	2.40
900	882	923	2.00	2.56
800	783	823	2.13	2.88
700	681	725	2.71	3.57
600	580	625	3.33	4.17

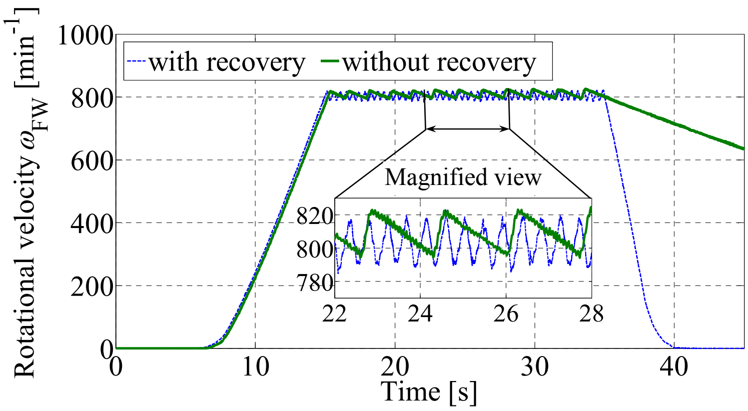

Figure 2.15: *Experimental results of flywheel velocity (ω_{ref} = 800 min^{-1}).*

Furthermore, Fig.2.15 shows the velocity of the flywheel with/without recovery corresponding to the flywheel reference velocity of 800 min^{-1}. With energy recovery process, the two ON/OFF valves VS_2 and VS_3 received the same control signal during Phase 2 to maintain the flywheel velocity around the reference velocity. When the velocity reached to the upper limit, the two valves were switched to close and the pump/motor PM acted as a pump. Consequently, the pressure p_2 in the suction line of this pump/motor became lower. At the same time, because of the closing of the ON/OFF valve VS_3, the pressure p_3 in

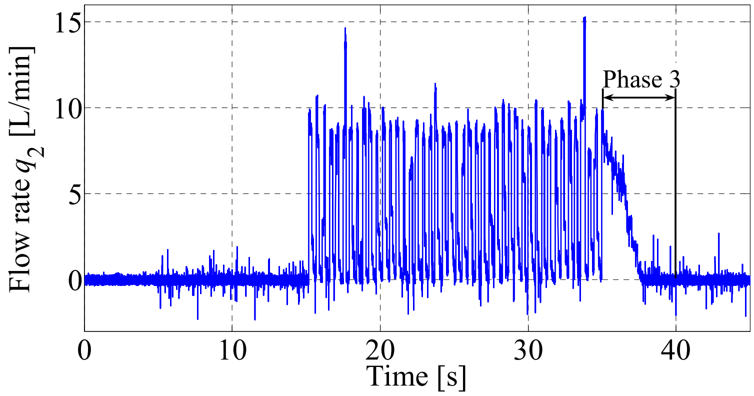

Figure 2.16: *Experimental result of flow rate* q_2 (ω_{ref} = *800* min^{-1}).

the discharge side of pump rose. Therefore, the big pressure difference made the flywheel velocity down rapidly. Conversely, whenever the rotational velocity of the flywheel decreased to the lower limit, the two valves were switched to open, and then the pump/motor acted as a motor.

The energy recovering was only realized in Phase 3. In case with energy recovery, all ON/OFF valves were closed during this phase. The pressure p_3 became higher because the pump/motor acted as a pump. The high pressure water was stored in the accumulator ACC_2 as the recovered energy after flowing through the check valve CV_1 and the recovered energy would be used as another driving source for next operation cycle. Figure 2.16 shows the flow rate q_2 to ACC_2 corresponding to the reference velocity of 800 min^{-1}.

Beside, in case with no energy recovery, the control algorithms of the two ON/OFF valves VS_1 and VS_2 were the same as with energy recovery. However, the valve VS_3 was opened during the full cycle. The rotational velocity of the flywheel in this case is shown in Fig. 2.15. The main deference between the rotational velocities of the flywheel with/without energy recovery was in the deceleration period when the valve VS_2 was closed and the valve VS_3 was opened. The load was decelerated only because of the pump loss and the friction loss, this made slower deceleration. Hence, in Phase 2, the rotational velocity error ratio in the velocity deceleration period was less than in the acceleration one. Likewise, in Phase 3, it took longer time to decelerate the flywheel velocity to zero. When the system is applied in real, mechanical brakes are required to make the deceleration process rapider; this implies that all of the kinetic energy of load will be dissipated in heat and/or acoustic energy.

2.4.2 Comparison of Simulated and Experimental Results

In this subsection, the comparison of the velocity errors and the energy recovery efficiency in the simulations and the experiments will be introduced. Figure 2.17 shows the experimental and simulated results of the flywheel velocity at the flywheel reference velocity of 800 min^{-1}. For more detail, Table 2.5 will show the velocity percentage errors e_{max} and e_{min} in the simulations and the experiments.

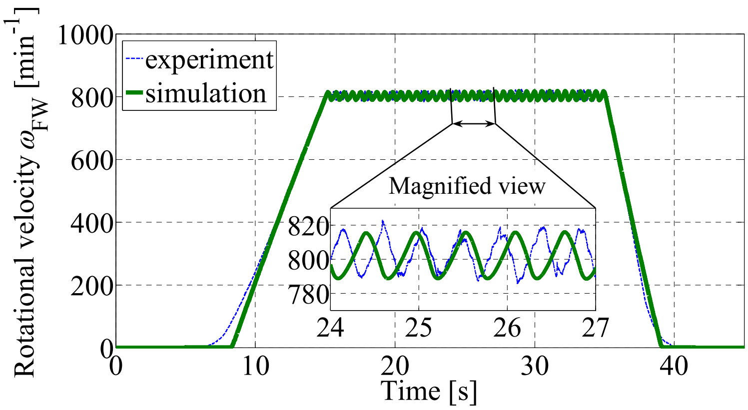

Figure 2.17: *Experimental and simulated results of flywheel velocity (ω_{ref} = 800 min^{-1}).*

Table 2.5: *Control performance of rotational velocity.*

	ω_{min} [min^{-1}]	ω_{max} [min^{-1}]	e_{min} [%]	e_{max} [%]
Experiment	783	823	2.13	2.88
Simulation	785	820	1.88	2.5

From Fig. 2.17 and Tables 2.5, it can be said that the experimental and simulated results were showed good agreement for the flywheel reference velocity of 800 min^{-1}. Even when the reference velocity was changed from

600–1000 min^{-1}, the experimental results were still similar to the simulated results. Therefore, it is concluded that the developed simulator has been built successfully. That makes an easy way to define the effect of each component to the full system, so that the system can be renewed or developed more simply.

2.4.3 Analysis of Velocity Control Performance

One of the most important requirements of the system is to reduce the rotational velocity error of flywheel in the working phase (Phase 2). In this subsection, the factors which affected to the velocity error will be pointed out and methods that made the velocity error attenuate will be discussed.

Figure 2.18 shows the control signal of the two ON/OFF valves SV_2, SV_3, the pressure p_2, and the flywheel rotational velocity ω_{FW} in the event when upper and lower limits are 805 min^{-1} and 795 min^{-1}, respectively. From this figure, the characteristics of the ON/OFF valves are estimated as follows: the opening time is approximately 40 ms, corresponding to the decreasing of 6 min^{-1}, and the maximum closing time is approximately 100 ms to the increasing of 14 min^{-1}. These are inherently based on the characteristics of the ON/OFF valves; the hold time which avoids frequent switching signal is introduced in the valve control algorithms. At least during this hold time, each valve keeps its state. For all of three valves of the FST system, the hold time of 0.12 s was applied in the control logic. Note that, before the control signals were sent to the ON/OFF valves, they were magnified via the solid state relay (SSR) devices from 5 V to 24 V. However, the time lags in the SSRs are not so big, they are only 0.5 ms and 2 ms for the opening and closing signals, respectively.

The two values of the upper and lower limit of the flywheel velocity also have effects on the velocity error. The two values should be chosen to guarantee that the valve open/close commands are kept more than the hold time.

The last factor which affects the velocity error is the conversion time of velocity transducer. In this research, the system adopted a high response velocity transducer with the conversion time of approximately 7.6 μs. The effect of the conversion time is introduced in the following subsection.

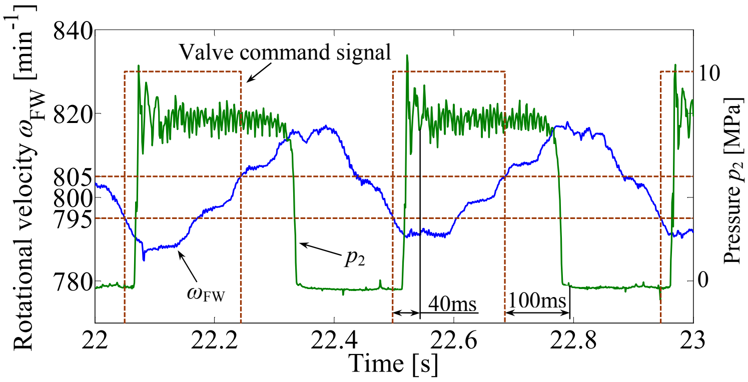

Figure 2.18: *Pressure p_2 response in experiment.*

2.4.3.1 Conversion Time of Velocity Transducer

To determine the effect of the conversion time on the flywheel rotational velocity error, this study compares the results of two transducers. The first one has time constant of 63 ms, which corresponding with conversion time of 300 ms. The second device has much quick response with the conversion time of 7.6 μs.

Tables 2.6 and 2.7 show the velocity errors for the reference velocity 600–1000 min^{-1} with the conversion time values of 300 ms and 7.6 μs, respectively. In both cases, the upper limit velocity ω_{close} is 810 min^{-1} and the lower limit velocity ω_{open} is 790 min^{-1}. The difference of the conversion time between the two devices nearly 300 ms made the maximum velocity of the flywheel decrease 11.4 min^{-1} in average and the minimum velocity of the flywheel increase 13.8 min^{-1} in average. Consequently, reducing the conversion time is one effective way to make the rotational velocity of the flywheel in the working phase better. The comparison of the percentage error e_{min} and e_{max} when the FV converters had the conversion time values of 300 ms and 7.6 μs will be shown in Figs.2.19 and 2.20, respectively. The transducer using in this research had sufficiently quick response, the delay time was only 7.6 μs; hence, it does not need further improvement.

2.4.3.2 Threshold Velocity

As mentioned above, the upper and lower limit (threshold) velocities ensure that the valve open and valve close commands are kept more than the hold time. In

Table 2.6: *Velocity error of various reference velocities with conversion time of 300 ms.*

Reference rotational velocity [min^{-1}]	$\omega_{\min}$ [min^{-1}]	$\omega_{\max}$ [%]	$e_{\min}$ [%]	$e_{\max}$
1000	964	1043	3.60	4.30
900	864	941	4.00	4.56
800	761	841	5.00	5.13
700	664	740	5.14	5.71
600	561	639	6.50	6.50

Table 2.7: *Velocity error of various reference velocities with conversion time of 300 ms.*

Reference rotational velocity [min^{-1}]	$\omega_{\min}$ [min^{-1}]	$\omega_{\max}$ [%]	$e_{\min}$ [%]	$e_{\max}$
1000	978	1029	2.20	2.90
900	877	928	2.56	3.11
800	778	830	2.75	3.75
700	676	730	3.43	4.29
600	574	631	4.33	5.17

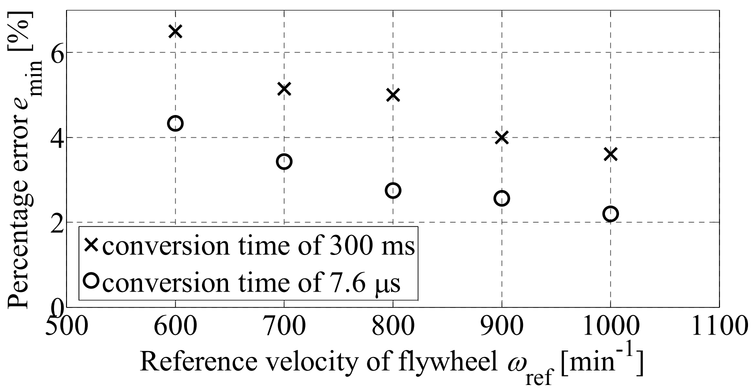

Figure 2.19: *Experimental results of percentage error* $e_{\min}$.

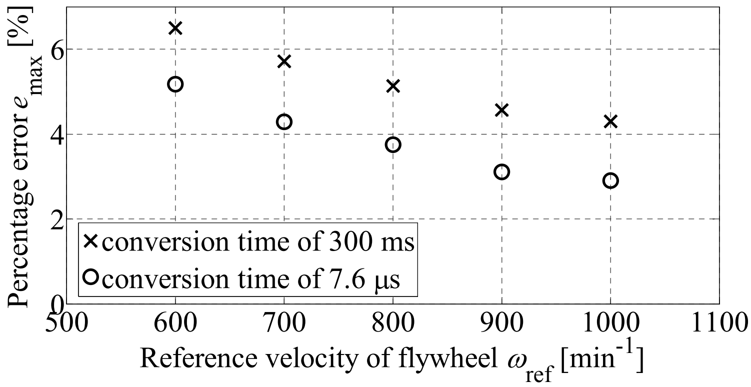

Figure 2.20: *Experimental results of percentage error* $e_{\max}$.

this FST system, the hold time of 0.12 s had to be maintained. With the same velocity transducer, the main factor which affects the hold time is to control the upper/lower deviations of the flywheel velocity. Thus, the criterion to choose the threshold velocities of the flywheel is to assure the hold time more than 0.12 s.

To evaluate the effect of the flywheel upper/lower limit velocities on accuracy of the velocity of the flywheel, following two cases of the limit velocities are considered.

Case 1: To control the upper/lower deviations of the flywheel velocity within 10 min^{-1}. The rotational velocity of the flywheel and its error for the reference velocity 600–1000 min^{-1} are shown in Table 2.7.

Case 2: To control the upper/lower deviations of the flywheel velocity within 5 min^{-1}. Corresponding results to *Case 1* are shown in Table 2.4.

Figure 2.18 shows the relationship of the ON/OFF valves SV_2, SV_3 control signal, the pressure p_2, and the flywheel rotational velocity ω_{FW} in *Case 2*. It is seen from this figure that the valve open and close commands are kept to 0.19 s and 0.25 s, respectively. This means that the hold time of the ON/OFF valves in *Case 2* is satisfied. Because of larger upper limit velocity and smaller lower limit velocity in *Case 1*, the period of the valve open and close commends are longer than that in *Case 2*. As a result, the hold time of the ON/OFF valves in *Case 1* is also satisfied.

Figures 2.21 and 2.22 show the comparison of the percentage error $e_{\min}$ and $e_{\max}$ in *Case 1* and *Case 2*. From these figures it is seen that *Case 2* gives smaller error compared with *Case 1*. The average of reducing percentage error is around 0.5%. Thus, for smaller upper and lower limits of the flywheel velocity, the percentage errors $e_{\min}$ and $e_{\max}$ were little improved; therefore, the flywheel velocity achieved better operation. This reduction, however, brought to the number of switching up; hence, it made the life of the valves shorten. Table 2.8 shows the number of the switching of the valves VS_1, VS_2 and VS_3 in the two cases with the reference velocity of 800 min^{-1}. Therefore, the designer should make a balance of the control specifications and the longevity of the ON/OFF valves.

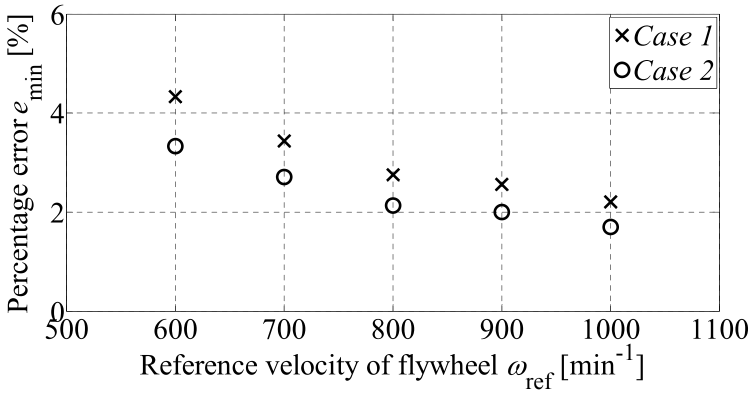

Figure 2.21: *Experimental results of percentage error* $e_{\min}$.

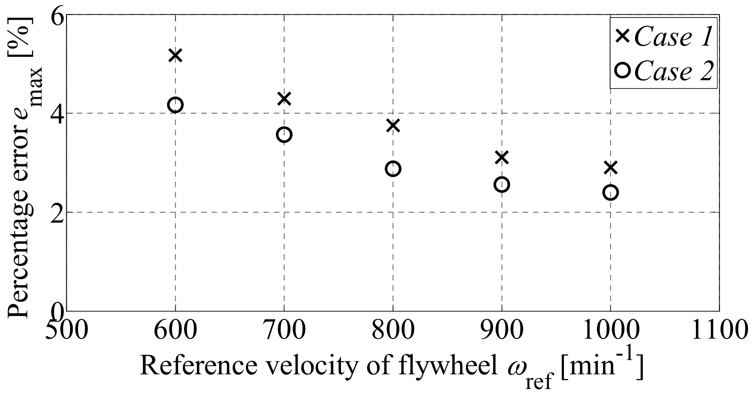

Figure 2.22: *Experimental results of percentage error* $e_{\max}$.

Table 2.8: *Number of valve switching in two cases ($\omega_{ref} = 800\ min^{-1}$).*

		Case 1	*Case 2*
Number	VS1	1	1
of	VS2	35	45
switching	VS3	35	45

2.4.3.3 Comparison of Velocity Responses from *Cases 1* to *4*

This subsection introduces the velocity responses of the flywheel FW for all four cases. The primary purpose for introducing methods from *Cases 1* to *4* is to analyze the energy efficiency; however, the velocity response is a critical aspect that needs to be considered initially.

The drive pattern, as shown in Fig. 2.14(a), consists of three phases; however, Phase 2 is the most important for velocity response because the system primarily works and achieves functionality during this phase. It is also called constant (velocity) or working phase; its reference velocity, ω_r, is constant and maintain a value from 600 to 1000 min^{-1}.

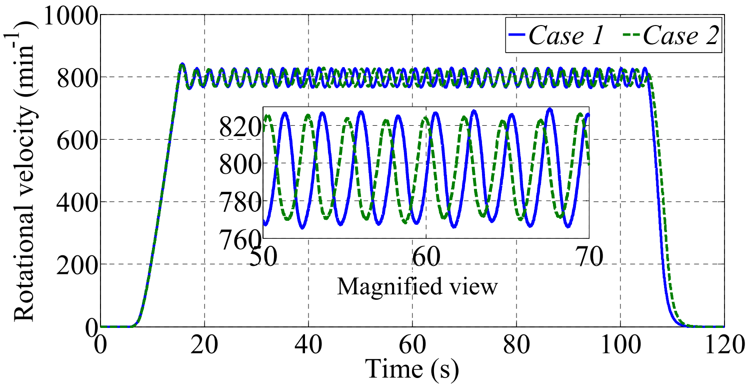

Figure 2.23: *Velocity responses in Cases 1 and 2 ($\omega_r = 800\ min^{-1}$).*

Figures 2.23 and 2.24 show the velocity responses in all four cases corresponding with the reference velocity of 800 min^{-1}. Because identical control logic for the ON/OFF valves and the same velocity of the electric motor M were used, the transient process for all cases is almost the same. During working phase,

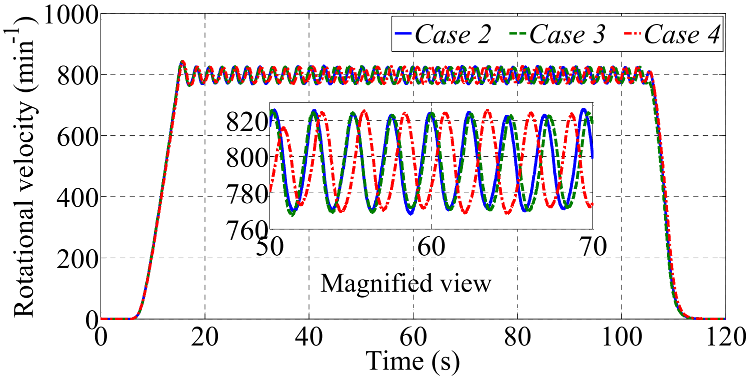

Figure 2.24: *Velocity responses in Cases 2, 3 and 4 ($\omega_r = 800$ min^{-1}).*

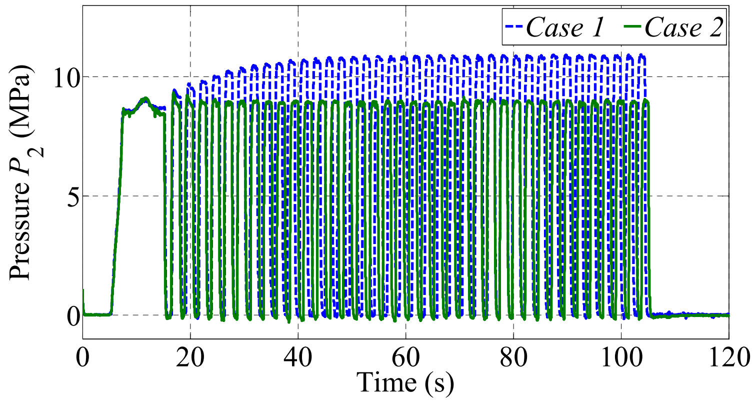

(a)

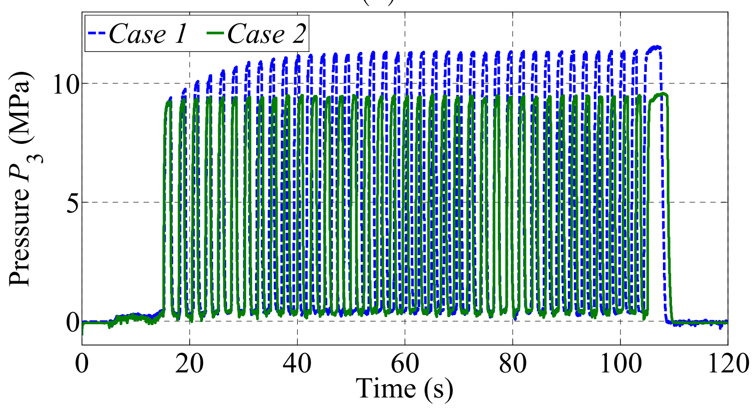

(b)

Figure 2.25: *Pressures: (a) $p_{2.i}$ ($i = 1, 2$) and (b) $p_{3.i}$ ($i = 1, 2$) in Cases 1 and 2 ($\omega_r = 800$ min^{-1}).*

there is a slight difference; the distinction is clearer in *Cases 1* and *2*. As shown in Fig. 2.23, the maximum and minimum velocities are 828.9 and 826.1 min^{-1} and 765.0 and 767.6 min^{-1} for *Cases 1* and *2*, respectively. This can be explained as follows: once the flywheel FW reached the reference velocity, the state was changed to Phase 2. In *Case 1*, the velocity of the electric motor was maintained at 1200 min^{-1} and halved in *Case 2*. Thus, the system in *Case 2* worked with lower pressures $p_{2.2}$ in high-pressure line of the pump/motor PM and $p_{3.2}$ in low-pressure line of the pump/motor PM, as shown in Fig. 2.25. This led to a decrease in the angular acceleration of the flywheel FW in both acceleration and deceleration processes; therefore, the effect of time lag in the system on the velocity of the flywheel FW was relatively reduced.

For *Cases 3* and *4*, the working pressures $p_{1.3}$ and $p_{1.4}$ were established within a range from 8.5 to 9 MPa; however, because of the delay in the supply response including the electric motor M, the hydraulic pump P, and the relief valve RV_1, the pressure $p_{1.i}$ $(i = 3, 4)$ increased beyond the established bounds. The range of the real value of the bounds of the pressures $p_{1.i}$ $(i = 3, 4)$ depends on the reference velocities and cases. Because of these limitations, the pressures $p_{1.3}$ and $p_{1.4}$ in *Cases 3* and *4* were lower than those in *Case 2*, and as a result, the system performed better in *Case 3* and *4*. However, this improvement is not extensive, as shown in Fig. 2.24, according to the velocity responses in *Cases 2*, *3*, and *4* at the reference velocity of 800 min^{-1}.

The velocity responses of the system for all cases in which the reference velocity varied from 600 to 1000 min^{-1} are listed in Table 2.9, and for easy comparison, the percentage errors, e_{min} and e_{max}, defined in Eqs. (2.23) and (2.24) are shown in Fig. 2.26. It is clear that the steady state errors reduced slightly from *Cases 1* to *4* for all reference velocities. The greatest difference is between *Cases 1* and *2*, primarily because of the much higher working pressure in *Case 1*. The improved velocity response in *Cases 3* and *4* is clear with a lower reference value and is more difficult to distinguish if the reference velocity is higher. In particular, the percentage error e_{min} in *Case 4* is even greater than in *Case 3* for reference velocities from 800 to 1000 min^{-1}. This can be explained as follows. In the working phase, when the velocity of the flywheel is lower than the lower limit, ω_{open}, the ON/OFF valves VS_2 and VS_3 will be opened to supply

Table 2.9: *Velocity responses in four cases.*

	ω_r (min^{-1})	ω_{min} (min^{-1})	ω_{max} (min^{-1})	e_{min} (%)	e_{max} (%)
	600	566.2	627.8	5.63	4.63
	700	665.2	728.4	4.97	4.06
Case 1	800	765.0	828.9	4.38	3.61
	900	865.0	929.3	3.89	3.26
	1000	963.9	1029.9	3.61	2.99
	600	567.8	624.7	5.37	4.12
	700	668.1	725.7	4.56	3.67
Case 2	800	767.6	826.1	4.05	3.26
	900	867.5	927.1	3.61	3.01
	1000	967.1	1027.3	3.29	2.73
	600	569.2	624.0	5.13	4.00
	700	669.8	724.7	4.31	3.53
Case 3	800	769.5	825.1	3.81	3.14
	900	869.0	926.3	3.44	2.92
	1000	968.3	1027.1	3.17	2.71
	600	570.4	623.0	4.93	3.83
	700	669.9	724.1	4.30	3.44
Case 4	800	768.3	824.5	3.96	3.06
	900	868.0	926.0	3.56	2.89
	1000	967.3	1026.8	3.27	2.68

energy to the hydraulic pump/motor PM and the acceleration of the flywheel FW during the acceleration period depends on the pressure $p_{2.i}$. Inversely, when the velocity of the flywheel FW reaches the upper limit, ω_{close}, the two ON/OFF valves VS_2 and VS_3 will be closed to cut the supplied energy and brake the hydraulic pump/motor PM, respectively, and the acceleration of the deceleration process depends on the pressure $p_{3.i}$. During the working phase, the value of the pressure $p_{1.i}$ determines the working values of the pressures $p_{2.i}$ and $p_{3.i}$. Figure 2.27 displaying the pressure $p_{1.i}$ in four cases when the reference velocity maintains a value of 800 min^{-1} shows that the pressure $p_{1.1}$ is highest in *Case 1*, which initiates the highest values of e_{min} and e_{max}. The value of $p_{1.i}$ $(i = 2, 3, 4)$ in *Cases 2*, *3*, and *4* are not significantly different, $p_{1.i}$ is only slightly higher in *Case 2*, and as a result, the error in this case is also slightly larger. In both *Cases 3* and *4*, the same boundary of the pressures $p_{1.i}$ $(i = 3, 4)$ was established from 8.5 to 9 MPa; however, because the time lag of the supply response in *Case 4* is much longer, the pressure $p_{1.4}$ in this case is normally lower and leads to a smaller steady state error. The exception is that e_{min} corresponding to the reference velocity reaches the values of 800 min^{-1} or higher. This is because the supply response does not include sufficient energy to maintain a higher pressure $p_{1.4}$ than the precharge pressure of the accumulator ACC_2 during very short time, so the pressure drops, as shown in Fig. 2.27.

In Phase 3, the deceleration process in *Case 1* was executed faster than the others a little bit while the processes in the last three cases are almost same. The reason is because of the working pressure $p_{1.1}$ in *Case 1* is much higher than the others as shown in Fig. 2.27, it leads to the braking pressure $p_{3.1}$ shown in Fig. 2.25(b) in this phase is also higher while there are not different much among the last three cases for both working pressure $p_{1.i}$ $(i = 2, 3, 4)$ shown in Fig. 2.27 and braking pressure $p_{3.i}$ $(i = 2, 3, 4)$.

2.5 Energy Performance

2.5.1 Energy Consumption

Energy consumption of the FST system, that is the average results of 5 times measurement by a power meter on the electric power supply line for the electric motor M, consists of three parts: the useful energy is the required energy to operate the flywheel a full cycle theoretically, the saving energy stored into the accumulator ACC_2 after a cycle, and the wasted energy. Because of the energy loss of the water hydraulic transmissions is considerably higher than the oil hydraulic transmission; thus, taking into account of the energy consumption and finding methods to reduce it is very important requirement for water hydraulic systems. This study introduces three ways to improve energy efficiency and this

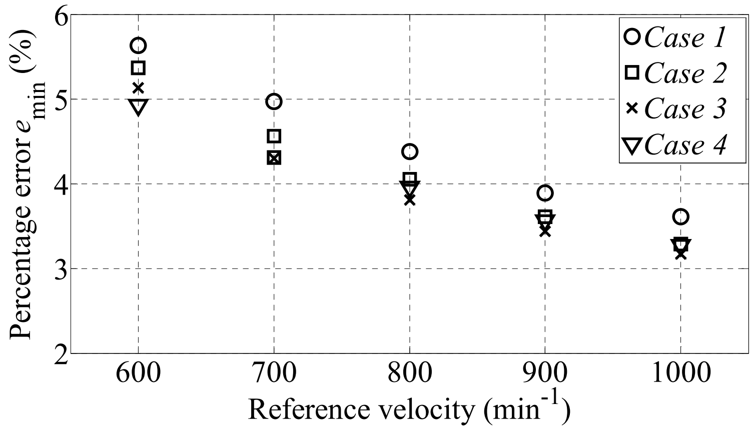

(a)

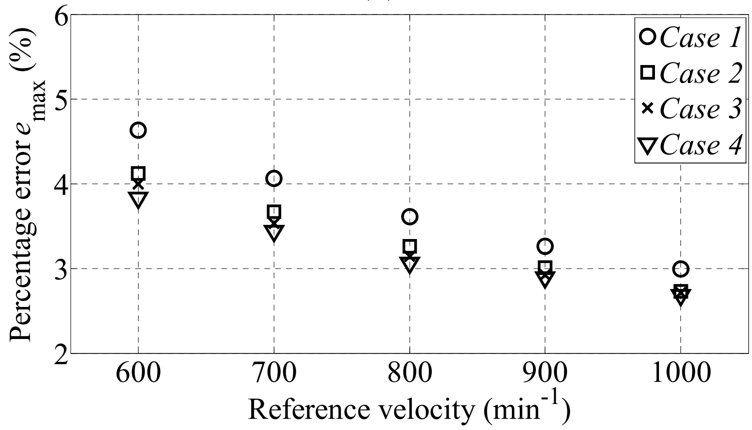

(b)

Figure 2.26: *Percentage errors: (a)* $e_{\min}$ *and (b)* $e_{\max}$ *in four cases.*

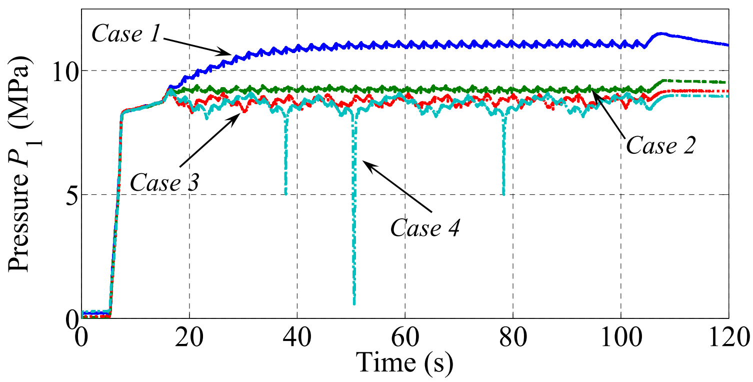

Figure 2.27: *Pressure* $p_{1.i}$ *in four cases* ($\omega_r = 800$ *min*$^{-1}$).

section aims to show the total energy consumption of the system that is denoted by $E_{\mathrm{con}.i}$ for *Case i* ($i = 1, ..., 4$) and compare them together, other analyses for energy saving performance will be proposed in the next sections.

Table 2.10 shows the energy consumptions in four cases when the reference velocity varies from 600 to 1000 min^{-1}, and to be seen more intuitively, the energy consumptions will also be shown in Fig. 2.28. For higher reference velocity, the energy consumption in *Case 1* was down while inversely, it increased for the other cases. The reason can be explained as follows. For each case, the velocity of the electric motor was set to the same value and the energy consumptions were almost same in deceleration phase for all reference velocity because the ON/OFF valve SV_1 was closed to cut down the supplied energy in *Case 1* and the electric motor M was stopped for the others, it leaded to the difference of the energy consumptions when the reference velocity changed only depends on Phase 1 and Phase 2. In the acceleration phase, the larger reference velocity required higher energy consumptions for all cases; however, in working phase or steady state, when the reference velocity was higher, the flow rate through the hydraulic pump/motor PM was higher as well while the supply flow rate from the hydraulic pump P was kept almost constant, it leaded to the working pressure $p_{1.i}$ and supply pressure $p_{s.i}$ that could be consider as the load of the electric motor M be smaller and therefore, the energy consumption that supplied from the electric motor decreased in this phase. From *Case 2*, the velocity of the electric motor M was halved in Phase 2; thus, the system worked with a lower pressure than *Case 1* and as a result, the changes of the energy consumption were smaller.

The energy consumption reduced from *Cases 1* to *4*. The largest reduction was between *Cases 1* and *2*, from 2.26 to 2.38 times, corresponding to reference velocity from 600 to 1000 min^{-1}. The gap between *Cases 3* and *4* is not extensive: approximately 1.2 times for all references. The supply power to the electric motor M and supply pressure $p_{s.i}$ for all cases are shown in Figs. 2.29 and 2.30, respectively. For the acceleration phase, the energy consumptions are the same for all cases because the same control logic and velocity of the electric motor M are used. The greatest difference occurs during the working phase, in which the supply pressure $p_{s.i}$ ($i = 1, \cdots, 4$) is the highest in *Case 1*, leading to a large gap between *Case 1* and the others. *Cases 3* and *4* used methods to force the working

Table 2.10: *Energy consumptions in four cases.*

ω_r (min^{-1})	$E_{\mathrm{con.1}}$ (Wh)	$E_{\mathrm{con.2}}$ (Wh)	$E_{\mathrm{con.3}}$ (Wh)	$E_{\mathrm{con.4}}$ (Wh)
600	168.5 (100%)	70.9 (42.1%)	43.7 (25.9%)	36.6 (21.7%)
700	167.8 (100%)	71.3 (42.5%)	46.4 (27.7%)	39.1 (23.3%)
800	167.2 (100%)	71.9 (43.0%)	49.5 (29.6%)	40.3 (24.1%)
900	166.3 (100%)	72.5 (43.6%)	53.0 (31.9%)	42.6 (25.6%)
1000	165.4 (100%)	73.1 (44.2%)	56.1 (33.9%)	47.1 (28.5%)

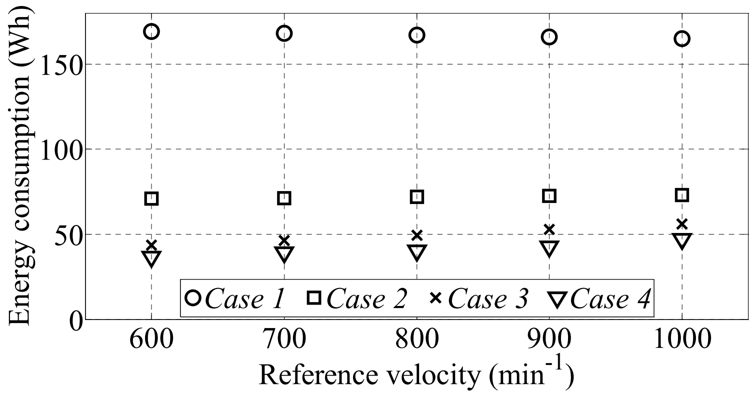

Figure 2.28: *Energy consumptions in four cases.*

pressures $p_{1.3}$ and $p_{1.4}$ inside a range from 8.5 to 9 MPa; however, this pressure still increased beyond the boundary because of the time lag of the devices. In particularly, the working pressure $p_{1.4}$ in *Case 4* occasionally dropped below the precharge pressure of 7.8 MPa during a very short period; this indicated that a working pressure range from 8.5 to 9 MPa causes the lowest supply pressure for the transmission. In this manner, the total energy consumption could reduce from 23.3 to 38.4% and from 35.6 to 48.4% in *Cases 3* and *4*, respectively. Finally, in

Phase 3, the energy consumption of the last three cases share the same values of almost zero because the electric motor M was stopped. The velocity of 1200 min^{-1} was maintained only in *Case 1* for determining the maximum wasted energy if the electric motor M was not used during a full cycle. Based on Fig. 2.29 for calculating the energy consumption in the deceleration phase for *Case 1* with a reference velocity value of 800 min^{-1} and experimental data for the other references, the energy consumption in this phase is approximately 24.5 Wh for all references, which occupies approximately 14.5% of the total energy consumption.

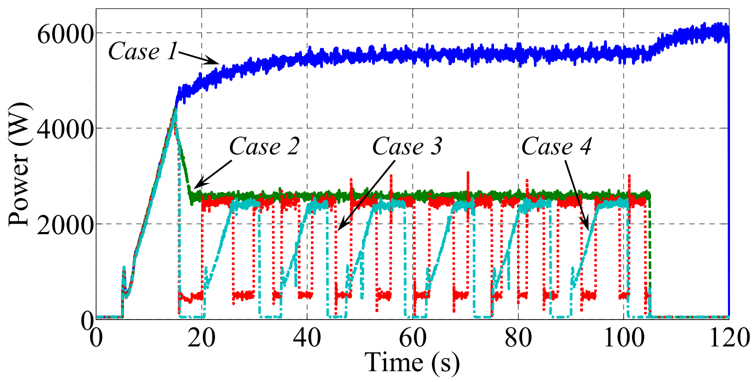

Figure 2.29: *Supply power to the electric motor M in four cases ($\omega_r = 800$ min^{-1}).*

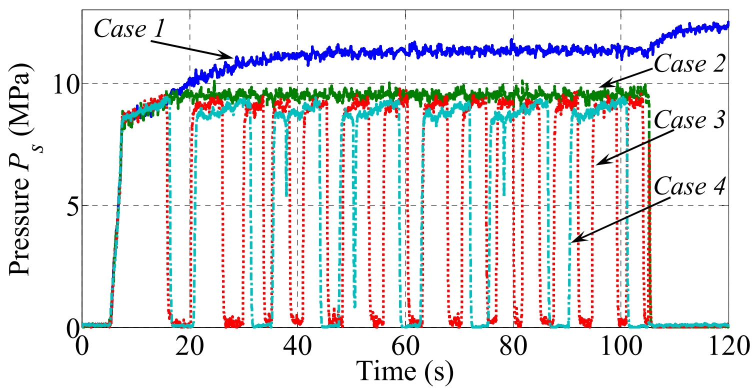

Figure 2.30: *Supply pressure $p_{s.i}$ in four cases ($\omega_r = 800$ min^{-1}).*

2.5.2 Energy Savings

The saved energy of the FST system is denoted by $E_{\text{save}.i}$, where i maintains values from 1 to 4 corresponding to *Cases 1* to *4*. This saved energy consists of two elements: the recovered energy generated in Phase 3 or the deceleration process of Phase 2, produced by converting the kinetic energy of the flywheel FW into high-pressure fluid stored into the accumulator ACC_2; and the charged energy supplied in the accumulator ACC_2 in Phases 1 and 2 by the pressure difference. The recovered energy can be defined via the pressure $p_{1.i}$ and flow rate $Q_{2.i}$, as discussed in the following.

2.5.2.1 Recovered Energy Efficiency

In Phase 3 or the deceleration process in Phase 2, the ON/OFF valves VS_2 and VS_3 are closed. The ON/OFF valve VS_3 is closed to brake the flywheel FW; at that time, the pump/motor PM acts as a pump and converts the kinetic energy of the flywheel FW into high-pressure fluid stored in the accumulator ACC_2. The recovered energy will be reused as an additional energy source during the acceleration process of the next cycle. The ON/OFF valve VS_2 is closed to directly halt the supplied energy to the hydraulic pump/motor PM and preserve the recovered energy. The recovered energy for one cycle in *Case i* ($i = 1, ..., 4$) can be calculated as follows

$$E_{\text{re}.i} = \int_{t_{\text{start}}}^{t_{\text{end}}} p_{\text{ACC}_2.i} \cdot Q_{\text{ACC}_2.i} dt \tag{2.25}$$

where $E_{\text{re}.i}$ is the recovered energy to the accumulator ACC_2 in *Case i*; $p_{\text{ACC}_2.i}$ and $Q_{\text{ACC}_2.i}$ are the pressure of the fluid inside the accumulator ACC_2 and the flow rate charged into the accumulator ACC_2 in the deceleration processes of *Case i*; t_{start} and t_{end} are the times at the beginning and end of a cycle, respectively.

Because the pressure $p_{\text{ACC}_2.i}$ and flow rate $Q_{\text{ACC}_2.i}$ are approximated to the working pressure $p_{1.i}$ and flow rate $Q_{2.i}$ in *Case i*, Eqn. (2.25) can be written as

$$E_{\text{re}.i} = \int_{t_{\text{start}}}^{t_{\text{end}}} p_{1.i} \cdot Q_{2.i} dt \tag{2.26}$$

Figure 2.31 shows the flow rate $Q_{2.1}$ in *Case 1* when the reference velocity is 800 min^{-1}, which represents the flow rate charged into the accumulator ACC_2

during the deceleration processes. Based on the pressure $p_{1.1}$ and flow rate $Q_{2.1}$, as shown in Figs. 2.27 and 2.31, the recovered energy in *Case 1* corresponding to the reference velocity of 800 min^{-1} was obtained as 11.1 Wh. Similarly, the recovered energies for all reference velocities of all four cases were calculated, listed in Table 2.11 and displayed in Fig. 2.32. The recovered energies do not differ greatly among four cases. The largest reduction, between *Cases 1* and *4*, only ranges from 23.2 to 25.2% corresponding to the reference velocity from 600 to 1000 min^{-1}. Because the same range of working pressures $p_{1.i}$ ($i = 3, 4$) from 8.5 to 9 MPa were used, the recovered energies in *Cases 3* and *4* are very similar, with a difference from 1.9 to 5.2%.

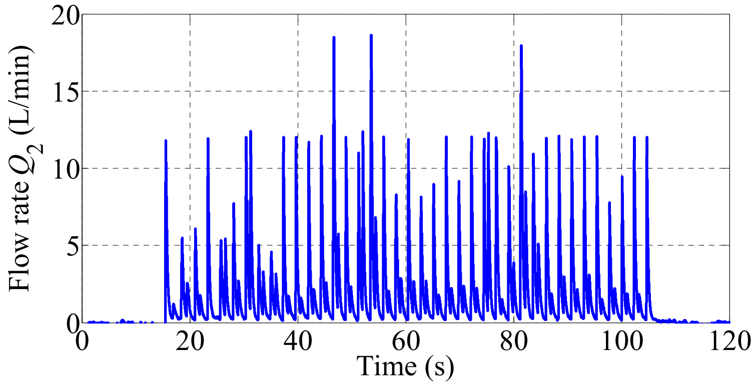

Figure 2.31: *Flow rate $Q_{2.1}$ in Case 1 ($\omega_r = 800$ min^{-1}).*

Table 2.11: *Recovered energies in four cases.*

ω_r (min^{-1})	$E_{\mathrm{re.1}}$ (Wh)	$E_{\mathrm{re.2}}$ (Wh)	$E_{\mathrm{re.3}}$ (Wh)	$E_{\mathrm{re.4}}$ (Wh)
600	9.5	8.5	7.7	7.3
700	10.4	9.1	8.0	7.6
800	11.1	9.7	8.4	8.0
900	12.4	10.5	9.5	9.3
1000	13.5	11.7	10.3	10.1

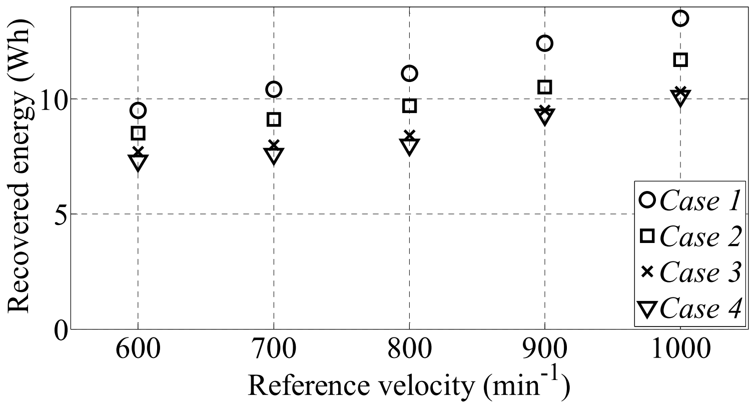

Figure 2.32: *Recovered energies in four cases.*

2.5.2.2 Estimation of Saved Energy

The saved energy is the energy remaining inside the accumulator ACC_2 after a working cycle, which is reused in the following cycle as an additional energy source. In Phases 1 and 2, energy is charged into the accumulator ACC_2 by the pressure difference between the working pressure $p_{1.i}$ and the accumulator pressure $p_{ACC_2.i}$; in Phase 3, the hydraulic pump/motor PM acts as a pump to convert the kinetic energy of the flywheel FW into high-pressure water and store it in the accumulator ACC_2. The saved energy in Phase 3 can be calculated via the pressure $p_{1.i}$ and the flow rate $Q_{2.i}$, but the energy charged into the accumulator ACC_2 in Phases 1 and 2 is quite difficult to measure, requiring further devices for determination because the charge and discharge processes occur alternately. This study proposes a method to estimate the saved energy, as discussed in the following.

- After one working cycle, turn off the electric motor M and operate the FST systems normally by using only the saved energy stored inside the accumulator ACC_2.
- Compare the velocity response of the flywheel for cases using saved energy and power supply; the saved energies of the FST systems are estimated as the part of electric energy that caused the systems to operate in the same manner as when using saved energy.

The estimation of saved energy does not share the exact result as energy stored inside the accumulator ACC_2, but represents a part of total energy consumption that can be reduced in the following cycle by using the saved energy as an additional energy source to the electric energy.

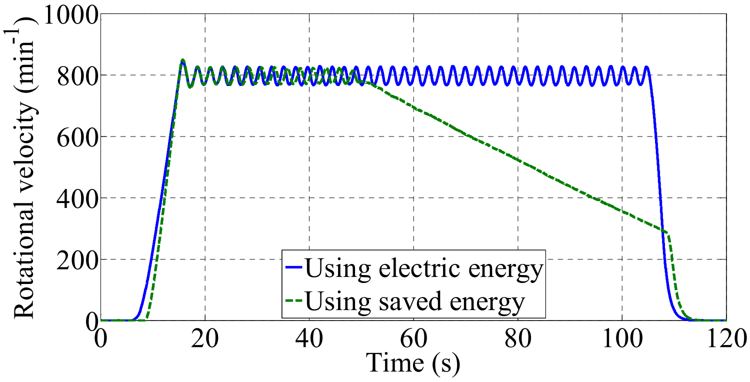

(a)

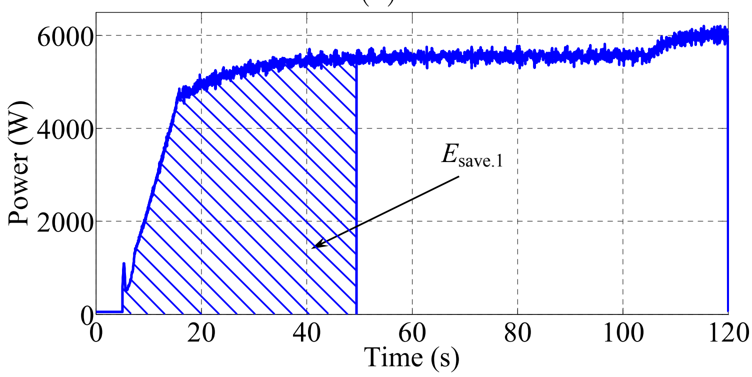

(b)

Figure 2.33: *Estimation of saved energy in Case 1 (ω_r = 800 min^{-1}): (a) velocity responses in cases of using only electric or saved energy, (b) estimation of saved energy.*

Figure 2.33(a) shows the velocity responses of the FST system in *Case 1* for two events: using only the electric energy source or the saved energy when the reference velocity is 800 min^{-1}. Fig. 2.33(a)indicates that the saved energy stored in the accumulator ACC_2 can initiate operation as though the system runs on electric energy for 49.5 s; this corresponds to electric energy of 58 Wh, as shown in Fig. 2.33(b). By using this method, as shown in Figs. 2.34, 2.35, and 2.36 for

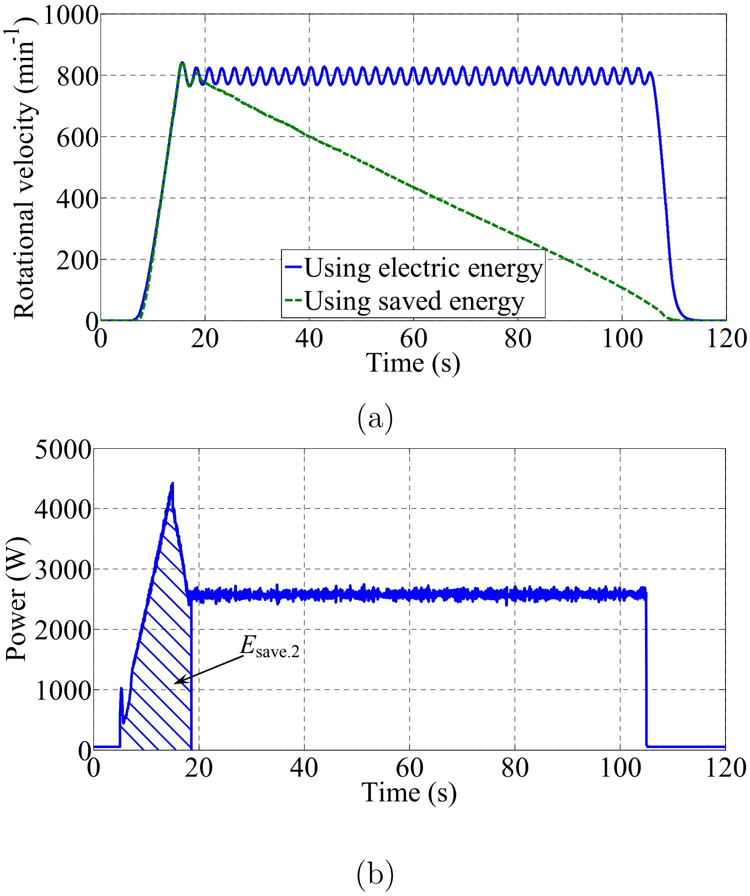

Figure 2.34: *Estimation of saved energy in Case 2 ($\omega_r = 800$ min^{-1}): (a) velocity responses in cases of using only electric or saved energy, (b) estimation of saved energy.*

Cases 2, *3*, and *4*, the saved energy of the system, with reference velocity from 600 to 1000 min^{-1} for all cases, is evaluated and listed in Table 2.12.

In *Cases 1* and *2*, the saved energy reduces for higher reference velocity but is inverted in the other cases. This can be explained as follows. As mentioned above, the saved energy is generated in all phases and divided into two parts: in Phases 1 and 2, energy is charged into the accumulator ACC_2 because of the pressure difference between the working pressures $p_{1.i}$ and the accumulator pressure $p_{\mathrm{ACC}_2.i}$. The second part is in Phase 3, during which the hydraulic pump/motor PM acts as a pump to convert the kinetic energy of the flywheel into high-pressure water and store it in the accumulator ACC_2; if the reference

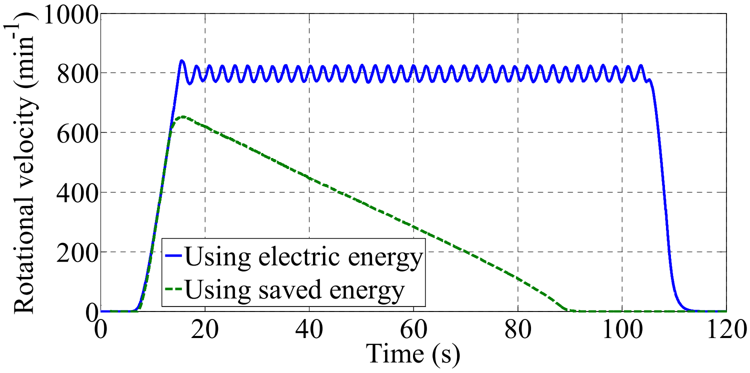

(a)

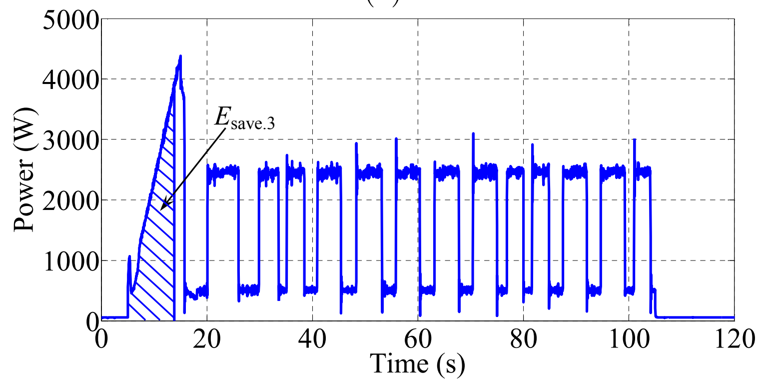

(b)

Figure 2.35: *Estimation of saved energy in Case 3 (ω_r = 800 min^{-1}): (a) velocity responses in cases of using only electric or saved energy, (b) estimation of saved energy.*

Table 2.12: *Saved energy in four cases.*

ω_r (min^{-1})	$E_{\text{save.1}}$ (Wh)	$E_{\text{save.2}}$ (Wh)	$E_{\text{save.3}}$ (Wh)	$E_{\text{save.4}}$ (Wh)
600	74.0	12.8	3.6	3.4
700	66.5	11.6	4.4	3.9
800	58.0	9.8	5.1	4.5
900	50.4	7.9	5.7	5.0
1000	42.5	6.9	6.5	5.7

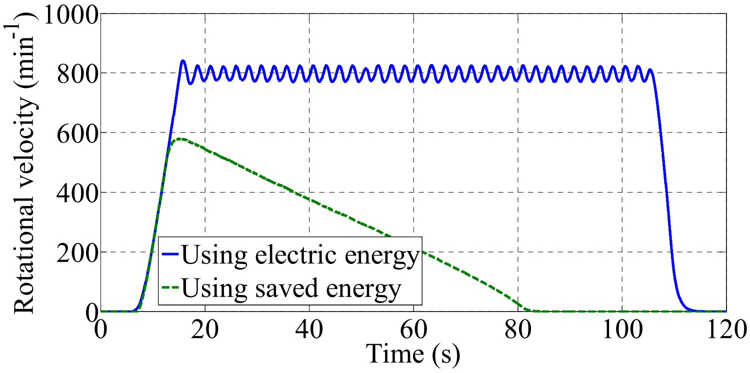

(a)

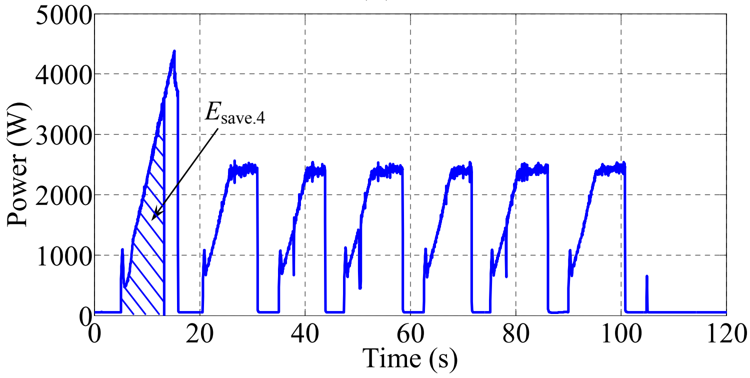

(b)

Figure 2.36: *Estimation of saved energy in Case 4 ($\omega_r = 800$ min^{-1}): (a) velocity responses in cases of using only electric or saved energy, (b) estimation of saved energy.*

velocity is higher, the kinetic energy of the flywheel is also larger, so the recovered energy in Phase 3 is large for all cases. However, the first part of the saved energy reverses: the higher the reference velocity, the lower the saved energy. This phenomena can be explained as follows: for one case, the velocity of the electric motor is maintained constantly for all references, so the supply flow rate via the hydraulic pump P does not change; however, the flow rate via the hydraulic pump/motor PM was greater for a higher reference velocity, which decreased the working pressure $p_{1.i}$. As a result, the saved energy charged into the accumulator ACC$_2$ in Phases 1 and 2 was smaller for higher references. The first part of the saved energy contributes more significantly in *Cases 1* and *2* than the other cases because of the limitations of the working pressures $p_{1.i}$ $(i = 3, 4)$ within the range from 8.5 to 9 MPa in Phases 1 and 2.

The saved energy in *Case 1* is much higher than that in the other cases, which is because the working pressure $p_{1.1}$ in this case is the highest, as shown in Fig. 2.27. Because the same thresholds are used for the pressures $p_{1.i}$ $(i = 3, 4)$, the saved energy in *Cases 3* and *4* does not differ extensively; however, it is 1.1 to 3.8 times smaller than the saved energy in *Case 2* for reference velocity from 600 to 1000 min^{-1}. The saved energies from *Cases 2* to *4* for the reference of 1000 min^{-1} only reduce slightly because the working pressure $p_{1.i}$ $(i = 2, 3, 4)$ is quite small and rarely exceeds the upper limit of 9 MPa.

2.5.2.3 Evaluation of Net Energy Consumption

To precisely estimate the energy consumption of the FST system and determine a basis for comparing the energy efficiency of the four cases, this subsection introduces the net energy consumption, which is the difference between the total energy consumption in a working cycle and the saved energy after the cycle, defined as follows:

$$E_{\text{net}.i} = E_{\text{con}.i} - E_{\text{save}.i} \tag{2.27}$$

where $E_{\text{net}.i}$, $E_{\text{con}.i}$, and $E_{\text{save}.i}$ are the net energy consumption, total energy consumption, and saved energy in *Case i* $(i = 1, \cdots, 4)$, respectively.

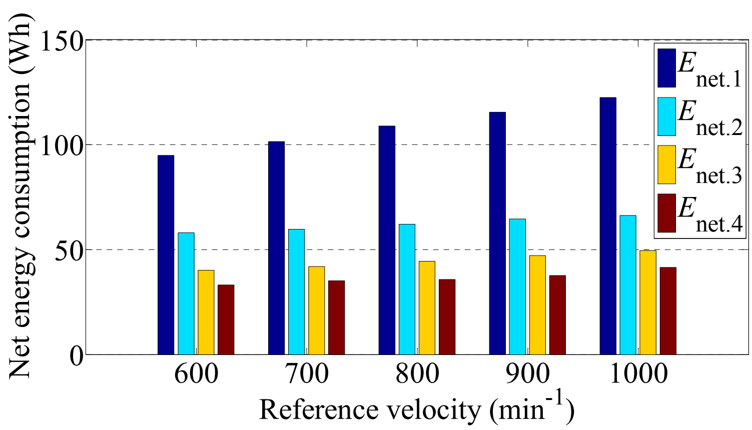

Figure 2.37: *Net energy consumptions in four cases.*

Table 2.13: *Net energy consumptions in four cases.*

ω_r (min^{-1})	$E_{\mathrm{net.1}}$ (Wh)	$E_{\mathrm{net.2}}$ (Wh)	$E_{\mathrm{net.3}}$ (Wh)	$E_{\mathrm{net.4}}$ (Wh)
600	95.0 (100%)	58.1 (61.2%)	40.1 (42.2%)	33.2 (34.9%)
700	101.5 (100%)	59.7 (58.8%)	42.0 (41.4%)	35.2 (34.7%)
800	109.0 (100%)	62.1 (57.0%)	44.4 (40.7%)	35.8 (32.8%)
900	115.6 (100%)	64.6 (55.9%)	47.3 (40.9%)	37.6 (32.5%)
1000	122.5 (100%)	66.2 (54.0%)	49.6 (40.5%)	41.4 (33.8%)

The net energy consumption of the system for all cases with reference velocity from 600 to 1000 min^{-1} were calculated and listed in Table 2.13, and to display them more intuitively, the results are also shown in Fig. 2.37. The net energy consumption in all cases increases if the system receives a higher reference velocity. The net energy consumption was reduced from 38.8 to 46.0% in *Case 2* and by using the limitation of the working pressures $p_{1.i}$ $(i = 3, 4)$ in *Cases 3* and *4*, net energy consumption was diminished from 57.8 to 59.5% and 65.1 to 66.2%, respectively.

The net energy consumption of the system in *Cases 3* and *4* does not vary significantly and the velocity responses are very similar. However, the idling stop method in *Case 4* requires the electric motor M and the hydraulic pump P to start and stop many times to maintain the working pressure inside a boundary, which shortens the duration of these devices. Thus, *Case 3* is the most promising method for saving energy.

2.6 Summary

This chapter was a whole view of a FST system, because it covered from simulation to experiment, examined the parameters which affected to control performance and energy saving, the two most important points of the system. In addition, three methods to improve the energy efficiency were introduced beside the original FST system.

First, the simulated and experimental results were almost same; that means the simulator has been build successfully and matched the actual.

The percentage error of the flywheel velocity could be reduced by using a quick response velocity transducer and restricting control upper and lower thresholds. The combination of both methods made the control accuracy of the FST system within ± 25 min^{-1}, that corresponds with the velocity error below 3% for given reference speeds equal or above 800 min^{-1}. However, the way of restricting the control upper and lower thresholds made the number of switching up; as a result, the life of the ON/OFF valves would be reduced. A requirement is to simulate the relationship between the upper and lower thresholds and the duration of the ON/OFF valves. It is a future work of this research.

The most important target of the research is to improve the energy efficiency of the water hydraulic FST. This chapter introduces the original FST system that does not act on the electric motor M during working cycles and proposes three methods to reduce energy consumption by lessening the velocity of the electric motor M, stopping the M during the working and deceleration phases, respectively, and limiting the working pressures $p_{1.i}$ $(i = 3, 4)$ by using an unload valve or idling stop method. Finally, both velocity and energy performances of these methods are compared.

Experiments on the FST system were executed with respect to energy efficiency and velocity responses for reference velocity from 600 to 1000 min^{-1}, and the primary conclusions can be summarized as follows:

- The velocity responses in the acceleration and deceleration phases were almost the same for all cases; in Phase 3, the deceleration process in *Case 1* was performed slightly faster than the others because of the difference of the working pressure $p_{1.1}$.

- The velocity response improved slightly from *Cases 1* to *4* with the most significant reduction between *Cases 1* and *2*: from 0.26 to 0.32% and from 0.26 to 0.51% when the reference velocity varies from 600 to 1000 min^{-1} for e_{min} and e_{max}, respectively.

- The difference in recovered energy generated in Phase 3 and the deceleration process in Phase 2, which converts the kinetic energy of the flywheel FW into high-pressure water stored in the accumulator ACC_2, is not significant among the four cases, particularly between *Cases 3* and *4*, the same limitations of the working pressures $p_{1.3}$ and $p_{1.4}$.

- The saved energy remaining inside the accumulator ACC_2 after a working cycle in *Case 1* is significantly higher than the others because the highest working pressure $p_{1.1}$ is used; however, this difference was not significant between the last two cases using the same thresholds for the pressures $p_{1.i}$ $(i = 3, 4)$.

- The energy and net energy consumptions of the system reduced from *Case 1* to *4*. The last two cases display many advantages in both energy and velocity performances, which are slightly better in *Case 4*; however, the electric motor M was turned on/off many times to maintain the working pressure $p_{1.4}$ inside the working range in this case, which leads to a shortened the durations of the electric motor M and the hydraulic pump P. As a result, the method of using a unload valve should be used in application.

Chapter 3

Water Hydraulic Pump Motor Transmission

3.1 PMT System

3.1.1 Overview of the PMT System

Figure 3.1 shows the novel water hydraulic PMT system. The PMT system is based on the FST system; some devices have been changed, and the control algorithms for the ON/OFF valves and electric motor M are different. Note that, Figs. 2.1 and 3.1 use the same symbols to represent the same devices in the real systems, and the specifications of the experimental devices of the PMT system are given in Table A.1. In the PMT system, the ON/OFF valve VS_1 is replaced by the check valve VC_1, the accumulator ACC_1 is eliminated, and the accumulator ACC_2 is used to both absorb pressure surges in the acceleration and constant phases and store recovered energy in the deceleration phase.

The most important feature of the PMT system is the control logic for the two ON/OFF valves VS_2 and VS_3 and the electric motor M. In the acceleration and constant phases, VS_2 and VS_3 are open, and they are closed throughout the deceleration phase. The controller receives the reference signal $r(t)$, as shown in Fig. 3.1, and the feedback of the flywheel velocity is provided by an encoder to generate the control signal $u(t)$. The hardware for the controller is installed on dSPACE 1104, and the software is MATLAB/Simulink; thus the control signal u_{M}

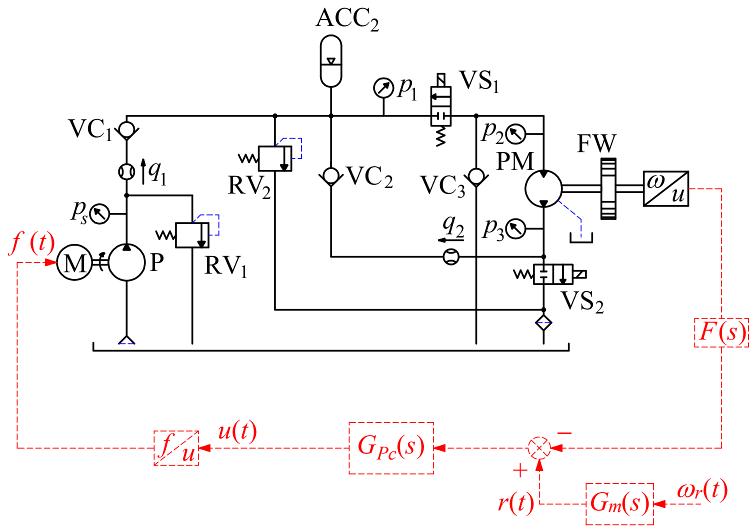

Figure 3.1: *Schematic of water hydraulic PMT system.*

is limited by ± 10 V. It is assumed that the rotational velocity of an electric motor $n(t)$ is related to the frequency of electrical power supply $f(t)$ by a first-order time lag system given by [57]

$$\tau_n \dot{n}(t) = n(t) + \frac{120}{P_{\mathrm{M}}} f(t) \tag{3.1}$$

where τ_n is the time constant of the electric motor and P_{M} the number of poles of the motor M, in this case $P_{\mathrm{M}} = 4$. Thus, the control signal that is delivered to the electric motor M is frequency. A frequency converter is used for converting the control signal out of dSPACE in voltage to frequency signal supplied to the electric motor M. The specification of the frequency converter can be derived by doing some tests on it. The experimental data of the tests will be shown in Table A.1, the results are the average of five times of experiments; for more detail, Fig. 3.2 shows the input-output mapping of the frequency converter.

From the experimental results, it is easy to realize that, the relationship of the input and output of the frequency converter can be considered as linear mapping, and it can be written approximately as following equation

$$f = \varepsilon u \tag{3.2}$$

where ε is the frequency coefficient and get the value of 6.1817 Hz/V.

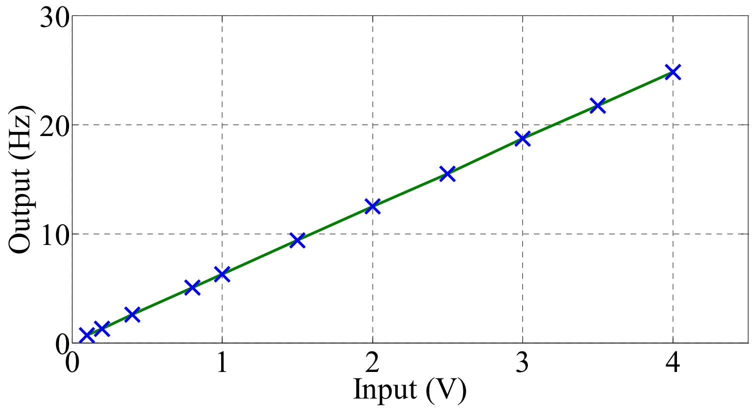

Figure 3.2: *Frequency converter input-output mapping.*

In the deceleration phase, all the ON/OFF valves were closed as mentioned above, and the electric motor M was also stopped. Thus, there was no energy supply to the hydraulic pump/motor PM but it still worked same as the FST system and also converted the kinetic energy of the flywheel FW into high pressure fluid stored in the accumulator ACC_2.

3.1.2 Control Logic of PMT System

The controller of the PMT system in Fig. 3.3 is a feedback control that matches the velocity of the flywheel track to a desired reference velocity $r(t)$, as shown in Fig. 3.1. The controller in this study is conventional proportional-integral-derivative (PID) controller. Each gain is tuned manually to attenuate the steady-state error and overshoot. The PID controller has the transfer function as follows:

$$G_{Pc}(s) = K_{PP} + \frac{K_{PI}}{s} + K_{PD}s \tag{3.3}$$

where K_{PP}, K_{PI}, and K_{PD} are the proportional, integral, and derivative gains; in the experiment, they had values of 0.002, 0.001, and 0.001, respectively.

In the feedback loop, a first-order low-pass filter $F(s)$ is used to eliminate the high-frequency noise caused by measurement devices, which comprise an encoder and frequency-velocity (FV) converter.

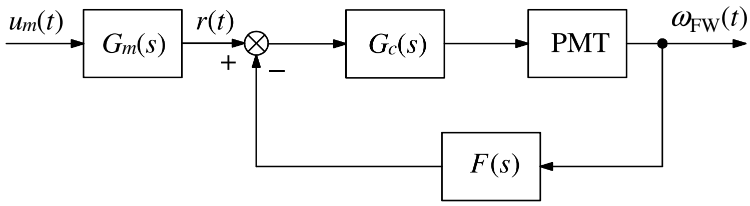

Figure 3.3: *Control structure of PMT system.*

The reference velocity $r(t)$ is generated according to the reference model $G_m(s)$ using the rectangular input signal $\omega_r(t)$, as shown in (3.4).

$$G_m(s) = \frac{1}{2s+1} \tag{3.4}$$

3.2 Velocity Response

The PMT system was controlled by a conventional PID as mentioned above, the target of the control is to make the velocity of the flywheel converge to a reference signal $\omega_r(t)$. To compare with the velocity response of the FST, the reference signal is also divided into three parts: an acceleration phase, a constant (working) phase, and a deceleration phase. The acceleration phase can be calculated when the velocity is the stationary state to get the constant value of the reference signal ω_{wr}, the constant and working phase is defined same as the FST system, the acceleration and constant phases also took 100 seconds for each cycle.

The velocity responses in working phase of the PMT system corresponding with the reference velocity ω_{wr} from 600 min^{-1} to 1000 min^{-1} are shown in Table 3.1, and Fig. 3.4 shows the velocity response in case of reference velocity $\omega_{wr} = 800\ \text{min}^{-1}$. Based on the Table 3.1, it is easy to realize that the limit of the bounds of the velocity errors is 3.92 min^{-1} and 4.18 min^{-1} corresponding with the bound of percentage errors e_{min} and e_{max} that also will be defined in Eqs. (2.23) and (2.24) to 0.49% and 0.52%, respectively, when the reference velocity changes from 600 min^{-1} to 1000 min^{-1}. As showed in Fig. 3.4, the transient time (in the acceleration phase) of the response takes longer time than the reference, it can

Table 3.1: *Experimental velocity response of the PMT system.*

ω_r (min^{-1})	ω_{min} (min^{-1})	ω_{max} (min^{-1})	e_{min} (%)	e_{max} (%)
600	598.34	603.13	0.28	0.52
700	697.22	704.10	0.40	0.59
800	796.08	802.99	0.49	0.37
900	896.88	904.18	0.35	0.46
1000	996.85	1003.20	0.32	0.32

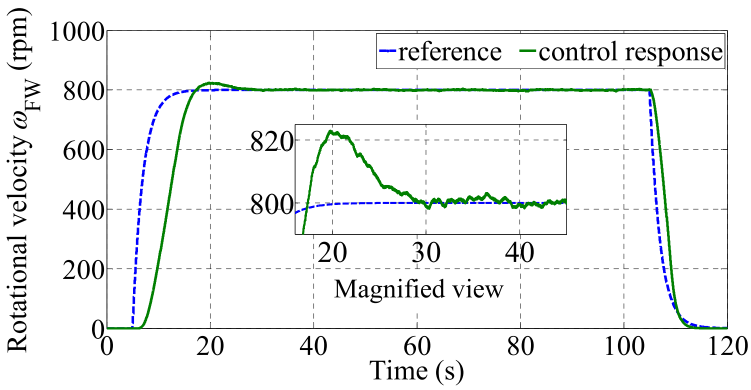

Figure 3.4: *Velocity response of the PMT system* ($\omega_{\text{wr}} = 800$ *min*$^{-1}$).

be improved by using larger gains of PID controller; however, it will bring the larger overshoot. Thus, finding a method to reduce the transient time and still keep a small overshoot is a requirement of this research in the future.

Figure 3.5 shows the control signal of the electric motor M. In the working phase, the controller sent to the motor a signal that is not changed much. This is really good for the duration of the motor. For all the time of the acceleration and working phases, the ON/OFF valve VS_2 and VS_3 were opened, that made the supply pressure for hydraulic pump/motor PM was steady; therefore, the lifetime of the both ON/OFF valves and also the hydraulic pump/motor is not affected.

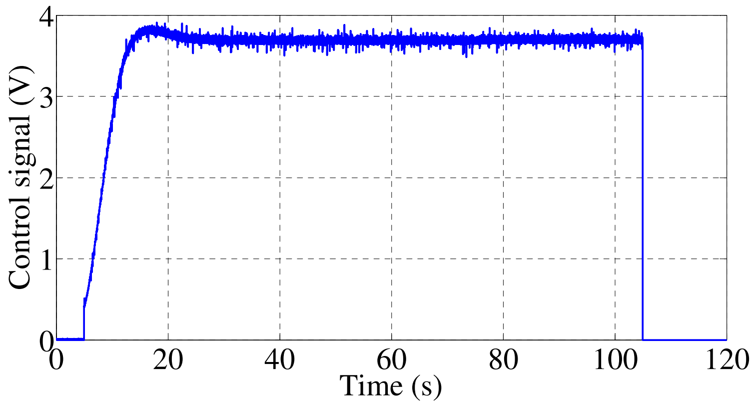

Figure 3.5: *Control signal of electric motor.*

3.3 Energy Performance

3.3.1 Energy Consumption

Energy consumption of the PMT system is only from the acceleration and working phases same as the FST system, because the electric motor M is also stopped in the deceleration phase. Energy consumption of the system when the reference velocity is from 600–1000 min^{-1} will be shown in Table 3.2 and the supply power to the electric motor M will be shown in Fig. 3.6. The energy consumption of the PMT system decreases if the reference velocity goes down. It is not difficult to understand because the velocity of the electric motor M also varies depending on the reference velocity.

Table 3.2: *Energy consumption of the PMT system.*

ω_r (min^{-1})	Energy consumption [Wh]
600	18.4
700	20.8
800	23.0
900	26.0
1000	28.5

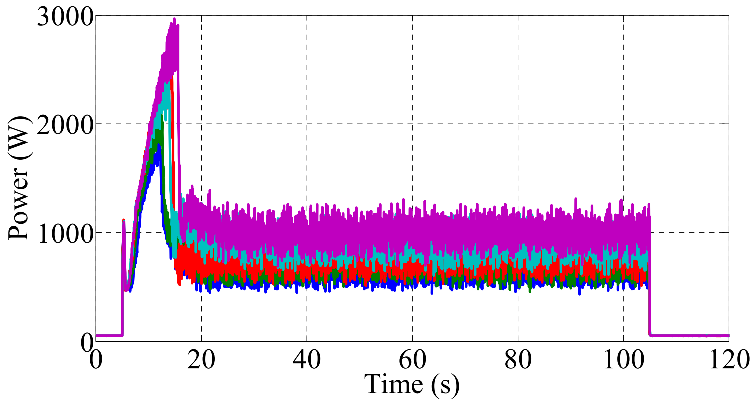

Figure 3.6: *Supply power to the electric motor M. Blue line* – $\omega_r = 600\ min^{-1}$, *green line* – $\omega_r = 700\ min^{-1}$, *red line* – $\omega_r = 800\ min^{-1}$, *cyan line* – $\omega_r = 900\ min^{-1}$, *violet line* – $\omega_r = 1000\ min^{-1}$

3.3.2 Energy Saving

Saved energy of the PMT system is the energy stored inside the accumulator ACC after a working cycle and reused in the following cycle. It generated only by converting the kinetic energy of flywheel into high pressure fluid stored in the accumulator ACC in the deceleration phase because in a working phase, the working pressure is less than the precharge pressure of ACC (7.8 MPa); therefore, there is no fluid charged into ACC in this phase. The recovered energy converted into high pressure fluid in the deceleration phase can be calculated via pressure and flow rate; however, more importantly, the useful part for the next action cycle of the recovered energy need to be defined. The saved energy can be estimated by following:

- After one working cycle, turn off the electric motor M and operate the PMT systems normally by using only the saved energy stored inside the accumulator ACC_2.

- Compared the velocity response of the flywheel in the cases of using saved energy and using power supply; the saved energies of the PMT system was estimated as the part of electric energy that made the systems operate same as using saved energy.

Note that the estimation of saved energy does not bring the exact result of energy stored inside the accumulator ACC_2 as well, but it represents a part of total energy consumption that can be reduced in the following cycle by using the saved energy as an additional energy source beside the electric energy.

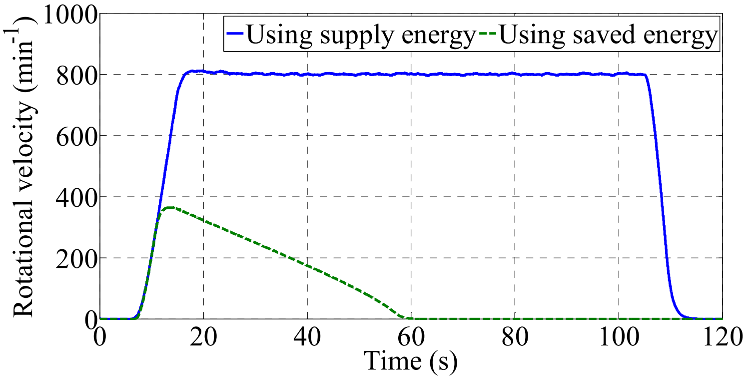

(a)

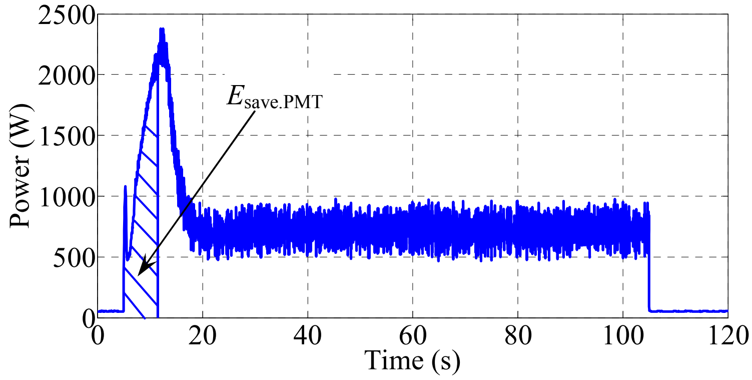

(b)

Figure 3.7: *Estimation of saved energy of the PMT system (ω_r = 800 min^{-1}): (a) velocity responses in cases of using only electric or saved energy, (b) estimation of saved energy.*

Figure 3.7 (a) shows the velocity responses of the PMT system in cases of using the supply energy and the saved energy when the reference velocity is 800 min^{-1}. By checking the figure, it can be concluded that the saved energy stored inside the accumulator ACC_2 can accelerate the flywheel to the highest velocity of 374.4 min^{-1} corresponding to the supply power can make the system operate 11.5 seconds. Based on the supply power for the electric motor curve as shown in Fig. 3.7 (b), the saved energy can be found out and get the value of 2.5 Wh. In the same way, the saving energies for other reference velocities form 600 to 1000 min^{-1} are also estimated and shown in Table 3.3. To evaluate the saved energy, a saved energy index η_{PMT} will be introduced and defined as

$$\eta_{\text{PMT}} = \frac{E_{\text{save.PMT}}}{E_{\text{con.PMT}}} \tag{3.5}$$

where $E_{\text{save.PMT}}$ is the saved energy of the PMT system and $E_{\text{con.PMT}}$ the total energy consumption of the PMT system.

Table 3.3: *Saved energy of the PMT system.*

ω_r (min^{-1})	$E_{\text{save.PMT}}$ [Wh]	η_{PMT} [%]
600	1.6	8.7
700	2.1	10.1
800	2.5	10.9
900	3.1	11.9
1000	3.9	13.7

Based on the Table 3.3, the saved energy index η_{PMT} gets the value from 8.7 to 13.7% when the reference velocity varies from 600 to 1000 min^{-1}. This saved energy will contribute to reduce the energy consumption of the next cycle and also shorten the transient response.

3.3.3 Net Energy Consumption and Comparison with the FST System

3.3.3.1 Net Energy Consumption

To estimate the energy consumption of the PMT system more correctly and get a basis for comparison with other transmission and system, the net energy consumption of the PMT system $E_{\text{net.PMT}}$ that is the difference of the total energy consumption in a cycle and the saved energy after the cycle, Eq. (3.6), will be introduced.

$$E_{\text{net.PMT}} = E_{\text{con.PMT}} - E_{\text{save.PMT}} \tag{3.6}$$

Table 3.4: *Net energy consumption of the PMT system.*

ω_r (min^{-1})	$E_{\text{con.PMT}}$ [Wh]	$E_{\text{save.PMT}}$ [Wh]	$E_{\text{net.PMT}}$ [Wh]
600	18.4	1.6	16.8
700	20.8	2.1	18.7
800	23.0	2.5	20.5
900	26.0	3.1	22.9
1000	28.5	3.9	24.6

The net energy consumption of the PMT system are shown in Table 3.4 for reference velocity from 600 to 100 min^{-1} and it increases from 16.8 to 24.6 Wh.

3.3.3.2 Relative Wasted Energy of FST to PMT

The total energy consumption and saved energy of each system was then obtained, but the work of defining the wasted energies of the both system is very difficult. Thus, to compare the advantage and disadvantage of the FST and PMT systems in energy efficiency, a relative wasted energy between the both systems that is denoted by E_{waste} will be introduced in Eq. (3.7). Note that the net energy consumption in *Case 3* and *Case 4* of the FST system are the smallest and not different much; however *Case 3* brings the longer life time of the supply response consisting of the electric motor M and the hydraulic pump P because they are not changed the state between on and off in working cycle while changed many times in *Case 4*. Thus, the results of *Case 3* of the FST system should be used to compare with other systems.

$$E_{\text{waste}} = E_{\text{net.3}} - E_{\text{net.PMT}} \tag{3.7}$$

Table 3.5: *Net energy consumptions of FST, PMT and relative wasted energy of FST.*

ω_r (min^{-1})	$E_{\text{net.FST}}$ [Wh]	$E_{\text{net.PMT}}$ [Wh]	E_{waste} [Wh]
600	58.1	16.8	41.3
700	59.7	18.7	41.0
800	62.1	20.5	41.6
900	64.6	22.9	41.7
1000	66.2	24.6	41.6

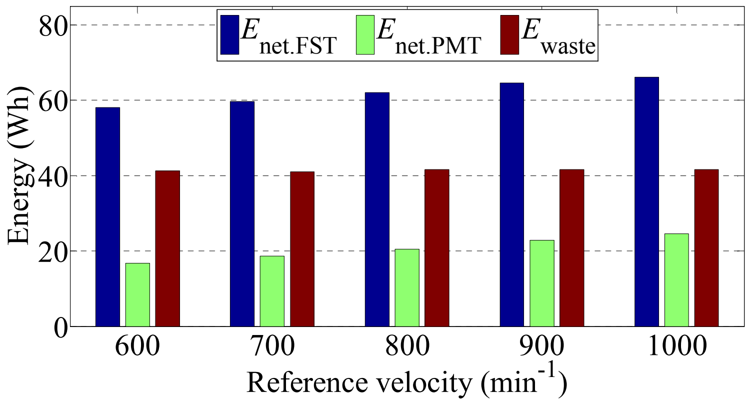

Figure 3.8: *Net energy consumption of FST, PMT and relative wasted energy of FST.*

Table 3.5 and Fig. 3.8 show the comparison of the net energy consumption of the both systems and the relative wasted energy of the FST system in comparison with the PMT system corresponding with the reference velocity from 600 to 1000 min^{-1}. It is very easy to realize the massive advantage of the PMT system in energy efficiency. To make the comparison clearer, the index η_w, which is the ratio between the relative wasted energy and net energy consumption of the FST system, is defined as follows

$$\eta_w = \frac{E_{\text{waste}}}{E_{\text{net.FST}}} \tag{3.8}$$

Table 3.6: *Wasted energy indexes.*

ω_r (min^{-1})	η_w [Wh]
600	71.1
700	68.7
800	67.0
900	64.6
1000	62.8

Table 3.6 shows the wasted energy index η_w when the reference velocity varies from 600 to 1000 min $^{-1}$. The result indicates that from 62.8 to 71.1 % of net energy consumption of the FST system was wasted in comparison with the PMT system. The energy loss of the FST system is mainly because of much higher working pressure that leads to the losses via the relief valves RV_1 and RV_2. Furthermore, the energy charged into the accumulator ACC_1 in Phases 1 and 2 would be dissipated after the working phase and the energy needed to make the flywheel fluctuate around the reference velocity are also the other reasons for the wasted energy.

3.4 Summary

This chapter gave a comparison between the water hydraulic the PMT and FST systems in terms of velocity response and energy saving performance.

The steady state error in the working phase decreased drastically in the PMT system in comparison with the FST system. For more detail, the steady state error downed from 6 to 18 times, it was from 1.66 to 4.1 min^{-1} corresponding to the percentage errors from 0.28 to 0.59%.

The more important feature of the study was the analysis of the energy saving performances of the PMT and FST system and compared them together. Total energy consumption of the PMT system was 2.56–3.85 times less than the FST system corresponding to the reference velocities of 600–1000 min^{-1}.

To realize the energy efficiencies of the PMT and FST systems precisely, this research proposed a method to estimate the saved energy stored in the accumulator ACC_2 and a method to calculate the relative wasted energy of the FST in comparison with the PMT system to show the significant advantage of the PMT system in improving energy efficiency. The results showed that the relative wasted energy is enormous from 62.8 to 71.1% of the total energy consumption of the FST system.

In addition, the PMT system could reduce noise and enlarged the lifetime of the devices such as the ON/OFF valves and hydraulic pump/motor PM because of smoother operation.

Chapter 4

Comparison among FST, PMT, and SMS

4.1 SMS

4.1.1 Overview of SMS

Figure 4.1 shows a conventional servo motor system (SMS), which was examined to evaluate the advantages of the FST and PMT systems. The SMS was set up similarly to the FST and PMT systems; however, the ON/OFF valves were replaced with a servo valve to control the velocity of the flywheel FW. Note that Figs. 2.1, 3.1, and 4.1 use the same symbols to represent the devices in the real systems; Table A.1 presents the main experimental devices of the SMS.

4.1.2 Control Logic of the SMS

The controller of the SMS uses feedback control to make the velocity of the flywheel FW track a desired reference signal $r(t)$ (same as the reference signal of the PMT system) that is generated after the reference model $G_m(s)$ by the rectangular input signal $\omega_r(t)$, as shown in (4.1). The SMS also uses a PID controller that is tuned manually to attenuate the steady-state error and overshoot with the transfer function

$$G_{Sc}(s) = K_{SP} + \frac{K_{SI}}{s} + K_{SD}s \tag{4.1}$$

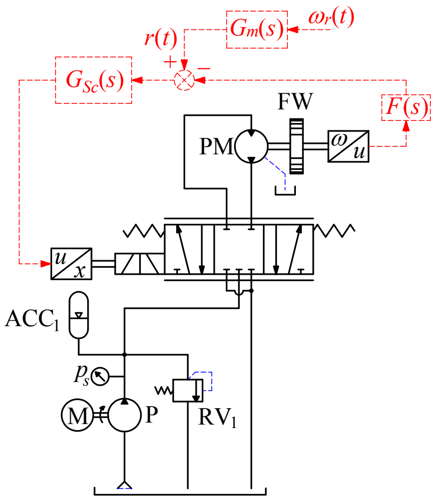

Figure 4.1: *Schematic of the water hydraulic SMS.*

where K_{SP}, K_{SI}, and K_{SD} are the proportional, integral, and derivative gains; in the experiments, they had values of 0.015, 0.002, and 0.005, respectively.

The same low–pass filter $F(s)$ used in the PMT system is also applied to the feedback loop to reduce the noise caused by the measurement devices, which comprise an encoder and FV converter. A similar reference model $G_m(s)$ is used in the control circuit as well.

4.2 Comparison of Velocity Response

The velocity responses of all three systems were analyzed. The main objective of this chapter is to analyze and compare the energy performances of the conventional SMS and digital FST and PMT systems. However, the velocity response is a very important performance that needed to be considered first.

Figure 4.2 shows the velocity responses of all systems at a reference velocity of 800 min^{-1}. In the deceleration phase, all three systems had almost the same responses. The transient responses of the FST and PMT systems were not much different, they only showed a difference at the end of the process, where the PMT system had a longer but smoother response in the PMT system. The SMS showed the best transient response with the shortest rise time and smallest maximum overshoot.

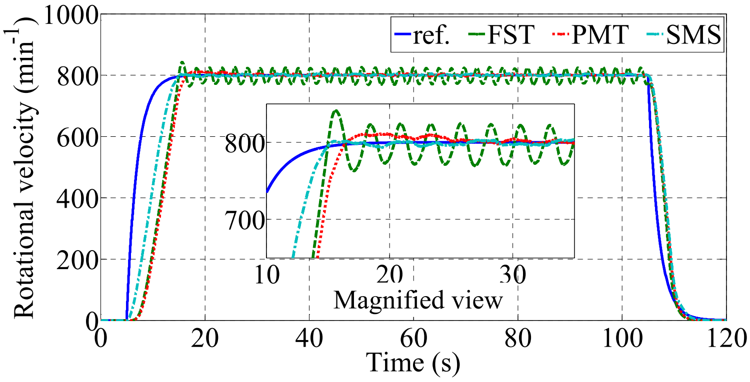

Figure 4.2: *Velocity response of FST, PMT, and SMS (ω_r = 800 min^{-1}).*

Table 4.1 presents the transient responses of all three systems in term of the rise time ($t_{r.\mathrm{F}}$, $t_{r.\mathrm{P}}$, and $t_{r.\mathrm{S}}$ for FST, PMT, and SMS, respectively), maximum overshoot ($M_{p.\mathrm{F}}$, $M_{p.\mathrm{P}}$, and $M_{p.\mathrm{S}}$ for FST, PMT, and SMS, respectively), and percentage overshoot defined in (4.2) (PO_{F}, PO_{P}, and PO_{S} for FST, PMT, and SMS, respectively) for reference velocities of 600–1000 min^{-1}. For all reference velocities, the SMS greatly reduced the overshoot: the overshoot was 7.3–11.4 times less compared to the FST system and 1.5–3.5 times less compared to the PMT system. This was because of the flexible and fast operation of the servo valve. The FST worked with a high velocity for the electric motor M in the acceleration phase, while the PMT operated with a lower velocity depending on the control signal. Therefore, the PMT system had a smaller overshoot and longer rise time for all reference velocities. The SMS had the shortest rise time for all reference velocities because it worked with a high supply pressure $p_{s.\mathrm{S}}$ from the start of the working cycle, while the others needed time to make the supply pressures ($p_{s.\mathrm{F}}$ and $p_{s.\mathrm{P}}$ for FST and PMT, respectively) increase from the stationary state. This problem is reduced in the next cycle when the systems use the saved energies stored in the accumulator ACC_2 as an additional energy source. The effects of the saved energy on the FST and PMT systems will be considered in future work.

$$PO_i = \frac{M_{p.i}}{\omega_r} \tag{4.2}$$

here, i denotes for F, P, and S corresponding to FST (*Case 3*), PMT, and SMS.

Table 4.1: *Transient responses of FST, PMT, and SMS.*

ω_r	FST			PMT			SMS		
(min^{-1})	$t_{r.\mathrm{F}}$ (s)	$M_{p.\mathrm{F}}$ (min^{-1})	PO_F (%)	$t_{r.\mathrm{P}}$ (s)	$M_{p.\mathrm{P}}$ (min^{-1})	PO_P (%)	$t_{r.\mathrm{S}}$ (s)	$M_{p.\mathrm{S}}$ (min^{-1})	PO_S (%)
600	8.3	40.0	6.67	10.3	12.0	2.00	8.1	3.5	0.58
700	9.2	40.4	5.77	10.7	11.4	1.63	8.8	3.7	0.53
800	10.0	41.3	5.16	11.5	11.2	1.40	9.5	4.3	0.54
900	10.9	44.8	4.98	12.2	10.3	1.14	10.2	5.4	0.60
1000	11.7	44.6	4.46	13.5	9.3	0.93	11.3	6.1	0.61

Table 4.2: *Steady-state responses of FST, PMT, and SMS.*

	ω_r (min^{-1})	$\omega_{\mathrm{min.i}}$ (min^{-1})	$\omega_{\mathrm{max.i}}$ (min^{-1})	$e_{\mathrm{min.i}}$ (%)	$e_{\mathrm{max.i}}$ (%)
FST	600	569.2	624.0	5.13	4.00
	700	669.8	724.7	4.31	3.53
	800	769.5	825.1	3.81	3.14
	900	869.0	926.3	3.44	2.92
	1000	968.3	1027.1	3.17	2.71
PMT	600	595.6	603.9	0.73	0.65
	700	695.7	704.0	0.61	0.57
	800	795.4	804.2	0.58	0.53
	900	895.4	904.5	0.51	0.50
	1000	995.5	1004.9	0.45	0.49
SMS	600	596.2	603.5	0.63	0.58
	700	696.0	703.7	0.57	0.53
	800	795.8	804.0	0.53	0.50
	900	895.6	904.5	0.49	0.50
	1000	995.5	1004.8	0.45	0.48

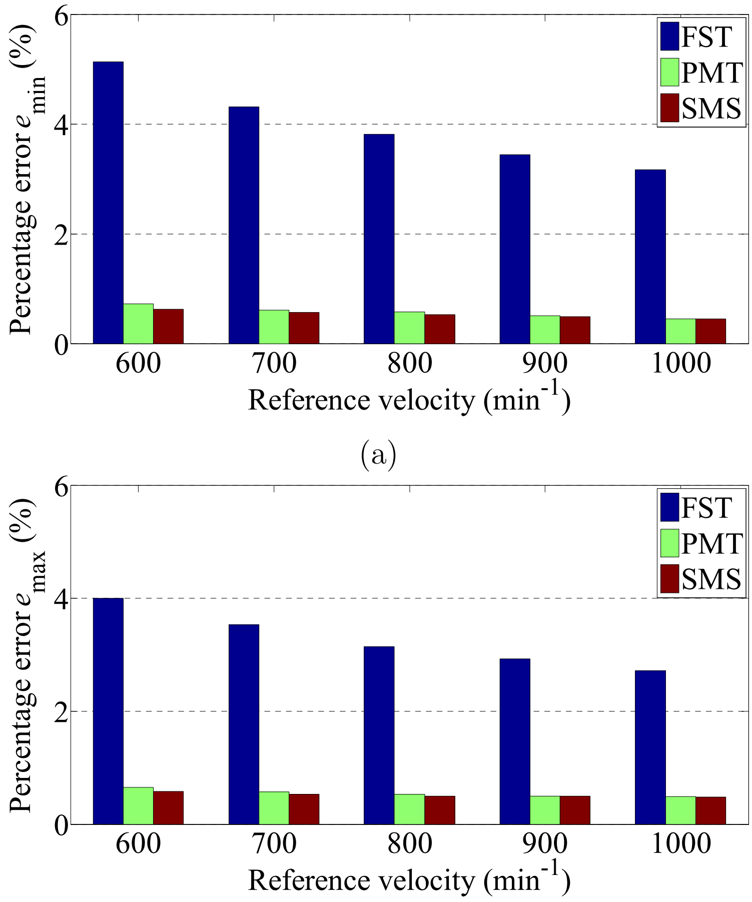

(b)

Figure 4.3: *Percentage errors: (a)* $e_{\min.i}$*, (b)* $e_{\max.i}$ *of FST, PMT, and SMS*

Table 4.2 presents the steady-state responses with the minimum velocities $\omega_{\min.i}$, maximum velocity $\omega_{\max.i}$, and percentage errors $e_{\min.i}$ and $e_{\max.i}$, which are defined in (2.23) and (2.24), respectively. Here, i denotes F, P, and S, which correspond to FST (*Case 3*), the PMT systems and SMS. As a more intuitively comparison of the steady-state responses of the three systems, Fig. 4.3 shows the percentage errors $e_{\min.i}$ and $e_{\max.i}$ as well. The percentage errors $e_{\min.i}$ and $e_{\max.i}$ of the PMT system and SMS were much smaller than those of the FST system for all reference velocities; the reduction was 5.5–8.1 times. The steady-state error of the FST system was mainly generated by the threshold in the control logic that guaranteed that the valve open/close commands were kept longer than the hold time of the valve and the response times of devices such as the ON/OFF valve, hydraulic pump/motor PM, and velocity transducer. The steady-state error of the FST system can be reduced by restricting the threshold velocity or using a better velocity transducer with faster conversion time [52]. However, these methods hare limited and increase the price of the system. The percentage errors $e_{\mathrm{min.F}}$ and $e_{\mathrm{max.F}}$ both tended to decrease quickly at higher reference velocities. This is because the steady-state error of the FST system does not greatly change in response to the reference velocity. Thus, FST is appropriate for high-velocity systems as this will reduce the percentage errors $e_{\mathrm{min.F}}$ and $e_{\mathrm{max.F}}$. The percentage errors of the PMT system and SMS did not greatly differ, the errors were only slightly smaller for the latter. This result demonstrates the high level of applicability of the PMT system.

Note that the steady-state responses of both the PMT system and SMS can be improved by using other control theories to reduce the effects of disturbances, noise, nonlinearity, etc. However, the main purpose of this chapter was to analyze and compare the energy performances of the three systems, as discussed in the following section. Therefore, the conventional PID controllers were applied to both systems.

4.3 Comparison of Energy Performance

Considering the energy performance is one of the most important requirements for water hydraulics because of the low energy efficiency of such systems. The total energy consumption was evaluated for all three systems. The FST and PMT systems can recover part of the total energy consumption and store it in the accumulator ACC_2 for reuse in the next working cycle.

4.3.1 Energy Consumption

Figure 4.4 shows the instantaneous value of the electric power supplied to the electric motor M of all three systems in the experiments with a reference velocity of 800 min^{-1}. The supply pressures $p_{s.i}$, where i denotes F, P, and S corresponding to the FST and PMT systems, and SMS, were considered to be the load of the supply response which consisted of the electric motor M and hydraulic pump P. The pressure $p_{s.\mathrm{S}}$ of the SMS also acted as the working pressure. Figures 4.5 and 4.6 show the supply pressures $p_{s.i}$ for FST, PMT, and SMS and the working pressures $p_{1.\mathrm{F}}$ and $p_{1.\mathrm{P}}$ for FST and PMT, respectively, at a reference velocity of 800 min^{-1}. To ensure a sufficient supply pressure $p_{s.\mathrm{S}}$ for operation of the servo valve in the SMS from the beginning, the electric motor M was started at the beginning of the experiment and the servo valve was only operated after 5 s based on the characteristics of the reference signal as shown in Fig. 4.2. Meanwhile, the electric motors M in the FST and PMT systems only began operation and energy consumption 5 s after the start of experiment as shown in Fig. 4.4. In the deceleration process, the electric motor M was stopped in the FST and PMT systems to save energy, but it was still used in the SMS to brake the flywheel FW. The SMS consumed a lage amount of energy, while the FST system showed greatly reduced energy consumption. The unload valve VS$_4$ of the FST system acted in the working phase and played an important role in reducing the energy consumption, as shown in Fig. 4.4. In the initial period of the acceleration phase, the FST and PMT systems had similar energy consumptions, but the latter consumed less energy at the end of the phase because of the lower velocity of the electric motor M during operation. There was a large difference during the working phase because the PMT system only needed a very small amount of energy to compensate for losses such as friction and leakage to ensure that the velocity of the flywheel FW tracked the reference velocity.

Table 4.3 presents the energy consumptions of the FST and PMT systems and SMS, denoted by $E_{\mathrm{con.F}}$, $E_{\mathrm{con.P}}$, and $E_{\mathrm{con.S}}$, for reference velocity of 600–1000 min^{-1}. The digital hydraulic systems (FST and PMT) demonstrated much less energy consumption than the conventional SMS. The FST system demonstrated a reduction of 52.7%–66.8%, while the PMT system demonstrated an even greater reduction of 76%–86%.

The energy consumptions of the FST and PMT systems tended to increase with the reference velocity, while the inverse was true for the SMS. The tendencies of the FST and PMT systems are intuitive because they require a greater energy supply with a higher reference velocity. The SMS was operated at a constant velocity for the electric motor M of 1100 min^{-1} to ensure that the system

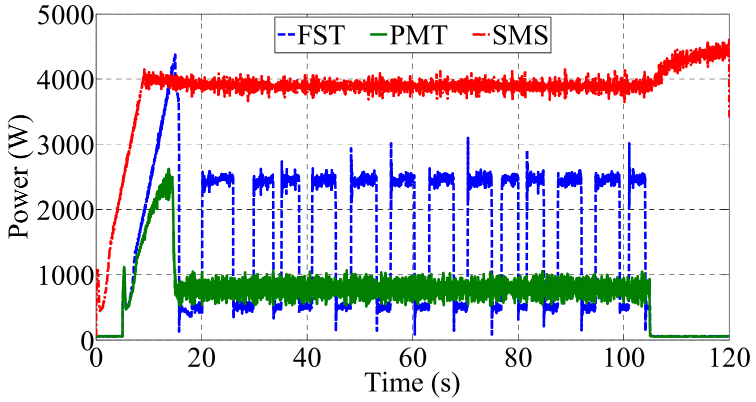

Figure 4.4: *Electric power supplied to the electric motor M of FST, PMT, and SMS* ($\omega_r = 800$ min^{-1}).

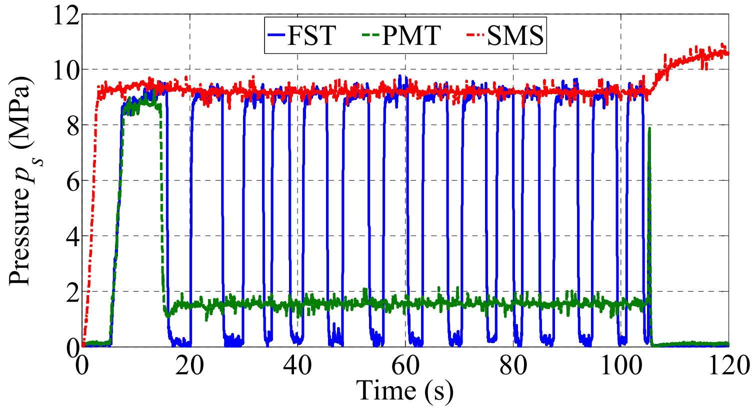

Figure 4.5: *Supply pressure* $p_{s.i}$ *of FST, PMT, and SMS* ($\omega_r = 800$ min^{-1}).

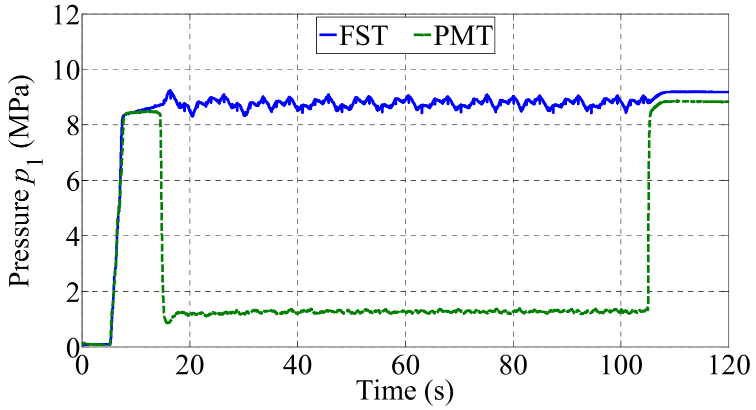

Figure 4.6: *Working pressure* $p_{1.\mathrm{F}}$ *and* $p_{1.\mathrm{P}}$ *for FST and PMT* ($\omega_r = 800$ min^{-1}).

Table 4.3: *Energy consumption of FST, PMT and SMS.*

ω_r (min^{-1})	$E_{\mathrm{con.F}}$ (Wh)	$E_{\mathrm{con.P}}$ (Wh)	$E_{\mathrm{con.S}}$ (Wh)
600	43.7 (33.2 %)	18.4 (14.0 %)	131.7 (100 %)
700	46.4 (35.6 %)	20.8 (16.0 %)	130.2 (100 %)
800	49.5 (38.8 %)	23.0 (18.0 %)	127.5 (100 %)
900	53.0 (42.6 %)	26.0 (20.9 %)	124.5 (100 %)
1000	56.1 (47.3 %)	28.5 (24.0 %)	118.6 (100 %)

performed its function in a full cycle for all reference velocities, especially the highest reference velocity of 1000 min^{-1}. In Phase 2, the flow rate through the hydraulic pump/motor PM increased with the reference velocity, while the supply flow rate from the hydraulic pump P did not change for all cases. This decreased the working pressure, which can be considered as a load on the electric motor M, and thus decreased the energy consumption.

4.3.2 Net Energy Consumption of FST and PMT Systems and Energy Consumption of SMS

The SMS does not recover energy; thus, the net energy consumption was only calculated for the FST and PMT systems. The net energy consumptions of the FST and PMT systems, as shown in (2.27) and (3.6), and the energy consumption of the SMS were then compared to assess the energy performance of each system with more precision and detail.

Table 4.4 lists the net energy consumption of the FST and PMT systems and the energy consumption of the SMS corresponding to reference velocities of 600–1000 min^{-1}. They are also shown in Fig. 4.7 for a more intuitive understanding. The massive increase in energy efficiency of the FST and PMT systems was clearly observed. The results indicate that the FST system only used 30.4%–41.8% of the total energy consumption of the SMS to complete a full cycle, while even the PMT system showed great results with 12.8%–20.7% of the total energy consumption of the SMS.

Table 4.4: *Net energy consumption of FST and PMT systems and energy consumption of SMS.*

ω_r (min^{-1})	$E_{\mathrm{net.F}}$ (Wh)	$E_{\mathrm{net.P}}$ (Wh)	$E_{\mathrm{con.S}}$ (Wh)
600	40.1 (30.4 %)	16.8 (12.8 %)	131.7 (100 %)
700	42.0 (32.3 %)	18.7 (14.4 %)	130.2 (100 %)
800	44.4 (34.8 %)	20.5 (16.1 %)	127.5 (100 %)
900	47.3 (38.0 %)	22.9 (18.4 %)	124.5 (100 %)
1000	49.6 (41.8 %)	24.6 (20.7 %)	118.6 (100 %)

Energy is lost in an SMS is because of the operation in the initial period (0–5 s), braking of the flywheel in Phase 3, and throttling loss in the servo valve during the working phase. A high working pressure leads to losses via the relief valve RV_1, and the energy stored in the accumulator ACC_1 dissipates after the cycle. In an FST system, losses mainly occur in the working phase because of the throttling loss in the ON/OFF valves, which is much smaller than the loss in the servo valve. Losses via the relief valves RV_1 and RV_2 and the energy charged into the accumulator ACC_1 dissipate after the working cycle as well; however, these losses are much smaller than those of the SMS because the unload valve VS_4 force the working pressure p_1 to stay between 8.5 and 9.0 MPa. Oscillation of the flywheel velocity around the reference velocity is another reason for the

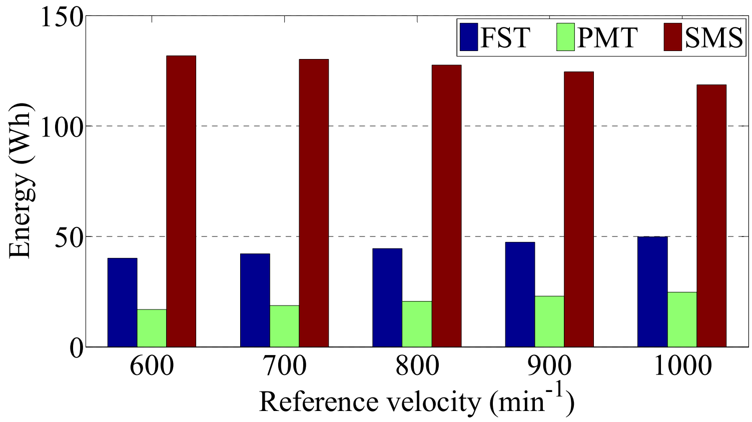

Figure 4.7: *Net energy consumption of FST and PMT systems and energy consumption of SMS.*

wasted energy. The PMT can greatly reduce the energy consumption because it is a direct connection between the hydraulic pump P and hydraulic pump/motor PM; therefore, it can eliminate almost all of the losses causing by intermediate devices. The only losses in a PMT system are the friction and leakage in the hydraulic pump P, the hydraulic pump/motor PM, and the piping loss.

4.4 Summary

This chapter compared the water hydraulic FST, PMT, and SMS in terms of the velocity response and energy performance.

The SMS showed the best transient response with the shortest rise time and smallest overshoot, while the steady-state error was only slightly less than that of the PMT system. The steady-state error of the FST system was relatively large at 5.5–8.1 times more than those of the PMT system and SMS for reference velocities of 600–1000 rpm. However, the percentage errors tended to decrease with higher reference velocities. Thus, the FST system is appropriate for high-velocity transmission.

Both FST and PMT can drastically reduce the energy consumption. The FST system only required 33.2%–47.3% of the total energy consumption of the SMS to complete a full cycle, while the PMT system required 14.0%–24.0%.

Both the FST and PMT systems could recover energy in the deceleration process. The energies saved in the accumulator ACC_2 after a working cycle were 8.2%–11.6% and 8.7%–13.7% of the total energy consumptions of the FST and PMT systems, respectively. These energies were reused in the next working cycle to reduce the energy consumption and rise time. The effect of the saved energy will be considered in future research.

The FST and PMT systems are much cheaper than the SMS because they only use inexpensive ON/OFF valves. Thus, they will help make water hydraulics more widely applicable, especially for systems that do not require very quick and precise control performance.

Chapter 5

Conclusions

The goal of this dissertation is to improve both energy and control performance in water hydraulic transmissions. This research introduces the two cheap FST and PMT systems beside the conventional servo motor system for comparison. As the results of this study, the following conclusions are made.

1. This research showed a whole view of the FST system, because it covered from simulation to experiment, examined the parameters which affected to control performance and energy saving, the two most important points of the system. In addition, three methods to improve the energy efficiency were introduced beside the original FST system.

   First, the simulated results had a good agreement with behavior of the experimental results in velocity, pressure, and flow of each part. That means the simulator has been build successfully and matched the actual.

   The percentage error of the flywheel velocity could be reduced by use a quick response velocity transducer and restricting control upper and lower thresholds. The combination of both methods made the control accuracy of the FST system within ± 25 min^{-1}, that corresponds with the velocity error below 3% for given reference speeds equal or above 800 min^{-1}. However, the restriction of the control upper and lower thresholds made the number of switching up; as a result, the life of the ON/OFF valves would be reduced much. A requirement is to simulate the relationship between the upper and lower thresholds and the duration of the ON/OFF valves. It is a future work of the research.

The most important target of the research is to improve the energy efficiency of the water hydraulic FST. Chapter 2 introduced the original FST system without acting on the electric motor M during working cycles and proposed three methods to reduce the energy consumption by lessening the velocity of the electric motor M and stopping it in the working and deceleration phases, respectively, and limited the working pressures $p_{1.i}$ $(i = 3, 4)$ by use an unload valve or idling stop method, and after that compared them together in both velocity and energy performances.

The experiments on the FST system with respect to energy efficiency and velocity response as well for the reference velocity from 600 to 1000 min^{-1} were executed and the main conclusions can be summarized as follows:

- The velocity responses in the acceleration and deceleration phases were almost same for all cases; only in Phase 3, the deceleration process in *Case 1* was performed slightly faster than the others because of the difference of the working pressure $p_{1.1}$.
- The velocity response improved a little bit from *Case 1* to *4* with the biggest reduction was between *Cases 1* and *2*: from 0.26 to 0.32% and from 0.26 to 0.51% when the reference velocity varied from 600 to 1000 min^{-1} for e_{min} and e_{max}, respectively.
- The difference of the recovered energy generated in Phase 3 and the deceleration process of Phase 2 by converting the kinetic energy of the flywheel FW into high pressure water stored into the accumulator ACC_2 was not much among the 4 cases, particularly between *Cases 3* and *4* because of use the same limitation of the working pressures $p_{1.3}$ and $p_{1.4}$.
- The saved energy remained inside the accumulator ACC_2 after a working cycle in *Case 1* was extremely higher than the others because of use the highest working pressure $p_{1.1}$ while the difference was not much between the last two cases using the same thresholds for the pressures $p_{1.i}$ $(i = 3, 4)$.

- The energy and also net energy consumption of the system reduced from *Case 1* to *4*. The last two cases showed many advantages in both energy and velocity performances and a little better in *Case 4*; however, the electric motor M was turned on/off many times to maintain the working pressure $p_{1.4}$ inside the working range in this case, it leaded to the duration of the electric motor M and also the hydraulic pump P shorten. As a result, the method of using a unload valve should be used in real application.

2. The steady state error in the working phase decreased drastically in the PMT system in comparison with FST system. For more detail, the steady state error downed from 1/6 to 1/18 times, it was from 1.66 to 4.1 $\min^{-1}$ corresponding to the percentage errors from 0.28 to 0.59%.

   The more important point of the study is analysis of the energy saving performances of FST and PMT system and compares them together. Total energy consumption of FST system was much larger than PMT system that was from 2.56 to 3.85 times corresponding to the reference velocities from 600 to 1000 $\min^{-1}$.

   To realize the energy efficiency of the systems more exactly, this research proposed a method to estimate the saved energy stored in the accumulator ACC_2 and a method to calculate the relative wasted energy of FST in comparison with PMT system. The results showed that the relative wasted energy was enormous from 62.8 to 71.1% of the total energy consumption of FST system. Inversely, PMT has shown its outstanding characteristics, it only used from 45.0 to 59.1% of the relative wasted energy of FST system to complete a full cycle.

   In addition, PMT system could reduce noise and also enlarged the lifetime of the devices such as the ON/OFF valves and the hydraulic pump/motor PM because of smooth operation.

3. The SMS showed the best transient response with the shortest rise time and smallest overshoot, while the steady-state error was only slightly less than that of the PMT system. The steady-state error of the FST system

was relatively large at 5.5–8.1 times more than those of the PMT system and SMS for reference velocities of 600–1000 rpm. However, the percentage errors tended to decrease with higher reference velocities. Thus, the FST system is appropriate for high-velocity transmission.

Both FST and PMT can drastically reduce the energy consumption. The FST system only required 33.2%–47.3% of the total energy consumption of the SMS to complete a full cycle, while the PMT system required 14.0%–24.0%.

Both the FST and PMT systems could recover energy in the deceleration process. The energies saved in the accumulator ACC_2 after a working cycle were 8.2%–11.6% and 8.7%–13.7% of the total energy consumptions of the FST and PMT systems, respectively. These energies were reused in the next working cycle to reduce the energy consumption and rise time. The effect of the saved energy will be considered in future research.

The FST and PMT systems are much cheaper than the SMS because they only use inexpensive ON/OFF valves. Thus, they will help make water hydraulics more widely applicable, especially for systems that do not require very quick and precise control performance.

Appendix A

Table A.1: *Specifications of experimental devices*

Symbols	Specifications	Values
P	Displacement volume	15×10^{-6}m^3
PM	Displacement volume	15×10^{-6}m^3
ACC_1	N_2 gas volume	0.005 m^3
	Precharge pressure	5.0 MPa
ACC_2	N_2 gas volume	0.01 m^3
	Precharge pressure	7.8 MPa
FW	Moment of inertia	1.58 kgm^2
	Mass	78.9 kg
	Diameter	0.4 m
	Thickness	0.08 m
Drive motor	Revolution	1200 rpm
Flow meter	Range of measurement	0-15 L/min
Rotational speed meter	Conversion time	7.6×10^{-6} s/cycle
	Range of measurement	1-120000 rpm

Table A.2: *Specifications of measurement devices.*

	Type	Specifications	Values
Encoder	OnoSokki RP–432Z	Maximum Speed	5000 min^{-1}
		Adjacent error	±1/20 Pitch
		Cumulative error	±1/5 Pitch
F/V converter	Onosokki FV–1400	Full–scale output	1 to 120000 min^{-1}
		Deflection output	±1%
		Conversion time	7.6 μs
Flow meter	Nippon Flow Controls F–100	Flow range	1.5 to 15 l/min
		Accuracy	1.5%
Pressure gauge	Nagano Keiki KH15	Pressure range	0 to 100 MPa
		Accuracy	±0.025% to ±0.1%

Appendix B

Application of Water Hydraulics

Industrial high pressure water cleaning

A very important industrial application of tap water hydraulics is high-pressure water cleaners. A typical example is cleaners for malt reservoirs in beer breweries shown in diagram in Fig. B.1. A pump, PAH 32, generates a pressure up to 160 bar. The pump supplies the two high-pressure clean guns connected to a main water supply ring net via quick couplings. The installation supplies the user with a very flexible and effective high pressure cleaning system.

The high power density gives a very compact cleaner unit. Further advantages are no oil lubrication due to lubrication of the components by the tap water itself, and the system requires minimum maintenance.

Humidification

Today's several installations of humidification units with pumps, nozzles and accessories are in use for high- pressure water mist. It is needed indoor such as in super markets selling fruits and in textile industry. Indoor air quality is determined by a number of factors. Humidity is one of the most important measures directly affecting human beings as well as animals, plants and almost any material. Therefore, the ability to adjust humidity, both humidifying and dehumidifying, is of importance and found in numerous applications and industries. Human beings, for example, feel most comfortable at humidity

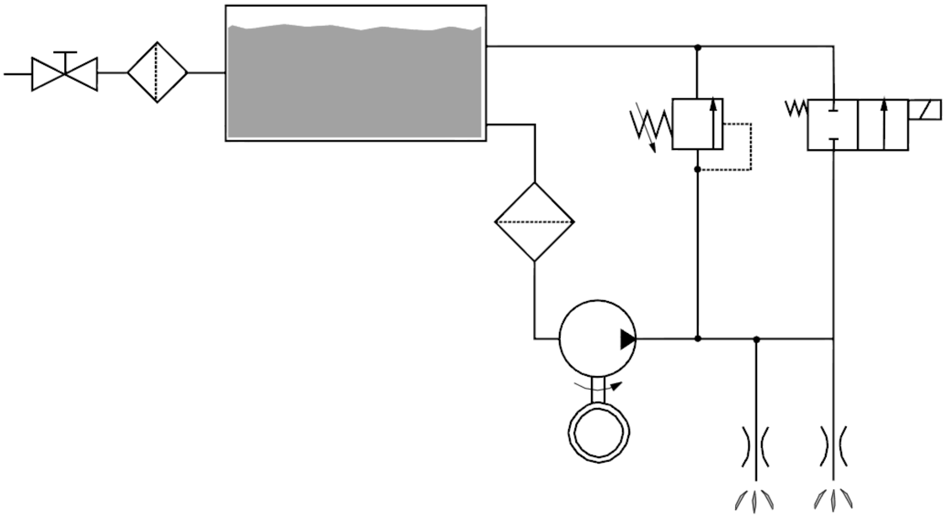

Figure B.1: *Diagram of a high pressure water cleaner [1].*

between 40 and 60% rH and a temperature of 22°C / 72°F. Correct humidity minimizes risk of infection with contagious disease, growth of bacteria or fungi, as well as impacts on performance of man and machine. There are hundreds of examples of how humidity affects productivity of manufacturing processes and the quality of products. A high-pressure pump boosts water to a pressure typically between 70-100 bar. Specially designed water nozzles atomize the water in billions of extremely small droplets. The water mist jets are injected either directly into the open space or into the duct system of an air-handling unit as shown in Fig. B.2. A humidification controlled green house for crops is shown in Fig. B.3.

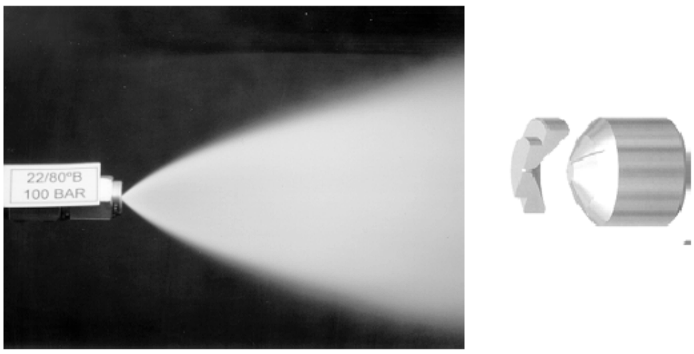

Figure B.2: *A nozzle and generation of water droplets [1].*

Figure B.3: *Humidification control in green house [1].*

Wood processing

Special designed water mist solutions are installed for wood processing, in particular for sawmills to avoid dust and to improve lubrication and cooling of saws as shown in Fig. B.4 as well as for lumber drying shown in Fig. B.5.

Fire protection and fighting systems

Very effective tap water hydraulic fire protection and fighting systems have been developed and taken in use. Figure B.6 shows an typical fire fighting application.

Water hydraulic maritime machinery

Novel Boatscrubbers, a developed automatic boat washer to control and drive by high pressure water hydraulics for motion control and rotation of the brushes to clean the boats is shown in Fig. B.7.

The benefits are significant due to the solution means that the boat–body can

Figure B.4: *Wood processing for sawmills [1].*

Figure B.5: *control Process for lumber drying in a kiln [1].*

be paint with a silicone process to eliminate the pollution from traditional boat painting that contains dangerous particles that seriously pollute the seabed of the harbors and sea–water.

Figure B.6: *Fire fighting by high pressure water hydraulics for generation of water mist [1].*

Figure B.7: *Automatic water hydraulic boat washer [1].*

References

[1] F. Conrad. Trend in design of water hydraulics – motion control and open-ended solutions. *Proc. of the 6th JFPS International Symposium on Fluid Power*, pages 420–431, 2005. vii, ix, x, 3, 4, 5, 6, 7, 9, 10, 11, 12, 13, 101, 102, 103, 104

[2] J. M. Garcia, G. W. Krutz, and L. Jr. John. Self propelled water hydraulic vehicle. *Proc. of The 10th Scandinavian International Conference on Fluid Power*, 2007. vii, xi, 3, 6, 7, 13, 14

[3] N. A. Peppiatt. Hydraulic seals for water and water–based fluids. *Proc. of 2012 Dutch Fluid Power Conference*, 2012. vii, 6, 8

[4] X. Liang and T. Virvalo. What's wrong with energy utilization in hyraulic cranes. *Proc. of the 5th International Conference on Fluid Power Transmission and Control*, pages 419–424, 2001. vii, xi, 15, 16, 17

[5] S. R. Majumdar. *Oil Hydraulic Systems Principles and Maintenance*. McGRAW-HILL, 2003. vii, 24, 25, 26, 27, 34

[6] B. Hollingworth. The past, present and future of (water) hydraulics. *Proc. of The Twelfth Scandinavian International Conference on Fluid Power, SICFP11*, 1:65–78, 2011. 1, 3

[7] F. L. Yin, S. L. Nie, and J. Ruan. Research on the realiability of sliding bearing support in a swash–plate type axial piston water hydraulic pump. *Proc. of International Conference on Fluid Power and Mechatronics FPM2011*, pages 282–286, 2011. 3

[8] Y. Minakawa, T. Yamochi, and H. Mutoh. Research on the water hydraulic drive mechanism powered by an accumulator. *Proc. of the 12th International Conference on Fluid Control, Measurements, and Visualization*, 2013. 3

[9] W. Kobayashi and K. Ito. Developement of gait–training orthosis with water hydraulic mckibben muscle. *Proc. of the 12th International Conference on Fluid Control, Measurements, and Visualization*, 2013. 3

[10] F. Yoshida and S. Miyakawa. Effect of design parameters on stability of water hydraulic proportional control valves. *Proc. of the 12th International Conference on Fluid Control, Measurements, and Visualization*, 2013. 3, 14

[11] P. N. Pham, K. Ito, and S. Ikeo. The application of simple adaptive control for simulated water hydraulic servo motor system. *Proc. of the 12th International Conference on Fluid Control, Measurements, and Visualization*, pages 204–209, 2013. 3, 14

[12] Y. B. Ham, Y. B. Lee, and B. O. Choi. A study on the application of birfield joint to a water hydraulic piston pump for low leakage and low friction pumping. *Proc. of the 6th JFPS International Symposium on Fluid Power*, pages 497–502, 2005. 3

[13] H. Zhou and W. Song. Optimization of floating plate of water hydraulic internal gear pump. *Proc. of the 8th JFPS International Symposium on Fluid Power*, pages 592–598, 2011. 3

[14] F. Majdič, J. Pezdirnik, and M. Kalin. Comparative tribological investigations of continuous control valves for water hydraulics. *Proc. of The 10th Scandinavian International Conference on Fluid Power*, 2007. 3

[15] A. Mitsuhata, C. Liu, A. Kitagawa, and M. Kawashima. Water hydraulic high–speed solenoid valve and its application. *Proc. of the 8th JFPS International Symposium on Fluid Power*, pages 605–610, 2011. 3

[16] F. Conrad and F. Rolim. Mechatronics system engineering for CAE\CAD, motion control and design of valve actuators for water robot applications.

Proc. of the 6th JFPS International Symposium on Fluid Power, pages 503–508, 2005. 3

[17] T. Kazama. Numerical simulation of a slipper model for water hydraulic pumps/motors in mixed lubrication. *Proc. of the 6th JFPS International Symposium on Fluid Power*, pages 509–514, 2005. 3

[18] S. Oshima, T. Hirano, S. Miyakawa, and Y. Oobayashi. Study on the output torque of a water hydraulic planetary gear motor. *Proc. of The 12th Scandinavian International Conference on Fluid Power*, 2011. 3

[19] D. Wu, Y. Liu, Z. Yang, H. Yang, and Z. Jiang. Tribological characteristics of Al_2O_3–3%TiO_2/Al_2O_3 under silt–laden water lubrication. *Proc. of The 12th Scandinavian International Conference on Fluid Power*, pages 79–88, 2011. 3

[20] Y. Yagi, H. A. Tasdemir, T. Tokoroyama, and N. Umehara. The development of friction tester in pressurized hot water at 30 mpa and 300°c. *Proc. of The 5th International Conference on Manufacturing , Machine Design and Tribology*, 2013. 3

[21] G. H. Lim, P. S. K. Chua, and Y. B. He. Modern water hydraulics – the new energy-transmission technology in fluid power. *Applied Energy*, 76:239–246, 2003. 3, 4, 13

[22] Danfoss. http://www.danfoss.com/BusinessAreas/High-Pressure+Systems/Waterhydraulics_info/water-hydraulics.htm. 4

[23] Hytar Oy. http://avs-yhtiot.fi/en/1244/hytar/water-hydraulics. 4

[24] SPX Fluid Power. http://www.spx.com/en/hydraulic-technologies/. 4

[25] Hauhinco. http://hauhinco.de/en/. 4

[26] Elwood Corporation. http://www.elwood.com/. 4

[27] Hunt Valve Company. http://www.huntvalve.com/. 4

[28] Schrupp, inc. http://www.hlhydraulic.com/water-hydraulic-control-valves.htm. 4

[29] The Oilgear Company. http://www.oilgear.com/Products/WaterandSpecialFluidProducts.htm. 4

[30] Hainzl Industriesysteme GmbH & CoKG. http://www.hainzl.at/index.php?id=1&L=1. 4

[31] Ebara Research Co., Ltd. https://www.ebara.co.jp/en/. 4

[32] Fluid Power Net International. http://www.fluidpower.net/fpni/index. 5

[33] National Fluid Power Association. http://www.nfpa.com/. 5

[34] British Fluid Power Association. http://www.bfpa.co.uk/. 5

[35] VDMA (Verband Deutscher Maschinen und Anlagenbau e.V). http://www.vdma.org/en/der-vdma. 5

[36] Japan Fluid Power System Society. http://www.jfps.jp/fluid_e/. 5

[37] K. Ito and S. Ikeo. Robust velocity control of a water hydraulic servomotor system with parameter uncertainty. *Proc. of SICE Annual Conference in Fukui*, 2003. 14

[38] K. Ito. Control performance comparison of simple adaptive control to water hyraulic servo cylinder system. *Proc. of The 19th Mediterranean Conference on Control and Automation*, pages 195–200, 2011. 14

[39] K. Ito, H. Takahashi, S. Ikeo, and K. Takahashi. Robust control of water hydraulic servo motor system using sliding mode control with disturbance observer. *Proc. of SICE-ICASE International Joint Conference*, pages 4659–4662, 2006. 14

[40] X. Wang, J. Zheng, S. Sun, and J. Chang. Research on hydrostatic bearing technology applied in water hydraulic servo valve. *Proc. of the IEEE 10th International Conference on Computer.Aided Industrial Design & Conceptual Design*, pages 2140–2145, 2009. 14

[41] K. A. Stelson. Saving the world's energy with fluid power. *Proc. of the 8th JFPS International Symposium on Fluid Power*, 2011. 15

[42] T. Wang and Q. Wang. An energy-saving pressurecompensated hydraulic system with electrical approach. *IEEE/ASME Transactions on Mechatronics*, 19(2):570–578, 2013. 15

[43] M. Linjama. Digital fluid power - state of the art. *The 12th Scandinavian International Conference on Fluid Power*, pages 331–353, 2011. 15

[44] R. Scheidl, H. Kogler, and B. Manhartsgruber. A cavitation avoidance strategy in hydraulic switching control based on a nonlinear oscillator. *The 10th Scandinavian International Conference on Fluid Power*, 2007. 15

[45] M. Linjama, M. Houva, P. Boström, A. Laamanen, L. Siivonen, L. Morel, M. Waldén, and M. Vilenius. Design and improvement of energy saving digital hydraulics control system. *Proc. of The 10th Scandinavian International Conference on Fluid Power, Tampere*, pages 341–359, 2007. 15

[46] P. Boström, M. Linjama, L. Morel, L. Siivonen, and M. Waldén. Design and validation of digital controllers for hydraulic systems. *The 10th Scandinavian International Conference on Fluid Power*, 2007. 15

[47] M. Karvonen, M. Heikkilä, M. Huova, M. Linjama, and K. Huhtala. Simulation study improving efficiency in mobile boom by using digital hydraulic power management system. *The 12th Scandinavian International Conference on Fluid Power*, pages 355–368, 2011. 17

[48] R. Inoguchi, K. Ito, and S. Ikeo. Pure-hydraulic hybrid cylinder drive system with hydraulic transformer. *JFPS International Journal of Fluid Power system*, 5(1):1–5, 2012. 17

[49] K. Sanada. A study on hils of fluid switching transmission. *Proc. of International Joint Conference SICE-ICASE*, pages 4668–4671, 2006. 17

[50] K. Ito, W. Kobayashi, P. N. Pham, and S. Ikeo. Control and energy saving performance of water hydraulic fluid switching transmission. *Proc. of The 12$^{\text{th}}$ Scandinavian International Conference on Fluid Power*, pages 103–114, 2011. 17

[51] P. N. Pham, K. Ito, W. Kobayashi, and S. Ikeo. Research on velocity error and energy recovery efficiency of water hydraulic fluid switching transmission. *Proc. of The 11$^{\text{th}}$ Inernational Conference on Automation Technology*, 2011. 17

[52] P. N. Pham, K. Ito, W. Kobayashi, and S. Ikeo. Analysis of velocity control performance and energy recovery efficiency of water hydraulic fluid switching transmission. *International Journal of Automation Technology*, 6(4):457–467, 2012. 17, 87

[53] P. N. Pham, K. Ito, and S. Ikeo. Investigation on velocity response and energy saving performance of water hydraulic system without using servo valve. *Proc. of The 13$^{\text{th}}$ Scandinavian International Conference on Fluid Power*, 2013. 17

[54] P. N. Pham, K. Ito, and S. Ikeo. Velocity response and energy consumption of water hydraulic pmt and servo motor systems. *Proc. of The 12$^{\text{th}}$ Inernational Symposium on Fluid Control, Measurement and Visualization*, 2013. 17

[55] S. Habibi and A. Goldenberg. Design of a new high performance electrohydraulic actuator. *Proc. of 1999 IEEE/ASME International Conference on Advanced Intelligent Mechatronics*, 1999. 18

[56] Y. Lin, Y. Shi, and R. Burton. Modeling and robust discrete-time sliding-mode control design for a fluid power electrohydraulic actuator(eha) system. *IEEE/ASME Transaction on Mechatronics*, 18(1):1–10, 2013. 18

[57] H. W. Beatly and J. L. Jirtley. *Electric Motor Hand Book*. McGRAW-HILL, 1998. 25, 70

[58] Y. Tanaka and K. Nakano. Energy balance of bladder type hydraulic accumulator (1^{st} report: Experimental investigation of thermal time constant). *Trans. of Japan Fluid Power System Society*, 22(6):96–102, 1991. 27, 29, 30

[59] Y. Tanaka and K. Nakano. Energy balance of bladder type hydraulic accumulator (2^{nd} report: Estimation of efficiency for energy storage during continous process). *Trans. of Japan Fluid Power System Society*, 23(3):99–105, 1992. 27

[60] M. Jelali and A. Kroll. *Hydraulic Servo-systems Modelling, Identification and Control*. Springer, 2004. 32, 35

[61] N. D. Manring. *Hydraulic Control Systems*. The National Fluid Power Association, USA, 2005. 32